

UCSF

UC San Francisco Electronic Theses and Dissertations

Title

Physiology-Behavior Transformation through Arcuate Feeding Circuit

Permalink

<https://escholarship.org/uc/item/79b3m4fn>

Author

Chen, Yiming

Publication Date

2018

Peer reviewed|Thesis/dissertation

Physiology-Behavior Transformation through Arcuate Feeding
Circuit

by

Yiming Chen

DISSERTATION

Submitted in partial satisfaction of the requirements for the degree of

DOCTOR OF PHILOSOPHY

in

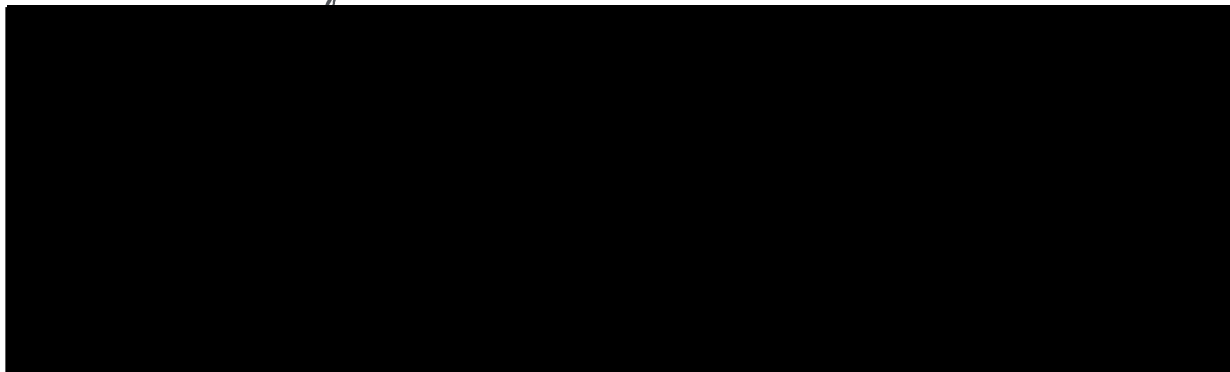
Neuroscience

in the

GRADUATE DIVISION

of the

UNIVERSITY OF CALIFORNIA, SAN FRANCISCO



Committee in Charge

Copyright 2018
by
Yiming Chen

Acknowledgement

I would like to thank Zack for his inspiration and insight.

Part of this thesis is a reproduction of material previously published and contains contributions from collaborators listed therein. Chapter 2 is reproduced in part with permission from: Chen, Y., Lin, Y.-C., Kuo, T.-W., & Knight, Z. A. (2015). Sensory Detection of Food Rapidly Modulates Arcuate Feeding Circuits. *Cell*, 160(5), 829–841. Chapter 3 is reproduced in part with permission from: Chen, Y., & Knight, Z. A. (2016). Making sense of the sensory regulation of hunger neurons. *BioEssays*, 38(4), 316–324. Chapter 4 is reproduced in part with permission from: Beutler, L. R.*, Chen, Y. *, Ahn, J. S., Lin, Y.-C., Essner, R. A., & Knight, Z. A. (2017). Dynamics of Gut-Brain Communication Underlying Hunger. *Neuron*, 96(2), 461–475.e5. Chapter 5 is reproduced in part with permission from: Chen, Y., Lin, Y. C., Zimmerman, C. A., Essner, R. A., & Knight, Z. A. (2016). Hunger neurons drive feeding through a sustained, positive reinforcement signal. *ELife*, 5(AUGUST), 1–21.

Abstract

Physiology-Behavior Transformation through Arcuate Feeding Circuit

Yiming Chen

Proper control of feeding is essential to the fitness of animals. This process involves transformation of homeostatic needs into behavioral control by specialized circuits in the hypothalamus. Agouti-related peptide (AgRP) and proopiomelanocortin (POMC) neurons in the arcuate nucleus (ARC) play dominant roles in this process: they integrate homeostatic information and control feeding. Altogether, 20 years of rigorous research has led to a comprehensive model of the homeostatic control of feeding through the arcuate circuit; this model is described in detail in Chapter 1. Nevertheless, it remains unclear how AgRP and POMC neurons are regulated *in vivo*.

In the Chapter 2 of this dissertation, we show the first recording of AgRP and POMC neuron activity *in vivo* during feeding. Contrary to past models, these key feeding neurons do not simply represent the current energy state of the body. Instead they anticipate future homeostatic consequences based on sensory cues associated with food. We discuss the implication of this finding extensively in Chapter 3.

In Chapters 4 and 5, we address two questions: how are homeostatic signals integrated *in vivo* in the arcuate feeding circuit in the context of the dominant sensory regulation, and how do AgRP neurons drive food intake despite the fact that their activity is reset before food consumption even starts? We show in Chapter 3 that sensory cues, intragastric nutrients and hormones converge onto AgRP neurons to estimate energy balance on different timescales. We then show in Chapter 4 that AgRP neurons promote food intake through a hunger signal that persists for tens of minutes and potentiates the reward value of food.

Table of Contents

Chapter 1: Introduction	1
Chapter 2: Sensory modulation of arcuate feeding circuit	
Summary	4
Introduction	4
Results	6
Discussion	23
Methods	28
Supplementary figures.....	38
Chapter 3: Making sense of the sensory regulation of hunger neurons	
Summary	41
Main content.....	41
Conclusion and outlook	60
Chapter 4: Hormonal and intragastric regulation of arcuate feeding circuit	
Summary	61
Introduction	61
Results	63
Discussion	84
Methods	89
Supplementary figures.....	97
Chapter 5: Control of feeding through sustained valence mechanism by hunger neurons	
Summary	103
Introduction	103
Results	105

Discussion	120
Methods	127
Supplementary figures.....	136
References	139

List of Figures

Chapter 1: Introduction

Figure 1.1. Homeostatic Control of Feeding Through Arcuate Nucleus.....	3
---	---

Chapter 2: Sensory modulation of arcuate feeding circuit

Figure 2.1. Optical recording of AgRP and POMC neuron activity in awake behaving mice	8
Figure 2.2. Ghrelin rapidly modulates AgRP and POMC neurons.....	10
Figure 2.3. Sensory detection of food rapidly regulates AgRP and POMC neurons.....	12
Figure 2.4. Food palatability determines the magnitude of the response to food detection	15
Figure 2.5. The response to food detection depends on food accessibility and is reversible.....	18
Figure 2.6. Intrameal dynamics of AgRP and POMC neurons	21
Figure 2.7. Natural dynamics of AgRP projections to the PVH.....	22
Figure 2.8 - Related to Figure 2.1. Location of viral infection and cannula placement for five AgRP and five POMC mice.....	38
Figure 2.9 - Related to Figure 2.4. Response of AgRP neurons to chocolate	39
Figure 2.10 - Related to Figure 2.5. Peanut butter accessibility	40
Figure 2.11 - Related to Figure 2.7. sEffect of ghrelin on AgRP (ARC → PVH) projections.....	40

Chapter 3: Making sense of the sensory regulation of hunger neurons

Figure 3.1. AgRP and POMC neurons regulate feeding in response to nutritional signals	43
Figure 3.2. Techniques for cell-type-specific recording of deep brain neural activity.....	46

Figure 3.3. Fast and slow regulation of AgRP and POMC neurons by anticipatory and homeostatic signals	47
Figure 3.4. Three models for the inactivation of AgRP neurons by feeding	55

Chapter 4: Hormonal and intragastric regulation of arcuate feeding circuit

Figure 4.1. Nutrient intake is necessary and sufficient for sustained AgRP neuron inhibition	64
Figure 4.2. Inhibition of AgRP neurons by nutrients is independent of macronutrient composition or nutritional state and is proportional to calorie ingestion.....	68
Figure 4.3. AgRP neuron inhibition in response to the sensory detection of food is inversely related to intragastric calorie infusion and predicts subsequent chow consumption	70
Figure 4.4. CCK, PYY, and 5HT are sufficient to inhibit AgRP neuron activity	72
Figure 4.5. PYY is necessary for inhibiting the basal firing rate of AgRP neurons. CCK is necessary for AgRP neuron inhibition caused by lipid.	74
Figure 4.6. Leptin gradually modulates the activity of AgRP and POMC neurons in fasted animals.....	77
Figure 4.7. Leptin is neither necessary nor sufficient for gating the sensory regulation of AgRP and POMC neurons.....	80
Figure 4.8. AgRP neurons are epistatic to leptin’s effect on food intake.....	84
Figure 4.9. – Related to Figure 4.1. Intragastric infusion of water causes stomach distension	97
Figure 4.10. – Related to Figure 4.2. AgRP neuron inhibition in response to intragastric and systematic administration of glucose	97
Figure 4.11. – Related to Figure 4.3. AgRP neuron inhibition in response to the sensory detection of food and subsequent chow intake are attenuated by LPS injection	98

Figure 4.12. – Related to Figure 4.4. Systemic hormones can have additive effects on AgRP neuron activity, and are effective in both fed and fasted mice.....99

Figure 4.13. – Related to Figure 4.6. Leptin has no acute effect on the calcium dynamics of AgRP and POMC neurons..... 100

Figure 4.14. – Related to Figure 4.7. Leptin is not necessary for gating the sensory regulation of AgRP and POMC neurons by palatable food. 101

Figure 4.15. Model for how AgRP neurons calculate energy balance by integrating three streams of information that develop on different timescales..... 102

Chapter 5: Control of feeding through sustained valence mechanism by hunger neurons

Figure 5.1. Prestimulation of AgRP neurons promotes sustained consummatory behavior 107

Figure 5.2. Prestimulation of SFO^{Nos1} neurons does not prime drinking behavior 109

Figure 5.3. Prestimulation of AgRP neurons promotes sustained appetitive behavior.. 110

Figure 5.4. Projections of AgRP neurons to PVH, BNST or LHA are sufficient to prime feeding behavior 112

Figure 5.5. Prestimulation of AgRP neurons conditions appetite and flavor preference 115

Figure 5.6. AgRP neuron activity is positively reinforcing in the presence of food..... 119

Figure 5.7. – Related to Figure 5.1. Prestimulation of AgRP neurons primes feeding .. 136

Figure 5.8. – Related to Figure 5.4. Prestimulation of specific AgRP neuron projections promotes feeding..... 137

Figure 5.9. – Related to Figure 5.6. AgRP neurons support positive, but not negative, reinforcement 138

Chapter 1. Introduction

Feeding behavior is controlled by conserved peptidergic neural circuits. Two neuropeptides, agouti-related peptide (AgRP) and neuropeptide Y (NPY), have played a pivotal role in our understanding of feeding (Andermann and Lowell, 2017; Cone, 2005; Krashes et al., 2016; Sternson and Eiselt, 2017). AgRP promotes feeding by antagonizing the melanocortin 4 receptor (MC4R), a Gs protein-coupled receptor (Lu et al., 1994; Ollmann et al., 1997). MC4R receptor is essential to satiety and loss of MC4R signaling leads to obesity and hyperphagia in both mice and humans (Balthasar et al., 2005; Huszar et al., 1997; Yeo et al., 1998). On the other hand, NPY promotes feeding by activating Gi protein-coupled NPY receptors (Kanatani et al., 2000; Marsh et al., 1998). NPY is one of the most potent orexigenic agent known; infusion of nanomolar concentrations of NPY into the third ventricle is sufficient to induce voracious feeding (Clark et al., 1985).

AgRP and NPY are co-expressed by the same GABAergic neurons in the arcuate nucleus (ARC) (Hahn et al., 1998). These neurons are considered *bona fide* hunger neurons, as their activation recapitulates the behavioral, physiological and affective aspects of hunger (Aponte et al., 2011; Burnett et al., 2016; Krashes et al., 2011; Steculorum et al., 2016); on the other hand, inhibition or ablation of these cells reduces feeding (Gropp et al., 2005; Krashes et al., 2011; Luquet et al., 2005). AgRP neurons project centrally to downstream targets implicated in the control of motivation, including lateral hypothalamic area (LHA), paraventricular hypothalamus (PVH), bed nucleus of stria terminalis (BNST) and parabrachial nucleus (PBN) (Betley et al., 2013). Optogenetic stimulation of the axonal terminals of AgRP neurons in each of these targets except PBN causes rapid food intake (Atasoy et al., 2012; Betley et al., 2013). While the projection of AgRP neurons to PBN is not sufficient to promote food intake, it plays an essential role in suppressing overeating and malaise (Campos et al., 2016; Wu et al., 2012).

Ablation of AgRP neurons in adult mice abolishes the motivation to eat and this effect can be rescued through chronic inhibition of PBN (Wu et al., 2009; Wu et al., 2012).

Pro-opiomelanocortin (POMC) neurons are intermingled with AgRP neurons in the ARC. These cells project to essentially the same targets as AgRP neurons and release α -MSH, a neuropeptide that suppresses feeding through activation of MC4R (Fan et al., 1997; Wang et al., 2015). While stimulation of AgRP neurons increases food intake in minutes, activation of POMC neurons promotes satiety on a timescale of tens of hours (Aponte et al., 2011; Fenselau et al., 2017). It is still controversial whether POMC neurons release the canonical fast neurotransmitters GABA and glutamate (Fenselau et al., 2017; Hentges et al., 2004; Vong et al., 2011). AgRP neurons project directly to inhibit POMC neurons but not vice versa, and this projection is not required for acute feeding control by AgRP neurons (Atasoy et al., 2012; Vong et al., 2011).

Arcuate feeding circuits sense the energy state of the body by integrating circulatory signals in the form of hormones and nutrients. How AgRP and POMC neurons are regulated by the hunger hormone ghrelin and the satiety hormone leptin has been widely studied (Cone, 2005; Schwartz et al., 2000). For example, leptin suppresses appetite and increases metabolism partially through inhibition of AgRP neurons and excitation of POMC neurons (Cowley et al., 2001; Friedman and Halaas, 1998). Meanwhile, ghrelin promotes feeding by activating AgRP neurons (Cummings and Overduin, 2007; Nakazato et al., 2001). Data also suggest that these cells directly monitor the glucose concentration in the circulation (Claret et al., 2007).

AgRP and POMC neurons receive neuronal inputs from various brain regions within and beyond the hypothalamus (Wang et al., 2015). Two upstream inputs have been scrutinized. PACAP-expressing neurons in the PVH directly activate AgRP neurons and promote hunger, while PACAP neurons in VMH activate POMC neurons (Krashes et al., 2014). In DMH, leptin

receptor neurons send direct inhibitory input to AgRP neurons and stimulation of those cells suppresses feeding (Garfield et al., 2016).

In summary, past research on the key arcuate feeding circuit led to the homeostatic control model, which has been the paradigm in the feeding field for decades (Gao and Horvath, 2007; Horvath and Diano, 2004; Schwartz et al., 2000; Spiegelman and Flier, 2001). In this model, AgRP neurons are activated by negative energy states signaled through humoral cues; activation of these cells promotes feeding; in return, food intake influences the interior milieu which then feeds back to AgRP neurons forming a closed control loop (**Figure 1.1**). While this model is intuitive and supported by hundreds of studies, one essential piece of data was missing when I started my study of feeding control: the neural dynamics of the arcuate feeding circuit *in vivo*.

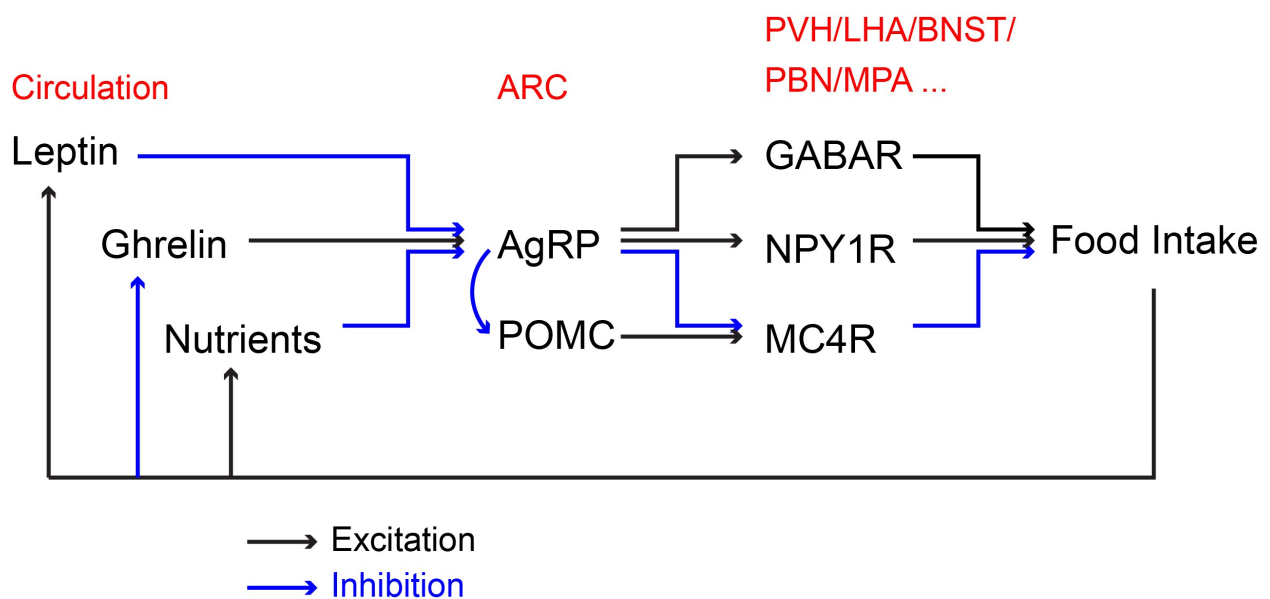


Figure 1.1. Homeostatic Control of Feeding Through Arcuate Nucleus.

AgRP neurons in arcuate nucleus (ARC) translates circulatory cues about homeostatic state of the body into neuronal control of feeding behavior through release of a cocktail of neurotransmitters in various downstream targets.

Chapter 2: Sensory modulation of arcuate feeding circuit

SUMMARY

Hunger is controlled by specialized neural circuits that translate homeostatic needs into motivated behaviors. These circuits are under chronic control by circulating signals of nutritional state, but their rapid dynamics on the timescale of behavior remain unknown. Here we report optical recording of the natural activity of two key cell types that control food intake, AgRP and POMC neurons, in awake behaving mice. We find unexpectedly that the sensory detection of food is sufficient to rapidly reverse the activation state of these neurons induced by energy deficit. This rapid regulation is cell-type-specific, modulated by food palatability and nutritional state, and occurs before any food is consumed. These data reveal that AgRP and POMC neurons receive real-time information about the availability of food in the external world, suggesting a primary role for these neurons in controlling appetitive behaviors such as foraging that promote the discovery of food.

INTRODUCTION

Food intake is controlled by evolutionarily hard-wired neural circuits that contain specialized neural cell types. Two cell types in the arcuate nucleus (ARC) of the hypothalamus are known to be particularly important for the control of feeding. These neurons are identified by expression of the neuropeptides Agouti-related Protein (AgRP) and Proopiomelanocortin (POMC) and have opposing functions. AgRP neurons are activated by energy deficit (Hahn et al., 1998) and promote food seeking and consumption. Optogenetic or chemogenetic activation of AgRP neurons induces voracious eating in sated mice (Aponte et al., 2011; Krashes et al., 2011), whereas inhibition or ablation of AgRP neurons results in aphagia (Gropp et al., 2005; Krashes et al., 2011; Luquet et al., 2005). These effects of AgRP neurons are mediated by release of GABA as well as two neuropeptides, AgRP and NPY, that stimulate food intake when

delivered into the brain (Clark et al., 1985; Fan et al., 1997; Ollmann et al., 1997; Tong et al., 2008). POMC neurons by contrast are activated by energy surfeit and their activity inhibits food intake and promotes weight loss. These two cell types interact in part through a common set of downstream neural targets that express melanocortin receptors, which are activated by POMC and inhibited by AgRP (Fan et al., 1997; Ollmann et al., 1997; Seeley et al., 1997). Thus AgRP and POMC neurons are two intermingled, interacting neural cell types that have opposing roles in the control of feeding.

Despite intense investigation of these cells over the past 20 years, their activity dynamics during behavior remain unknown. This knowledge gap reflects the difficulty of recording cell-type-specific neural activity within heterogeneous deep brain structures such as the hypothalamus. As a result our current understanding of the regulation of AgRP and POMC neurons is based on a combination of approaches that include *in vitro* electrophysiology, *c-fos* staining, pharmacology, and genetic manipulations. These pioneering studies have revealed a dominant role for circulating hormones and nutrients in the control of these cells (Williams and Elmquist, 2012). AgRP and POMC neurons are modulated by hormones such as ghrelin and leptin (Cowley et al., 2001; Cowley et al., 2003; Nakazato et al., 2001; Pinto et al., 2004) as well as circulating nutrients (Blouet and Schwartz, 2010) in part via their metabolic effects on mitochondrial dynamics (Dietrich et al., 2013; Schneeberger et al., 2013). Together these findings have led to a generally accepted model in which AgRP and POMC neurons function as interoceptors that monitor the concentration of hormones and nutrients in the blood and then gradually adjust their activity in parallel with changes in nutritional state. This model provides a compelling explanation for how nutritional changes can be translated into counterregulatory responses but leaves unanswered the question of whether these neurons are also subject to rapid regulation on the timescale of behavior.

AgRP and POMC neurons also receive abundant synaptic input which provides the potential for more rapid modulation. However the function of this afferent input is not well

understood. Fasting increases excitatory tone onto AgRP neurons (Liu et al., 2012; Yang et al., 2011), and one source of such excitatory input is neurons in the paraventricular hypothalamus (PVH) (Krashes et al., 2014). AgRP neurons also receive inhibitory input from the dorsomedial hypothalamus (DMH) among other sources (Krashes et al., 2014). POMC neurons by contrast receive inhibitory input from cells in the ARC, including neighboring AgRP neurons, as well as excitatory input from the ventromedial hypothalamus (VMH) and other regions (Cowley et al., 2001; Krashes et al., 2014; Pinto et al., 2004; Sternson et al., 2005; Vong et al., 2011). As these circuit connections have only recently been described, their regulation and function are not yet clear. An important open question regards the nature of the information that these presynaptic cells communicate to their AgRP and POMC targets.

In the present study we have used an optical approach to record the natural activity of AgRP and POMC neurons in awake behaving mice. These experiments have unexpectedly revealed that AgRP and POMC neurons are strongly regulated *in vivo* by the sensory detection of food. This rapid sensory regulation resets the activation state of these cells induced by food deprivation prior to the start of food consumption. This rapid regulation also contains information about the food's hedonic properties and depends on the animal's nutritional state. These findings reveal that AgRP and POMC neurons receive real-time information about the availability of food in the outside world, which they then use to anticipate the nutritional value of a forthcoming meal and adjust their activity in advance. This anticipatory regulation provides a mechanism to rapidly inhibit foraging upon food discovery, suggesting a primary role for these neurons in the regulation of appetitive behaviors *in vivo*.

RESULTS

Optical recording of AgRP and POMC neuron activity in awake behaving mice

In order to gain deeper insight into the regulation of AgRP and POMC neurons we sought to record their natural activity during feeding behavior. To do this we used fiber

photometry (Cui et al., 2013; Gunaydin et al., 2014), an approach that employs a multimode optical fiber to record the total fluorescence from a population of neurons expressing a calcium reporter for neural activity (**Figure 2.1F**). By targeting the calcium reporter to a specific cell type, this method enables optical recording of the real-time activity of a molecularly defined population of neurons within a deep brain structure. The resulting trace represents the integrated activity of the neurons defined by a genetic marker and anatomic location and therefore is particularly well-suited for use in the hypothalamus, which contains genetically separable populations of neurons with distinct functions.

We first confirmed that calcium signals from AgRP and POMC neurons correlate with changes in firing rate *ex vivo*. We targeted the sixth generation calcium reporter GCaMP6s (Chen et al., 2013) to AgRP and POMC neurons by stereotaxic injection of Cre-dependent AAVs into AgRP-IRES-Cre and POMC-Cre mice (**Figure 2.1A**) and then prepared acute brain slices for imaging and intracellular recording. Fluorescent cells in the ARC were identified for whole-cell patch clamp recordings and held at -70 mV in current clamp. Activation by depolarizing current ramp (0-40 pA, 10s) induced bursts in firing accompanied by increased GCaMP6s fluorescence (**Figure 2.1B**). To quantify the relationship between firing rate and fluorescence signal we applied step currents (-20 pA to +120 pA, 10 pA increments), which resulted in progressive increases in spikes and fluorescence (**Figure 2.1C**). Quantification of this response revealed a linear correlation between action potential number and GCaMP6s signal (**Figure 2.1D-E**). Thus GCaMP6s can report on activity dynamics in AgRP and POMC neurons as shown for other cell types (Chen et al., 2013).

To apply this approach *in vivo*, we injected AAVs expressing GCaMP6s into the ARC of the corresponding Cre mice and in the same surgery installed an optical fiber unilaterally above the ARC (**Figure 2.8**). After allowing two weeks for transgene expression, we connected mice to a photometry rig and recorded fluorescence from these cells as mice explored a feeding chamber without access to food. Baseline recordings from AgRP and POMC neurons showed

dynamic fluctuations ($\sim 10\text{-}20\%$ $\Delta F/F$) that resembled bursts of synchronous activity observed in other cell types (Cui et al., 2013; Gunaydin et al., 2014) (**Figure 2.1H**). These dynamics were unrelated to mouse movement, unaffected by changes in ambient lighting, and absent from recordings from control mice expressing GFP in AgRP or POMC neurons (**Figure 2.1H**), indicating that they represent calcium-dependent GCaMP6s signals.

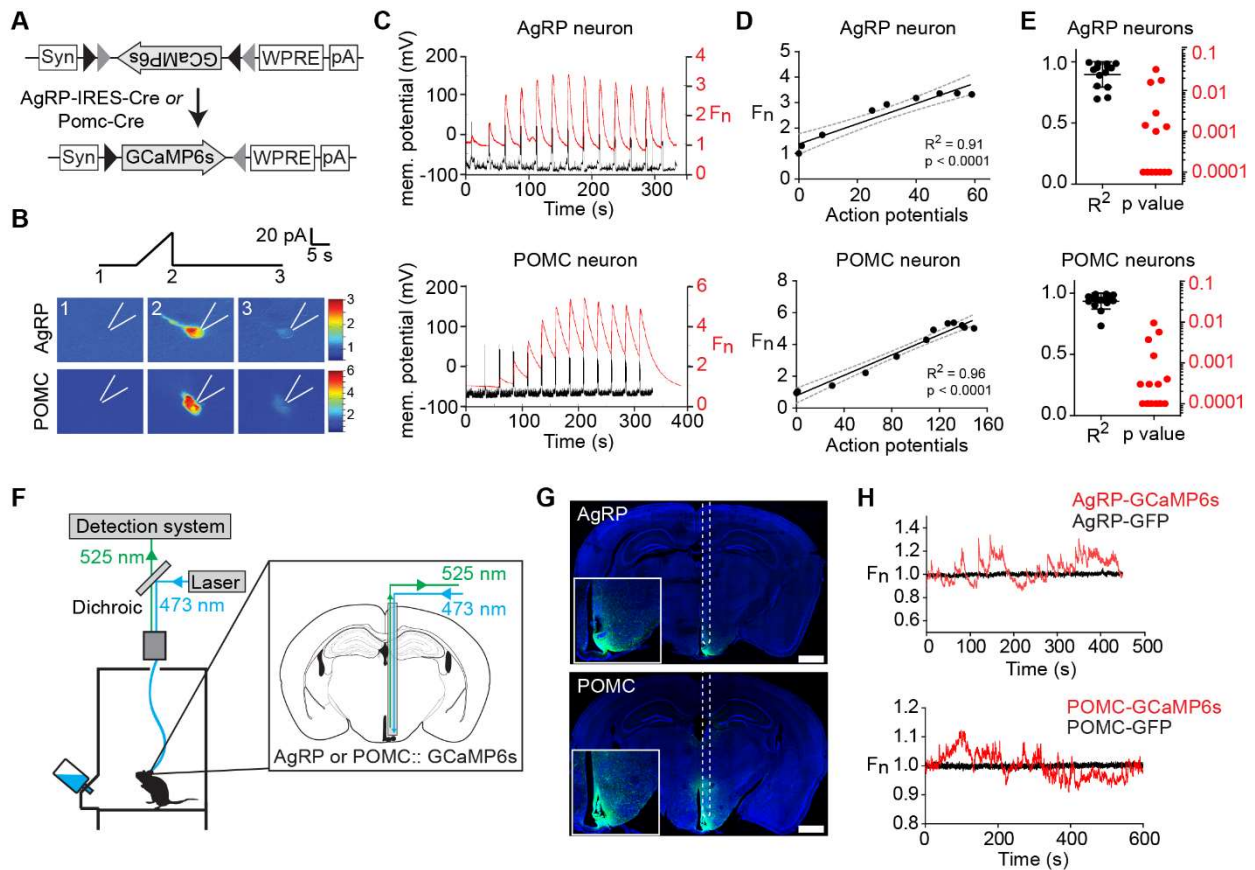


Figure 2.1. Optical recording of AgRP and POMC neuron activity in awake behaving mice. (A) FLEX AAV used to drive GCaMP6s expression. (B) Response of AgRP and POMC neurons to current ramp. Scale bar indicates GCaMP6s fluorescence normalized to 1.0 at start of the experiment (Fn). (C) Membrane potential and GCaMP6s fluorescence in response to sequential 10 pA current steps of duration 2s separated by 20s. (D) Relationship between action potential number and fluorescence for cells in panel C. (E) R-squared and p values for the linear regression of fluorescence versus action potential number for 16 POMC and 14 AgRP neurons. (F) Schematic of the fiber photometry setup. (G) Coronal section from AgRP and POMC mice showing path of optical fiber and injection site. Scale bar = 1 mm (H) Fluorescence trace during cage exploration for mice expressing GCaMP6s or GFP in AgRP neurons or POMC neurons. See also Figure S1.

To test the sensitivity of this assay to detect changes in neural activity, we challenged mice with ghrelin, a hormone that activates AgRP neurons and inhibits POMC neurons (Cowley et al., 2003; Nakazato et al., 2001). Mice expressing GCaMP6s in either AgRP or POMC neurons were acclimated to a behavioral chamber, given an intraperitoneal injection of ghrelin, and then returned to the chamber. Ghrelin sharply increased calcium signals from AgRP neurons ($\Delta F/F = 71 \pm 10\%$ at 5 min, $p < 0.001$ compared to vehicle; **Figure 2.2A,B**). This increase began within seconds of injection (mean latency = 33 ± 7 s) and reached a plateau within two minutes ($\tau = 76 \pm 12$ s, where τ is the exponential time constant corresponding to the time after injection resulting in $\sim 63.8\%$ of the total change). In the absence of further intervention, this increase in AgRP activity was sustained for the duration of the recording ($\Delta F/F = 62 \pm 10\%$ at 15 min; **Figure 2.2B**). By contrast injection of vehicle (PBS) had no effect on the activity of AgRP neurons ($\Delta F/F = -3 \pm 2\%$ at 5 min **Figure 2.2B**).

POMC neurons showed the opposite response, with ghrelin injection rapidly and potently inhibiting POMC activity ($\tau = 160 \pm 17$ s; $\Delta F/F = -49 \pm 4\%$ at 15 min, $p = 0.001$ compared to vehicle; **Figure 2.2C,D**). Interestingly vehicle injection alone produced a small but reversible drop in POMC activity (**Figure 2.2D**). This transient decline in POMC activity was consistently observed following animal handling, suggesting that POMC but not AgRP neurons receive an inhibitory stress regulated input.

We next tested the effect of food on the response to ghrelin. Our prediction based on the known nutritional regulation of these cells was that food consumption would gradually inhibit AgRP neurons and activate POMC neurons as animals transitioned from hunger to satiety. To test this we challenged mice with ghrelin and then 20 minutes later presented them with a pellet of chow. Unexpectedly we found that food presentation alone rapidly reversed much of the effect of ghrelin treatment ($\Delta F/F = -29 \pm 3\%$ at 2 min for AgRP neurons and $\Delta F/F = 80 \pm 3\%$ at 2 min for POMC neurons; **Figure 2.2**). This response began immediately upon placing food in

the cage and was complete within seconds ($\tau = 12 \pm 2$ s for AgRP neurons; $\tau = 44 \pm 3$ s for POMC neurons). All animals tested showed this response to food presentation (traces for ten mice are shown in **Figure 2.2E**), suggesting that it represents a general mechanism that regulates the activity of these neurons *in vivo*.

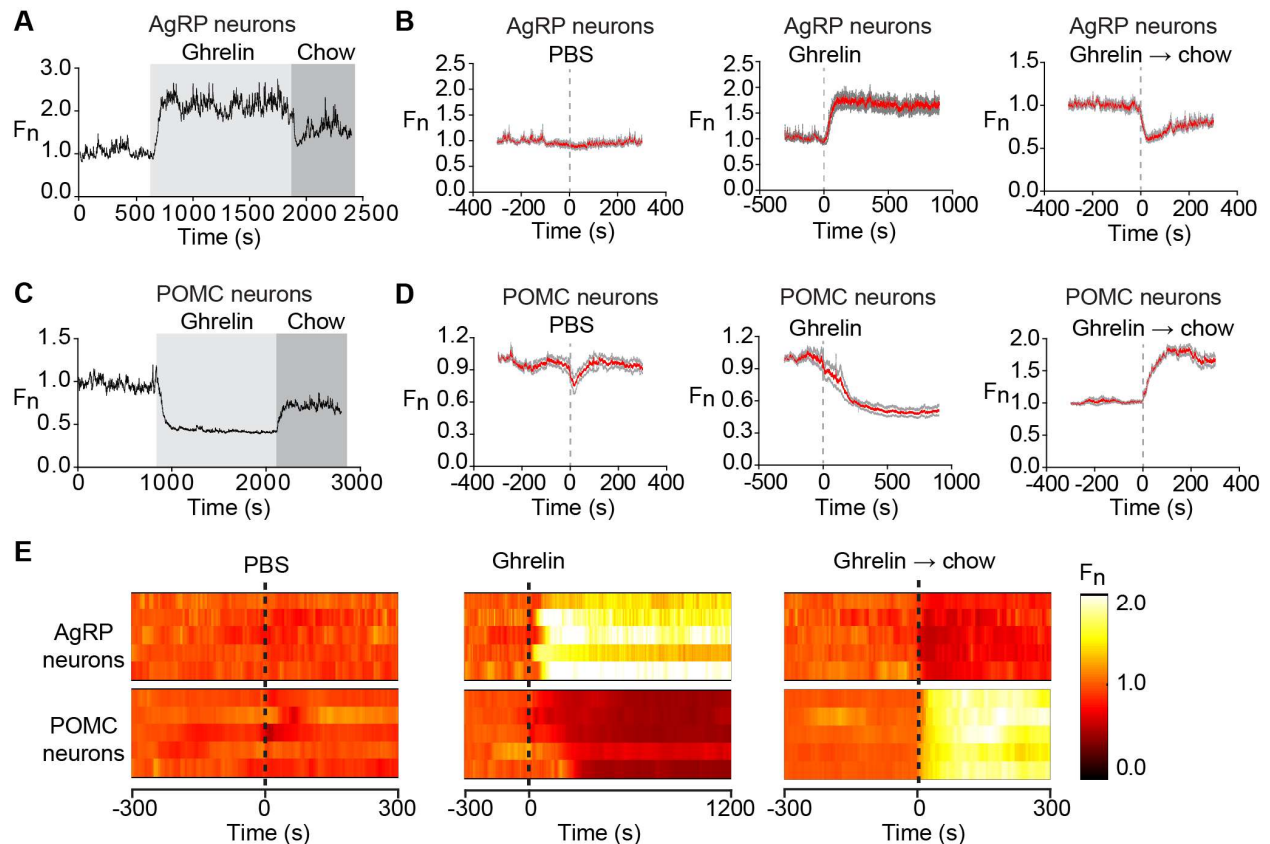


Figure 2.2. Ghrelin rapidly modulates AgRP and POMC neurons.

(A and C) Recordings from a mouse expressing GCaMP6s in AgRP or POMC neurons that was challenged with injection of ghrelin (light gray) followed by presentation of a pellet of chow (dark gray). **(B and D)** Calcium signals from AgRP and POMC neurons aligned to the time of PBS or ghrelin injection, or chow presentation to ghrelin treated mice. Red and gray indicate the mean response and standard error (AgRP, $n=7$; POMC, $n=5$). In each trial fluorescence was normalized by assigning a value of 1.0 to the median value of data points within a two minute window at -5 min before treatment. **(E)** Peri-event plots showing the response from a single trial of five AgRP mice and five POMC mice.

Food detection reverses the effects of fasting on AgRP and POMC activity

The regulation of AgRP and POMC neurons by sensory detection of food has not previously been described. To investigate this phenomenon under more physiologic conditions, we fasted mice overnight and then presented a pellet of chow. As observed for ghrelin-treated animals, food presentation to fasted mice strongly inhibited AgRP neurons ($\Delta F/F = -37 \pm 4\%$, at 5 min, $p < 0.001$ compared to object) and activated POMC neurons ($\Delta F/F = 38 \pm 5\%$ at 5 min, $p < 0.001$ compared to object; **Figure 2.3**). These responses began the moment that food was presented and were rapidly complete ($\tau = 20 \pm 4$ s for AgRP neurons and $\tau = 42 \pm 18$ s for POMC neurons). To quantify the extent to which these changes required food consumption, we analyzed video data to estimate the moment at which the first bite of food was consumed in each trial and then aligned calcium traces to this event. This revealed that most of the activity changes in these neurons were already complete by the time food intake was initiated ($96 \pm 6\%$ complete before feeding in AgRP neurons, $85 \pm 5\%$ in POMC neurons; **Figure 2.3H,I**). Thus the response of AgRP and POMC neurons to food is triggered primarily by food detection rather than food consumption. Of note, these stereotyped responses to food presentation were consistently observed in the first trial of each mouse (**Figure 2.3G**), indicating that this effect does not require prior training.

We investigated the determinants of this rapid response to food discovery. Presentation of an inedible object (a rubber stopper similar in size to a piece of chow) had little effect on the activity of AgRP neurons ($\Delta F/F = 4.9 \pm 2.2\%$) and induced a small change in POMC neurons in the opposite direction of food ($\Delta F/F = -10 \pm 2\%$). Thus the response of these neurons to food presentation is food-specific (**Figure 2.3**). The sensitivity of these cells to food presentation also depended on nutritional state, as AgRP neurons from *ad libitum* fed mice showed no response to food presentation ($\Delta F/F = -4.7 \pm 1.0\%$, $p = 0.21$ compared to object) whereas POMC neurons from *ad libitum* fed mice showed a greatly diminished response ($\Delta F/F = 4.7 \pm 2.4\%$, $p = 0.01$ compared to object; **Figure 2.3E,F**). Thus conditions that reflect energy deficit,

such as fasting or ghrelin treatment, potentiate the response of AgRP and POMC neurons to food detection.

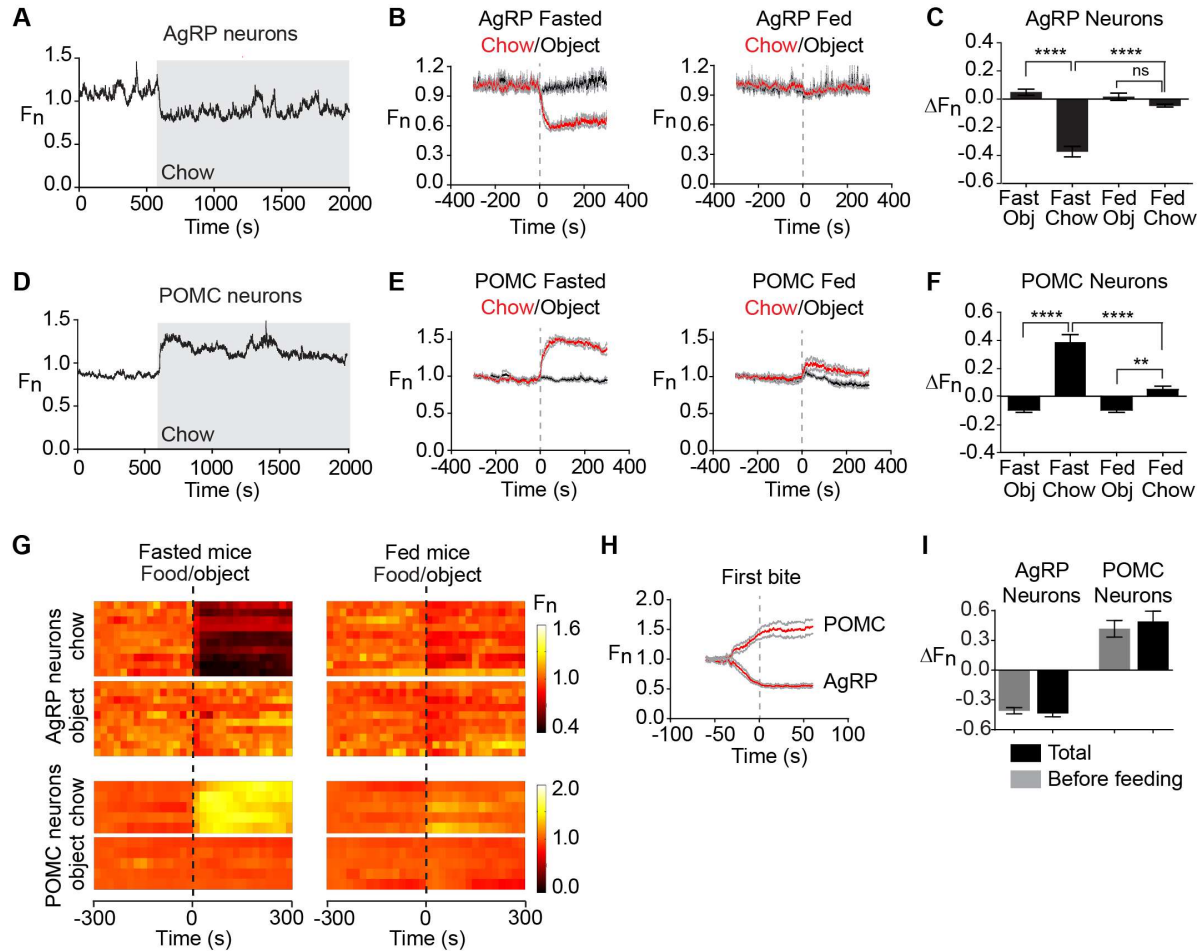


Figure 2.3. Sensory detection of food rapidly regulates AgRP and POMC neurons. (A and D) Recordings from fasted mice expressing GCaMP6s in AgRP or POMC neurons presented with a pellet of chow (gray). (B and E) Plots of calcium signals from AgRP and POMC neurons aligned to the time of presentation of a pellet of chow (red) or inedible object (black). Mice were either subjected to an overnight fast (left) or fed ad libitum (right) prior to experiment. Gray indicates standard error (AgRP, n=10; POMC, n=5). (C and F) Quantification of fluorescence changes 5 min after event, as indicated. (G) Peri-event plots aligned to the time of event. Each row is a single trial of a different mouse. (H) Calcium signals aligned to the initiation of feeding for AgRP and POMC neurons. (I) Quantification of change in fluorescence occurs before feeding is initiated versus the total change in the trial. * p<0.05, ** p<0.01, *** p<0.001, **** p<0.0001.

Food quality influences the magnitude of the response

We considered the possibility that the response of AgRP and POMC neurons to food presentation depends on the food's hedonic properties. In this regard sensory cues associated with palatable or energy dense foods trigger activation of brain regions involved in reward, but how this hedonic information is integrated with homeostatic signals remains poorly understood. To investigate this we first measured the response to peanut butter, an energy dense food that mice will eat in preference to chow and is considered rewarding. Mice were fasted overnight, acclimated to a behavioral chamber, and then presented with either pellet of chow or a dollop of peanut butter. Presentation of peanut butter strongly inhibited AgRP neurons ($\Delta F/F = -54 \pm 6\%$ at 5 min; **Figure 2.4A**) and activated POMC neurons ($\Delta F/F = 101 \pm 31\%$ at 5 min; **Figure 2.4C**). These responses began immediately upon food presentation and were complete in less than one minute ($\tau = 23 \pm 6$ s for AgRP and $\tau = 29 \pm 6$ s for POMC). The responses to peanut butter were significantly larger than the responses to chow (**Figure 2.4E**) and indeed were comparable in magnitude (but opposite in sign) to the effect of injection with pharmacologic doses of ghrelin (**Figure 2.4F**), which to our knowledge is the strongest known stimulus that modulates these cells.

A defining feature of palatable foods is that animals will consume them in the absence of hunger because they are intrinsically rewarding (e.g. eating dessert after a meal). We therefore tested whether AgRP and POMC neurons from *ad libitum* fed mice, which show little or no response to chow (**Figure 2.3**), would nonetheless respond to the presentation of peanut butter. Indeed we found that presentation of peanut butter to *ad libitum* fed mice strongly inhibited AgRP neurons ($\Delta F/F = -24\% \pm 4\%$, at 5 min, $p < 0.001$ compared to chow) and activated POMC neurons ($\Delta F/F = 55 \pm 11\%$, at 5 min, $p = 0.14$ compared to chow; **Figure 2.4A,C**). Thus more palatable food can modulate these neurons even in the absence of signals of energy deficit.

To further probe this relationship, we tested whether the response of these neurons to different foods depended on the order in which they were presented. Mice were fasted overnight and then sequentially presented with an inedible object, peanut butter, or chow in randomized order at 10 minute intervals. We then calculated the change in activity that occurred following each of these presentations. This revealed that presentation of peanut butter could completely block the subsequent neural response to presentation of chow (**Figure 2.4B,D**). By contrast, presentation of chow had no effect on the response to peanut butter in POMC neurons (**Figure 2.4D**) and only partially diminished the response in AgRP neurons (**Figure 2.4B**). The asymmetry in the response to these two foods is consistent with their differential effects in fasted and fed mice.

To extend these findings we tested a chocolate, a second food that is commonly used in rodent studies of reward. We found that presentation of chocolate (Hershey Kiss) to fasted mice inhibited AgRP neurons to a greater extent than chow (**Figure 2.9A**). Like peanut butter, chocolate also elicited a response in AgRP neurons from *ad libitum* fed mice that are unresponsive to chow (**Figure 2.9B**). Sequential presentation experiments revealed that chocolate could block the neural response to subsequent presentation of chow, but not vice versa, similar to our observations with peanut butter (**Figure 2.9D,E**). Although chocolate was a novel food for these animals, we observed responses to chocolate presentation in the first trial, indicating mice could identify it as food without prior experience. However the speed of the response to chocolate increased during subsequent tests, suggesting involvement of a learning process as well ($\tau = 40 \pm 8$ s in trial 1 versus 17 ± 2 s in trial 4, $p < 0.01$; **Figure 2.9C**). Collectively these data show that the rapid sensory regulation of AgRP and POMC neurons contains information about the hedonic properties of the food that has been detected.

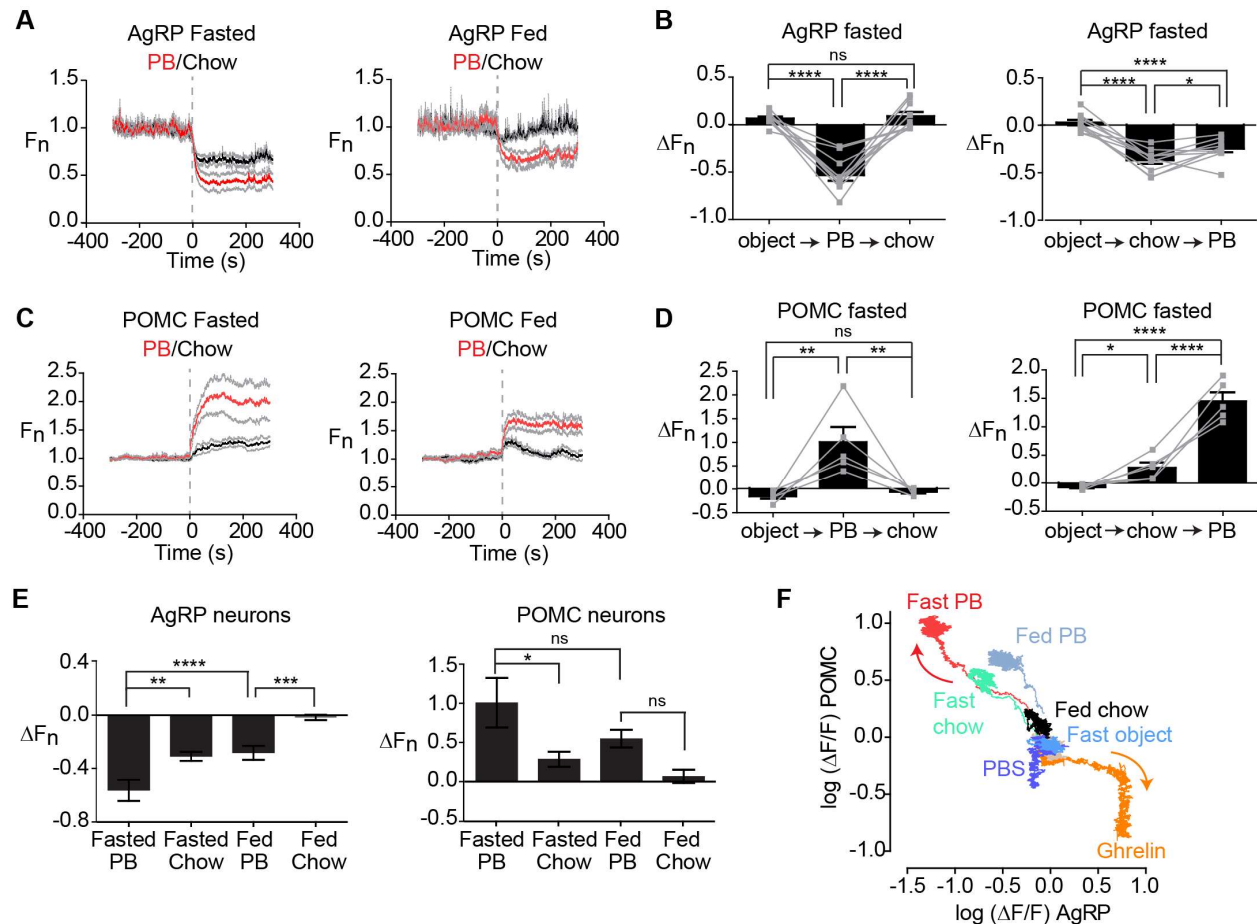


Figure 2.4. Food palatability determines the magnitude of the response to food detection. (A and C) Calcium signals from AgRP and POMC neurons in fasted and fed mice aligned to the time of presentation of peanut butter or chow. (B and D) Fluorescence change of AgRP and POMC neurons upon sequential presentation of an inedible object, chow, and peanut butter in fasted mice. (E) Quantification of responses of AgRP and POMC neurons 5 min after food presentation. (F) Plot showing the response of AgRP and POMC neurons over 5 min to different foods and pharmacologic treatments in the context of varying nutritional states. All traces start at the origin (0,0) and emanate outward. Arrows indicate the direction of movement. See also Figure S2.

Food accessibility modulates the response to food discovery

Most of the response of AgRP and POMC neurons to food presentation occurred before food intake was initiated (Figure 2.3H,I). We therefore wondered whether food consumption played any role in this response. To test this mice were fasted overnight and then presented with peanut butter in a container that allowed the food to be seen and smelled but not consumed (Figure 2.5A). Presentation of this inaccessible peanut butter rapidly activated

POMC neurons ($\Delta F/F = 43 \pm 9\%$ after 2 min; $\tau = 31 \pm 8\text{s}$) and inhibited AgRP neurons ($\Delta F/F = -39 \pm 4\%$ after 2 min; $\tau = 21 \pm 4\text{s}$; **Figure 2.5B,C**). Similar responses were observed in mice pretreated with ghrelin (**Figure 2.10A,B**). These responses occurred as quickly as the response to accessible food, but were somewhat smaller in magnitude (**Figure 2.10C,D**) and the response of POMC neurons was less durable (**Figure 2.5B,C**). This indicates that food accessibility can modulate the strength of the response to food presentation.

To further dissect this effect we tested whether an isolated sensory cue could modulate the activity of these two cell types. As mice rely heavily on the sense of smell, we tested whether the smell of peanut butter could elicit an activity change in AgRP and POMC neurons. Mice were fasted overnight and then exposed to peanut butter placed underneath the cage in a covered container so that it could be smelled but not seen or accessed (**Figure 2.5D**). We found that this “hidden peanut butter” rapidly modulated AgRP and POMC neurons in a way that resembled food presentation ($\Delta F/F = -12 \pm 5\%$ after 1 min in AgRP neurons and $\Delta F/F = 17 \pm 6\%$ after 1 min in POMC neurons; **Figure 2.5E,F**). However this effect was much smaller in magnitude and transient, with neural activity returning to baseline within eight minutes ($\Delta F/F = 8.3 \pm 4.5\%$ after 8 min in AgRP neurons and $\Delta F/F = -3.0 \pm 4.0\%$ after 8 min in POMC neurons; **Figure 2.5F and 2.10**). Together these data suggest that food-associated sensory cues can modulate these two cell types, but that the magnitude and durability of this response depends on the extent to which these cues are interpreted as representing access to food.

Food removal reverses the effects of food presentation

The response of AgRP and POMC neurons to food presentation is consistent with a model in which these neurons anticipate the change in their activity that will occur after food consumption and then enact this change in advance, taking into account factors such as the food’s energy density, the food’s accessibility, and the animal’s nutritional state. A prediction of this model is that the response to food presentation should be reversed if the food is removed

before it can be consumed. To test this mice were fasted overnight, presented with accessible chow, and then the food was removed after either a 2, 10, or 30 minute interval. As predicted we found that food removal reversed the effects of food presentation, resulting activation of AgRP neurons and inhibition of POMC neurons (**Figure 2.5G, J**; for clarity only data after 2 and 10 min removal are shown). The magnitude and kinetics of this reversal depended on the duration that mice were given food access. For example, mice given access to food for 30 minutes showed a smaller reversal of AgRP and POMC neuron activity following food removal than mice given access to food for 2 or 10 minutes (**Figure 2.5H, K**). Extended food access also slowed the response to food removal in AgRP but not POMC neurons (**Figure 2.5I, L**). These findings are consistent with food consumption during the feeding interval partially resetting the activation state of these neurons.

The response to food removal exhibited hysteresis, occurring approximately ten-fold more slowly than the initial response to food presentation (**Figure 2.5I, L**). This asymmetry was observed after only 2 min food access in both AgRP ($\tau=15 \pm 1$ s versus 258 ± 26 s, $p<0.0001$) and POMC neurons ($\tau=19 \pm 3$ s versus 269 ± 66 s, $p=0.03$) and therefore was unlikely to be caused by the post-ingestive effects of food consumption. Rather this suggests that the circuit interprets the sensory detection of food in such a way that food removal induces a more gradual change than food discovery.

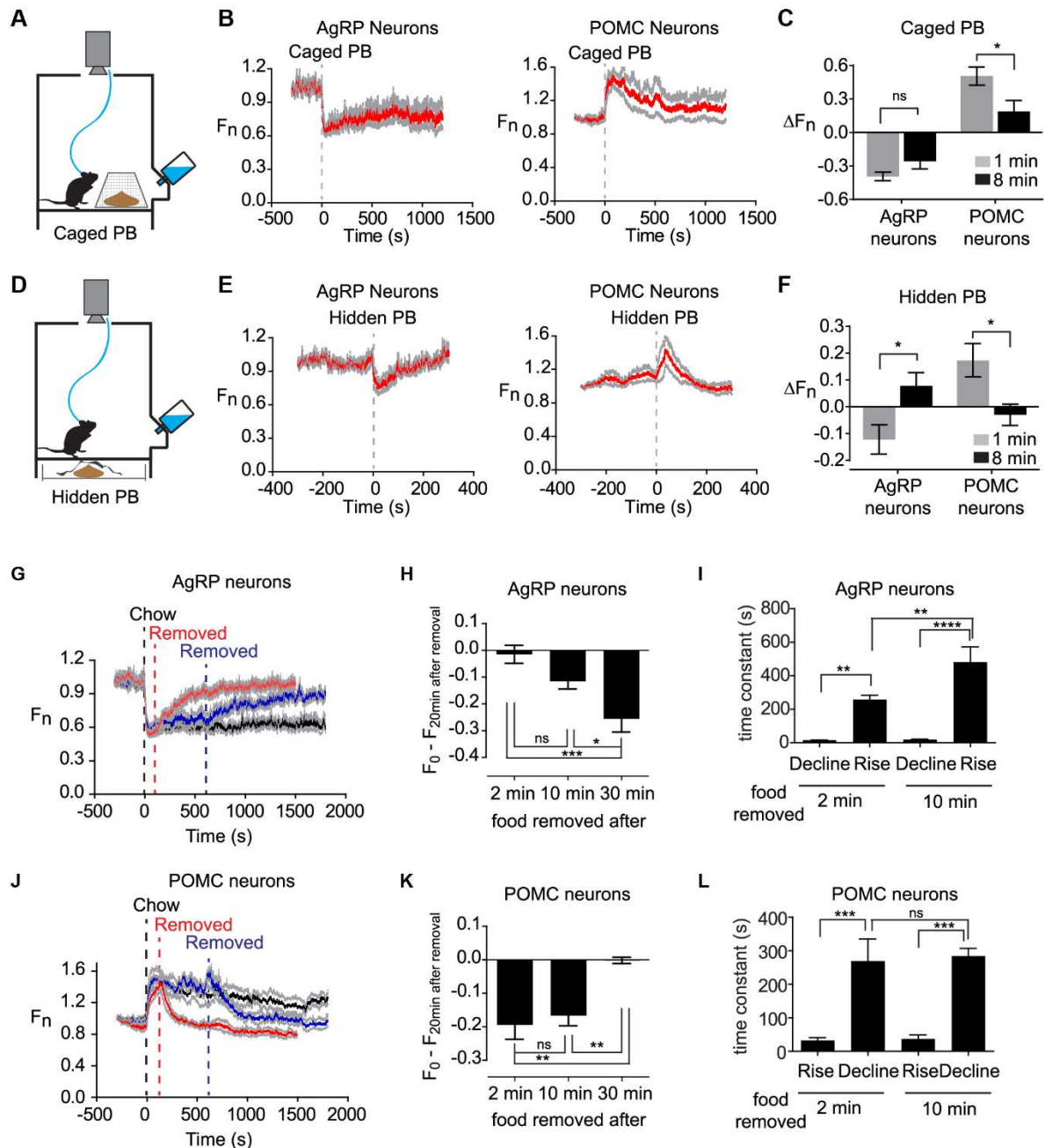


Figure 2.5. The response to food detection depends on food accessibility and is reversible. (A) Schematic of caged peanut butter. (B) Calcium signals aligned to the time of presentation of a caged peanut butter. (C) Change in fluorescence in 1 and 8 min after caged peanut butter presentation. (D) Schematic of hidden peanut butter. (E) Calcium signals aligned to the time of presentation of a hidden peanut butter. (F) Change in fluorescence in 1 and 8 min after hidden peanut butter presentation. (G and J) Chow was presented at time 0, and then food was removed at 2 min (red), 10 min (blue) or not removed (black). (H and K) Recovery in fluorescence 20 min after food removal for experiments in which food was removed after 2, 10, or 30 min. (I and L) Time constant for the response to upon food presentation and food removal after 2 and 10 min. See also Figure S3.

Neural dynamics within feeding bouts

We have focused on the initial response of AgRP and POMC neurons to food presentation, because this response is much larger than the fluctuations in the activity of these neurons that occur during feeding (**Figure 2.3A,D**). However we considered the possibility that these smaller intrameal dynamics might also be correlated with components of behavior. To test this we switched to a system in which mice were fed a liquid diet (vanilla Ensure) via a lickometer, so that we could align individual feeding bouts to photometry data with millisecond precision.

Mice were transitioned from a solid to liquid diet over several days, then fasted overnight and tested in an one hour trial. Licks were aligned to photometry traces, and individual feeding bouts defined as clusters of licks separated from their nearest neighbor by >20 seconds. This resulted in identification of an average of 17 +/- 2 feeding bouts in each one hour trial, with each bout lasting an average of 17 +/- 3 seconds and containing 53 +/- 10 licks. The start of each bout in a representative trial is indicated by gray lines in **Figure 2.6A, B**.

We compared the average activity of these neurons during active feeding (inrabout) versus intermeal intervals (interbout), by calculating the difference in fluorescence between these stages (interbout - intrabout). This revealed that POMC neurons were more active during feeding whereas AgRP neurons were less active ($\Delta F/F = 0.042 \pm 0.011$ for AgRP versus $\Delta F/F = -0.029 \pm 0.004$ for POMC, $p = 0.001$; **Figure 2.6C**). To investigate the dynamics underlying these differences, we aligned each feeding bout so that the start of the bout (first lick) corresponded to time zero and then analyzed a ten-second window flanking this moment. We found that AgRP and POMC neurons showed a consistent pattern of activity that predicted the onset of each meal. AgRP neurons declined in activity until the moment of the first lick and then their activity flattened (**Figure 2.6D**) whereas POMC neurons increased in activity prior to and throughout the start of feeding (**Figure 2.6E**). Cross-correlation analysis between AgRP and

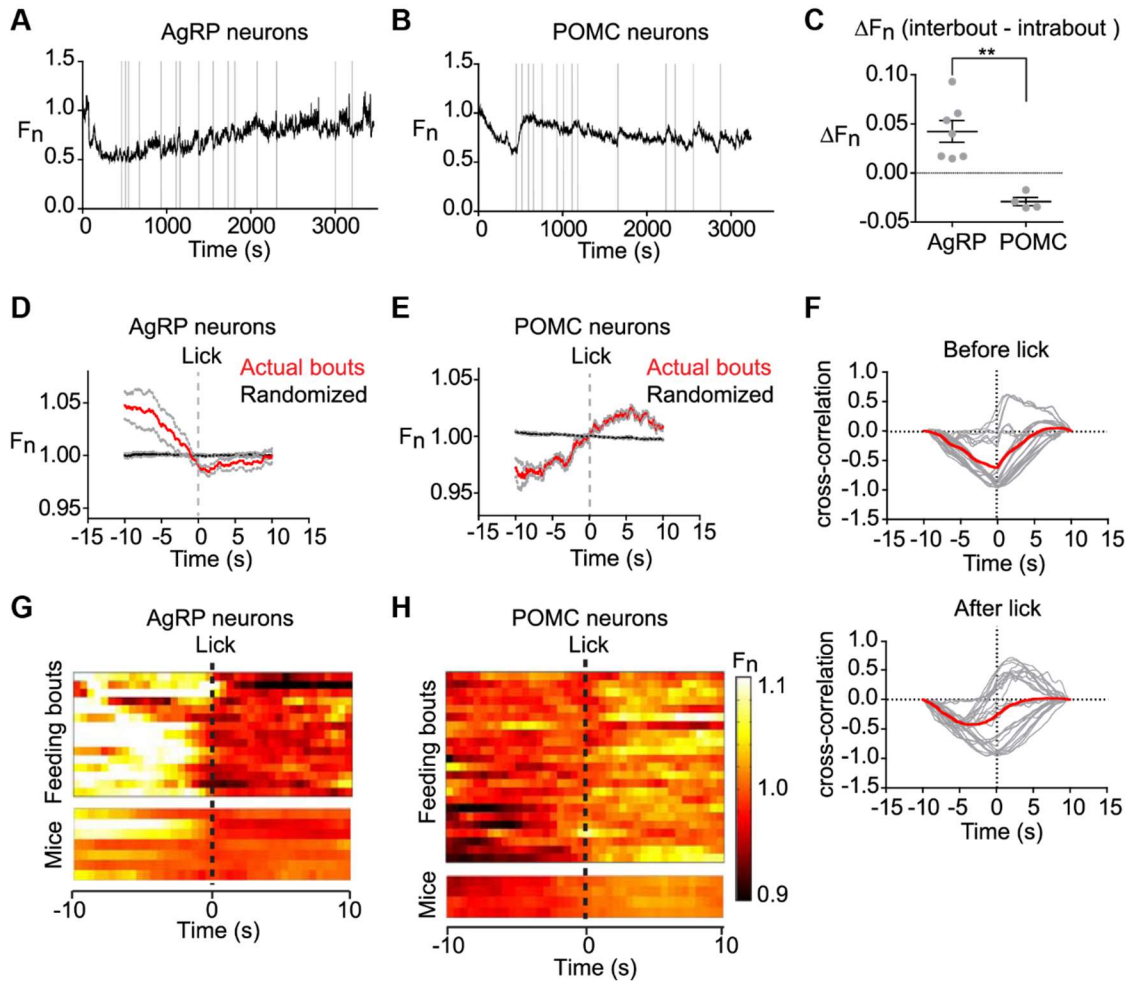


Figure 2.6. Intrameal dynamics of AgRP and POMC neurons.

(A and B) Traces of AgRP and POMC activity in mice during consumption of a liquid diet. Licks that mark initiation of a feeding bout are shown in gray. (C) Difference in average fluorescence between periods of feeding (intrabout) and intermeal intervals (interbout) for each mouse. (D and E) Calcium signals from AgRP and POMC neurons aligned to the moment of the first lick that initiates a feeding bout. Data from actual feeding bouts shown in red; data from simulated randomly generated feeding bouts in black. (F) Cross-correlation plots showing the correlation between activity of AgRP and POMC neurons before and after licking. Red is mean, gray is 28 individual comparisons between AgRP (n=7) and POMC (n=4) mice. (G and H) Peri-event plots showing the activity of AgRP and POMC neurons aligned to the start of feeding bouts. The top plot shows all of the bouts for one trial of a mouse. The bottom plot shows the average response across all bouts for 7 AgRP and 4 POMC mice.

POMC showed that there was an inverse correlation between the activity of these two cell types that reached a peak at approximately time zero (**Figure 2.6F**). These effects were tightly linked to behavioral state, as they were robust to changes in the definition of a feeding bout (e.g. changes in the minimum intermeal interval) yet were completely absent when the data was re-analyzed using randomly generated feeding bouts (**Figure 2.6D,E black**). Remarkably, these intrameal anticipatory changes in AgRP and POMC activity appear to recapitulate, on a smaller scale, the dramatic changes in activity that occur in these neurons in response to food presentation.

Dynamics of AgRP projections to the PVH

AgRP neurons project broadly to brain regions involved in the control of food intake in a primarily one-to-one configuration (Betley et al., 2013). Optogenetic experiments have identified AgRP projections to the PVH as being particularly important for the control of feeding (Atasoy et al., 2012). As fiber photometry enables direct monitoring of axonal calcium transients (Gunaydin et al., 2014), we sought to record the activity of these key AgRP (ARC → PVH) projections during behavior.

AAVs expressing Cre-dependent GCaMP6s were delivered to the ARC of AgRP-IRES-Cre mice and in the same surgery an optical fiber was implanted ipsilaterally in the PVH (**Figure 2.7A**). Photometry recordings four weeks after surgery revealed spontaneous synchronous activity in these projections (**Figure 2.7B**) that resembled calcium dynamics observed in AgRP cell bodies (**Figure 2.1H**), albeit somewhat smaller in magnitude. Intraperitoneal injection of ghrelin but not vehicle induced a rapid increase in calcium signals in these projections ($\Delta F/F = 17 \pm 5\%$ for ghrelin versus $-9 \pm 3\%$ for PBS at 5 min, $p=0.02$; **Figure 2.11**), indicating that they are appropriately regulated by hormonal signals.

We next tested the effect of food presentation. Mice were fasted overnight and then presented with either an inedible object, chow, or peanut butter. Presentation of either chow or

peanut butter rapidly and potently inhibited calcium dynamics in AgRP (ARC → PVH) projections ($\Delta F/F = -30 \pm 2\%$ for peanut butter versus $-21 \pm 3\%$ for chow at 5 min) whereas presentation of an inedible object had no effect (**Figure 2.7C,E**). Of note, peanut butter almost completely eliminated detectable synchronous activity in PVH axons (**Figure 2.7B, C**), suggesting that palatable food presentation is particularly potent in suppressing the activity of this pathway. Assays utilizing sequential food presentation revealed a pattern of responses in PVH projections that closely resembled responses observed in AgRP cell bodies (**Figure 2.7D, F**). Likewise chow presentation partially reversed the activation of these PVH projections by ghrelin (**Figure 2.11**).

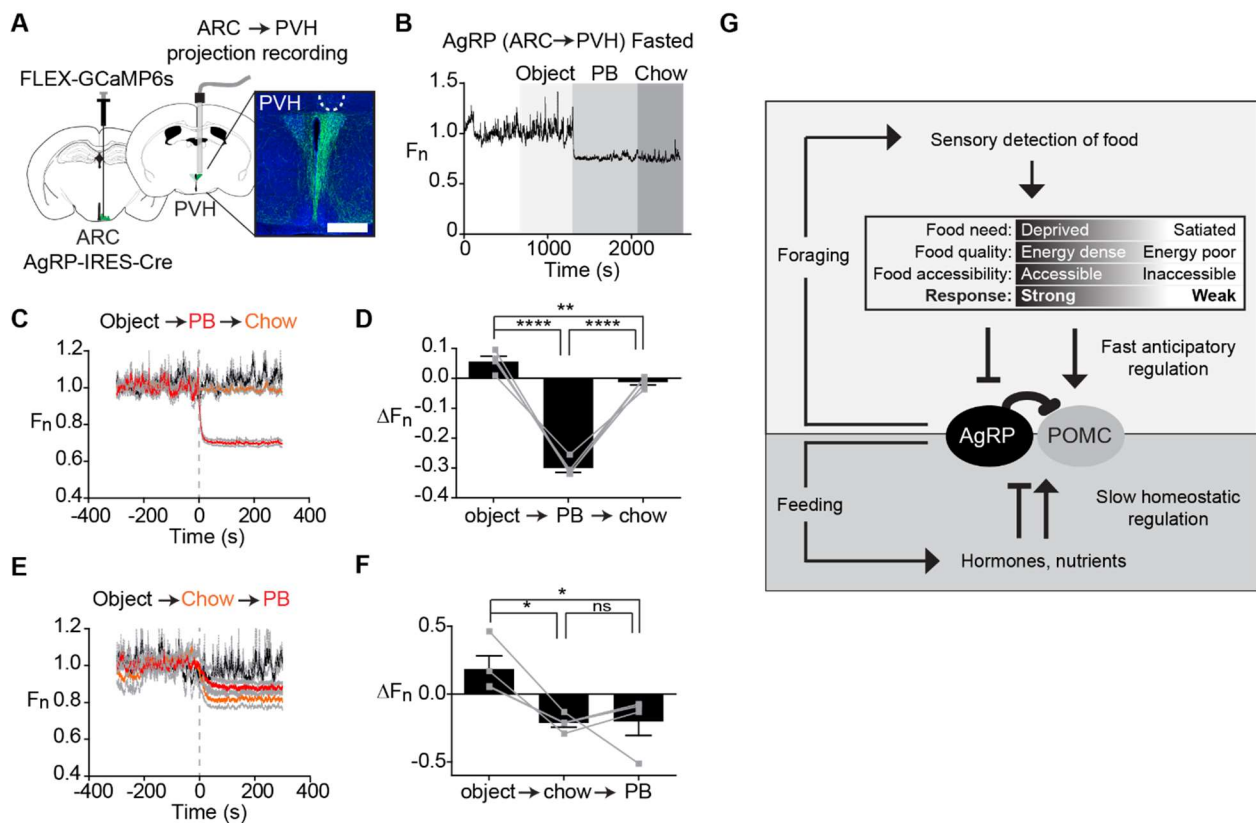


Figure 2.7. Natural dynamics of AgRP projections to the PVH.

(A) Schematic showing infection of cell bodies in the ARC and installation of optical fiber in the PVH. Scale bar = 0.5 mm (B) Recording from PVH of a fasted mouse presented sequentially with an inedible object, peanut butter, and chow. (C and E) Calcium signals from from PVH of mice presented sequentially with an inedible object, peanut butter, and chow. (D and F)

Quantification of calcium signals five minutes after event. (n=4 mice). **(G)** Model for regulation of AgRP and POMC neurons by homeostatic and sensory information. See also Figure S4. Thus the activity of AgRP (ARC → PVH) projections is regulated by ghrelin and food presentation in a way that mirrors the population response in the ARC.

DISCUSSION

It has been known for more than 75 years that the hypothalamus plays a critical role in the control of food intake (Hetherington and Ranson, 1939), yet the dynamics of the hypothalamic circuits that give rise to feeding behavior have remained a mystery. Here we have used an optical approach to record the natural dynamics of the two most widely-studied cell types that control feeding, AgRP and POMC neurons, in awake behaving mice. These experiments have revealed unexpectedly that these neurons are potently regulated by the sensory detection of food. This rapid regulation resets the activation state of AgRP and POMC neurons induced by orexigenic signals such as ghrelin or fasting. The magnitude and robustness of this response suggests that it is a primary mechanism that controls the activity of these neurons *in vivo*. The speed of this response suggests that it is likely mediated by neural input. The dependence on food palatability suggests that this response contains information about the food's hedonic properties or energy content, possibly through a learned association with smells or other sensory cues. Collectively, these findings reveal that AgRP and POMC neurons receive real-time information about the availability of food in the external world, which they then integrate with homeostatic signals arising from the body (**Figure 2.7G**). This demonstrates a more complex and dynamic role for these circuits in the control of feeding behavior than is currently appreciated.

Sensory feedback enables rapid inhibition of appetitive processes

The rapid sensory regulation of AgRP and POMC neurons is counterintuitive, since it appears to “short circuit” their well-established function as interoceptive sensors of nutritional

state. In this model energy deficit activates AgRP neurons and inhibits POMC neurons, thereby generating a motivational drive that promotes food intake and is only relieved when energy stores are replenished. An assumption of this model is that internal signals generated during feeding (e.g. accumulation of circulating nutrients or hormones) are responsible for resetting the activation state of these neurons and thereby reducing the drive to eat.

Our data by contrast show that food detection alone rapidly resets the activity of these two cell types and that this resetting precedes the onset of actual food consumption. This is surprising in light of the fact that stimulation of AgRP neurons is sufficient to promote food intake (Aponte et al., 2011; Krashes et al., 2011). However, our data also show that if food is removed before it can be consumed, then these neurons revert to their activity level prior to food presentation (**Figure 2.5G,J**). We have likewise found that inaccessible food induces smaller and less durable changes in AgRP and POMC neuron activity (**Figure 2.5C,F**). Together these findings suggest that food detection modulates AgRP and POMC neurons in a way that anticipates the change in their activity that will occur following food consumption, taking into account factors such as the food's energy density, perceived accessibility, and the nutritional state of the mouse (**Figure 2.7G**).

What is the purpose of this anticipatory regulation? We propose that it represents a mechanism to rapidly inhibit foraging and other appetitive behaviors once food has been discovered (**Figure 2.7G**). In this regard activation of AgRP neurons induces not only food consumption but also motivational processes that drive food obtainment, including dramatic foraging behavior and a willingness to work for food (Atasoy et al., 2012; Krashes et al., 2011). These appetitive processes are blocked by food discovery as part of the natural transition from foraging to feeding, but the mechanisms by which this transition is regulated have not been described. Our data show that food discovery results in rapid feedback inhibition of AgRP neurons themselves, rather than some downstream circuit element, which provides a direct mechanism to inhibit foraging once food has been obtained. The fact that this feedback occurs

at the level of AgRP neurons is surprising and suggests that the activity of these neurons is particularly important for generating the motivation to search for food relative to other aspects of feeding behavior.

Models for AgRP driven food consumption

The natural dynamics of AgRP neuron activity are consistent with a primary function for these neurons in regulating appetitive behaviors that promote food discovery. Yet multiple lines of evidence have suggested a role for these neurons in controlling food consumption as well. We discuss below two possible mechanisms by which AgRP neurons could drive food intake that are consistent with our data.

Subpopulations of AgRP neurons with specialized functions: A limitation of fiber photometry is that it measures the average activity of a population of a neurons, which can mask heterogeneity in the responses of individual cells. AgRP neurons that project to different downstream targets differ in their ability to induce food intake and in their expression of the leptin receptor (Atasoy et al., 2012; Betley et al., 2013; Wu et al., 2012). It is therefore unlikely that all AgRP neurons show identical responses to stimuli such as hormone challenge or food presentation. One possibility is that a subset of AgRP neurons are activated, rather than inhibited, by food presentation, and that this subpopulation of AgRP neurons is responsible for driving food consumption. Testing this possibility will require measuring the single-cell dynamics of AgRP neurons during behavior, using approaches such as optogenetic phototagging combined with *in vivo* recording (Lima et al., 2009) or fluorescence microendoscopic imaging (Ziv et al., 2013).

While future experiments are likely to uncover additional heterogeneity in these cells, three observations argue against this heterogeneity being the primary explanation for how AgRP activity drives food consumption. First, the magnitude of the decrease in AgRP calcium dynamics that we observe following food presentation, particularly for palatable foods (**Figure**

2.4F), is inconsistent with a major subset of these neurons having the opposite regulation. Therefore if some AgRP neurons are activated during feeding, they must represent a minority of the population. Second, our analysis of AgRP dynamics during individual feeding bouts reveals that AgRP activity declines immediately preceding meal initiation and then is relatively flat during the course of food intake (**Figure 2.6D**). These intrameal dynamics are not what would be predicted for a neuron whose activity directly drives food consumption. Third, and most importantly, we have shown that food presentation potently inhibits AgRP projections to the PVH (**Figure 2.7**). Optogenetic experiments have strongly implicated these ARC → PVH projections in the control of food intake (Atasoy et al., 2012; Betley et al., 2013). The fact that these PVH projections show the same activity pattern as the population as a whole argues that projection-specific dynamics are unlikely to be the primary explanation for how these neurons can drive feeding.

Learning mediated by AgRP activity: An alternative possibility is that AgRP neurons drive food consumption indirectly via a learning process. In this regard we have shown that the inhibition of AgRP activity following food discovery is contingent on subsequent food intake, since this inhibition is reversed if the food is removed before it can be consumed (**Figure 2.5G**). If AgRP activity has negative motivational valence (analogous to the unpleasant sensation of hunger), then this might enable animals to learn the consequences of failing to eat after obtaining food. In this model food discovery would temporarily relieve the sensation of hunger, but animals would learn through experience that this sensation returns if the food is not consumed. Over time this would result in appetitive and consummatory aspects of feeding becoming linked in sequence, so that food discovery is always followed by food intake, even though AgRP activity itself would largely be extinguished before the onset of feeding. Alternative models based on negative reinforcement and learning are also conceivable, and untangling these possibilities will be an important area for future investigation.

Neural input into AgRP and POMC neurons communicates the discovery of food

AgRP and POMC neurons receive abundant neural input and indeed the activation of AgRP neurons by fasting is mediated primarily by increased excitatory tone (Liu et al., 2012; Yang et al., 2011). Yet most studies of these cells have focused on the role of hormones and nutrients, and the role of this afferent neural input has remained unclear. Our data indicate that one function of this neural input is to communicate to AgRP and POMC neurons the discovery of food. This is appealing because it demonstrates a function for this synaptic input that extends beyond merely serving as a redundant source of homeostatic information. The fact that the strength of this neural input varies depending on the hedonic properties of the detected food suggests that, at some level, the upstream circuit encodes an association between sensory information and the food's nutritional content (i.e. a "food memory"). Identification of the neural substrate of this association may provide an entry point into the study of the maladaptive associations between sensory cues and food that develop in some eating disorders. As several cell types that provide input into AgRP neurons have recently been identified (Krashes et al., 2014), it should be possible to elucidate this afferent pathway using modern circuit mapping techniques.

Information processing by arcuate feeding circuits

Feeding is influenced by diverse types of signals including sensory, hedonic, homeostatic, and visceral cues. A longstanding question has been whether there exists a site in the brain where the neural circuits that sense these signals converge, thereby enabling integration of this information into a single decision to eat or not to eat (Friedman, 2014). The arcuate nucleus in this model is traditionally viewed as a sensor for homeostatic cues, which it then relays to higher centers where more complex integration occurs. This viewpoint is encapsulated in the fact that AgRP and POMC neurons are often described as "first order"

neurons, analogous to primary sensory afferent neurons such as rods and cones in the visual system.

A complication for this model as mentioned previously is that AgRP and POMC neurons are strongly regulated by neural input and therefore are not merely sensors of circulating nutritional signals. However absent an understanding of the function of this afferent input it has not been possible to assemble a complete picture of the role of these cells. The discovery that this input contains information about the sensory and hedonic properties of food reveals that these long-studied neurons themselves integrate multiple types of food-related information and indeed may represent a key convergence point in the feeding circuit. The further application of new methods for recording cell-type-specific neural activity is likely to provide additional insight into how this complex integration is achieved.

METHODS

Animals

AgRP-ires-Cre (#012899) and POMC-Cre (#005965) mice were obtained from Jackson laboratories and POMC-Cre mice backcrossed onto a C57Bl/6J background. All animals were singly housed on a 12h light/dark cycle and given ad libitum access to chow (PicoLab Rodent Diet 5053) and water. Mice were 6-8 weeks old at the time of surgery. For studies of AgRP neurons a combination of male and female mice were used and no differences between sexes were observed. Male mice were used for studies of POMC neurons. All experimental protocols were approved by the University of California, San Francisco IACUC following the National Institutes of Health guidelines for the Care and Use of Laboratory Animals

Virus

Recombinant AAV expressing GCaMP6s (AAV1.Syn.Flex.GCaMP6s.WPRE.SV40: titer: 1.03E+13) was purchased from Penn Vector Core (Gene Therapy Program, University of Pennsylvania School of Medicine).

Stereotaxic Viral Injection and Cannula Implantation

Animals were anesthetized with 2% isoflurane and placed in a stereotaxic head frame on a heat pad. Ophthalmic ointment was applied to the eyes and a subcutaneous injection of carprofen (10 mg/kg) was given to each mouse prior to surgery and one day after. The scalp was shaved, local anesthetic applied (lidocaine, 0.5%), and then incised through the midline. A craniotomy was made using a dental drill (0.5 mm). A Nanofil Hamilton syringe (2 μ L; WPI, Sarasota, FL) with a 26 gauge beveled metal needle was used to infuse virus. Virus was infused at a rate of 100 nL per min. Following infusion, the needle was kept at the injection site for 10min and then slowly withdrawn. AgRP-ires-Cre mice were injected with a total of 1 μ L of virus at two sites in the ARC (-1.85 mm anteroposterior (AP); -0.3 mm mediolateral (ML); 5.7 or 5.8 mm dorsoventral (DV) relative to bregman). POMC- Cre mice were injected with a total of 1 μ L of virus at two sites in the ARC (-1.75 mm AP; -0.3 mm ML; 5.7 and 5.8 mm dorsoventral DV).

Photometry cannulas were implanted after virus injection in the same surgery. For somatic recording in AgRP-ires-Cre mice, photometry cannulas were placed in the ARC (-1.85 mm AP; -0.3 mm ML; 5.7 mm DV relative to bregma). For somatic recording in POMC-Cre mice, photometry cannulas were placed in the ARC (-1.75 mm AP; -0.3 mm ML; 5.7 mm DV). For PVH recordings in AgRP-ires-Cre mice, photometry cannulas were targeted to the PVH using an angled injection (5°) with the coordinates (-0.65 mm AP; -0.75 mm ML; -4.5 mm DV relative to bregma). Photometry cannulas were secured to the skull using a thin base layer of vetbond (Santa Cruz Biotechnology, sc-361931) and adhesive dental cement (a-m systems 525000 and 526000). The incision was closed with vetbond and animals were given a subcutaneous

injection of buprenorphine (0.05 mg/kg) prior to recovery over a heat pad. Mice were monitored daily for wound healing, food intake and body weight, and allowed to recover for a minimum of two weeks before the initiation of photometry experiments.

Immunohistochemistry

Mice were transcardially perfused with PBS followed by formalin. Brains were postfixed overnight in formalin and placed in 30% sucrose for 2 days. Free floating sections (40 μ m) were prepared with a cryostat, blocked (3% BSA, 2% NGS and 0.1% Triton-X in PBS for 2 h), and then incubated with primary antibody (chicken anti-GFP, Abcam, ab13970, 1:1000) overnight at 4°C. Samples were washed, incubated with secondary antibody (goat anti-chicken Alexa 488 secondary antibody; Invitrogen, 1:500) for 2h at room temperature, and then coverslipped and imaged by confocal microscopy to confirm GCaMP6s expression localized to the arcuate nucleus.

For histology (Figure 2.8), all images were taken in the same day with the same microscope settings. The images were converted to a heatmap of pixel intensity using MATLAB. Photometry cannula location was estimated by examining slices with visible fiber tract. As most of those slices were damaged, the intact slices that were closest to the cannula in the rostral-caudal axis were used for Figure 2.8 and the cannula tract was drawn.

Fiber Photometry

A rig for performing fiber photometry recordings was constructed following basic specifications previously described (Gunaydin et al., 2014) with minor modifications. A 473 nm laser diode (Omicron Luxx) was used as the excitation source. This was placed upstream of an optic chopper (Thorlabs MC2000) that was run at 400 Hz and then passed through a GFP excitation filter (Thorlabs MF469-35). This signal was then reflected by a dichroic mirror (Semrock FF495-Di03-25x36) and coupled through a fiber collimation package (Thorlabs F240FC-A) into a home-

made patchcord made with optical fiber (400 μ m, 0.48 NA; Thorlabs BFH48-400). This patchcord was then linked to a home-made implant fiberoptic (Thorlabs BFH48-400, CF440-10) through ceramic splitting sleeve (Thorlabs ADAF15). Fluorescence output was filtered through a GFP emission filter (Thorlabs MF525-39) and focused by a convex lens (Thorlabs LA1255A) onto a photoreceiver (Newport 2151). The signal was output into a lock-in amplifier (Stanford Research System, SR810) with time constant at 30 ms to allow filtering of noise at higher frequency. Signal was then digitized with LabJack U6-Pro and recorded using software provided by LabJack (<http://labjack.com/support/software>) with 250Hz sampling rate.

Optical fibers and cannulas were prepared using multimode fiber with 400 μ m core (Thorlabs BFH48-400) that was stripped with a fiber stripper, lightly scored by a fiber optic scribe (Thorlabs S90R), pulled off by hand using bare fiber gripper (Thorlabs BFG1) to create an optical fiber with length suitable for implant. The ends of the fiber were then inspected by fiber inspection scope (Thorlabs FS200) and only fibers with at least one end having >90% smooth surface were used. Each optical fiber was then inserted into a ceramic ferrule (Thorlabs CF440-10). Fiber epoxy (F112) was applied to both end and allowed to cure for 24 h at room temperature. The next day each fiber was polished with a set of aluminum oxide lapping (polishing) sheets with grit ranging from 5 μ m to 0.3 μ m and a polishing disk (Thorlabs Fiber Polishing Supplies). Each implant cannula was then inspected again with a fiber inspection scope and test with photometry laser before used for implant to check autofluorescence and fluorescence attenuation.

Behavior

All experiments were performed in behavioral chambers (Coulbourn Instruments, Habitest Modular System) and video recorded using infrared cameras installed above each cage. To synchronize the video to the photometry data, we used an infrared light controlled by an

environmental control board (Coulbourn Instruments, Habitest Modular System) to send a 5 ms pulse passing through a TTL converter (Coulbourn Instruments H03-14) into the same DAQ used for fluorescence recording every time it flashes.

All experiments were performed at the beginning of the dark cycle (CT12 – CT14) to control for circadian factors and performed in a dark environment with illumination of red or infrared light. Mice were acclimated to the behavioral chamber for at least 15 min prior to the beginning of each testing session.

Hormone injection: Ghrelin (Tocris, 1465) was dissolved in PBS to stock concentration (1 mg/mL), aliquoted and stored at -80 C until use. Mice were removed from the behavioral chamber, given an intraperitoneal injection of ghrelin (60 μ g/mouse) or vehicle (PBS) in a total volume of 200 μ L and then returned immediately to the chamber. For peristimulus plots the time injection was defined as the moment that the mouse was returned to the cage as determined by video recording.

Food and object presentation: To eliminate any effects of novelty mice were exposed prior to testing to an inedible object (black rubber stopper) and peanut butter. In the basic experiment mice were either fasted overnight (16 h) or fed ad libitum, acclimated to the behavioral chamber, and then either a pellet of chow (PicoLab 5053), dollop of peanut butter, or object were placed in the cage. In sequential presentation experiments these items were presented at 10 min intervals without removing the prior object from the cage. In removal experiments the pellet of chow was removed at the times indicated. For peristimulus plots time zero was defined as the moment that the experimenters hand became visible in video recording to open the cage and deliver the food object. The time of the initiation of feeding was estimated by analysis of video data. Hershey Kisses milk chocolate was used in the chocolate experiments.

Lickometer assay: Mice were habituated to a liquid diet (Ensure vanilla flavor) for 3 days prior to the experiment. Liquid diet was prepared fresh every day during habituation or for experiments. Mice were fasted overnight, acclimated to the behavioral chamber for 15 min, and then a bottle filled with liquid diet was plugged into the lickometer system and the trial was run for 1h. Signal detected by lickometer was translated into a 1 ms TTL pulse by a TTL converter (Coulbourn Instruments H03-14) and Graphic State 4 software (Coulbourn Instrument). The TTL pulses were sent to the DAQ and then aligned to photometry traces.

Slice Physiology

Acute Hypothalamic Slice Preparation and Slice Electrophysiology

Hypothalamic slices were prepared from 8- to 15-week-old AgRP-ires-Cre and POMC-ires-Cre mice with recombinant AAV expressing GCaMP6s for 2-4 weeks. Slices were sectioned in ice-cold cutting saline containing (in mM) 26 NaHCO₃, 1.25 NaH₂PO₄, 3 KCl, 10 glucose, 210 sucrose, 2 CaCl₂ and 2 MgCl₂ and incubated in the oxygenated (95% O₂/ 5% CO₂) cutting saline in a holding chamber at 34°C for 30 min. Slices were then stored at room temperature until used. During experiments, slices were placed in a recording chamber and superfused with oxygenated artificial CSF containing (in mM) 125 NaCl, 25 NaHCO₃, 1.25 NaH₂PO₄, 2.5 KCl, 15 glucose, 2 CaCl₂ and 1 MgCl₂. Recording electrodes (3–8 MΩ) were pulled from borosilicate glass (O.D. 1.5 mm, I.D. 0.86 mm; Sutter Instrument). Whole-cell recordings were made at 28°C using an Axopatch 700B amplifier (Molecular Devices). Data acquisition (filtered at 5 kHz and digitized at 10 kHz) and pulse generation were performed using a Digidata 1550 and pClamp 10.5 software (Molecular Devices). To activate the recorded cells, step currents (10 pA, 2 s) from -20 pA to +120 pA and ramp currents (40 pA, 10 s) were injected under current clamp mode by an Axopatch 700B amplifier (Molecular Devices).

Calcium Imaging

Ca²⁺ imaging was performed using a digital CCD camera (ORCA-ER, Hamamatsu) mounted on an Olympus upright microscope (BX51WI). Micro-manager software (version 1.4) was used as microscope control interface (Edelstein et al. 2014). Internal solution contains (mM) 125 K gluconate, 10 KCl, 4 Mg₃ATP₂, 0.3 Na₃ATP, 5 Na₂-phosphocreatine and 10 HEPES. After loading, the cells were imaged (10 ms exposure time; 10 Hz) with 470 nm excitation through a filter set (U-N41017, E.X. 470 nm, B.S. 495 nm, E.M. 5, Olympus). Ca²⁺ responses were expressed as relative changes in fluorescence ($\Delta F/F$).

To achieve synchronization between electrophysiology data and calcium imaging data, a customized Arduino board was used to send an electric pulse both to a light bulb near the slice chamber so that a flash can be detected by the camera and to the DAQ for electrophysiology. Data from two devices were then time-stamped based on the light flash and electric pulse using customized MATLAB code.

Data Analysis

Slice Calcium Imaging Data Analysis:

Data analysis followed the basic logic described previously (Chen *et al.* 2013). Motion correction was done with TurboReg plug-in in ImageJ (Thévenaz et al. 1998). Regions of interest (ROIs) were selected using oval selection tool in ImageJ with cell nucleus included. Plot Z-Axis Profile function in ImageJ was then used to measure the mean grey value of each ROI versus frame number. Neuropil fluorescence was selected and estimated using the same protocol with polygon selections. Only regions located near the cell with no detectable fluorescent neural processes were used.

The true fluorescence signal of each cell was estimated with function (Chen *et al.* 2013):

$$F_{\text{cell_true}(t)} = F_{\text{cell_measured}(t)} - r \times F_{\text{neuropil}(t)}, \text{ with } r=0.7.$$

For establishing the relationship between spike number and peak dF/F , the data points with saturated firing were excluded (defined as sweeps with higher current injection but decreasing number of spikes). Linear regression statistics were calculated using Prism 6.

Photometry Analysis:

For photometry data analysis, data were subjected to minimal processing consisting of only autofluorescence background subtraction and within trial fluorescence normalization.

Photometry Background Correction: The raw fluorescence output contains activity-dependent fluorescence from GCaMP6s as well as background fluorescence from the optical fiber and brain tissue. To estimate and correct for this autofluorescent background, we used a protocol in which we measured fluorescence for each mouse on the day following surgery, at which point no GCaMP6s is expressed and therefore all fluorescence represents background signal. We measured this background at a range of laser intensities (0.002 to 0.12 mW) for each mouse to generate an autofluorescence curve at various laser powers. This value was then subtracted from the recorded data obtained in actual experiments. Any mice having an autofluorescence value larger than 50% of the total baseline fluorescence intensity following GCaMP6s expression were not used for experiments.

Fluorescence Normalization: For peri-stimulus time plots, unless otherwise specified, the median value of data points within a 2 min window flanking the -5 min time point before each treatment was used as the normalization factor to calculate $F_n = 1.0$. Correction for photobleaching was not necessary due to the low laser power used during photometry recordings (~0.07 mW), the short time windows for most experiments (10-20 min), and the fact that all experimental groups had control groups treated with identical laser powers.

Internal controls: Ghrelin was used as a positive control in the initial testing of each new animal to validate the functionality of the experimental setup; every animal that we tested was ghrelin responsive. In addition at the beginning of each experiment animals were monitored to confirm that the baseline fluorescence showed fluctuations characteristic of these neurons (~10-20% $\Delta F/F$) that were uncorrelated with motion. For GFP controls, optical implants were installed in Pomc-GFP mice (Jackson #009593) or in AgRP-ires-Cre Rosa26-GFPL10 mice (Jackson #022367).

Time constant estimation: To estimate the exponential time constant τ_1 (τ) we used the following protocol. We first low-pass filtered the normalized fluorescence at 10 Hz to eliminate bias introduced by high-frequency fluctuations, as we are only interested in the slower components of the signal change. The resulting smoothed data was essentially monotonic following stimuli such as ghrelin or food. We then determined the maximum fluorescence change in response to the stimulus (within a range of 5 or 20 min depending on the experiment) and identified the earliest time point at which 63.8% of this change had occurred and defined this as τ_1 .

Lickometer Data Analysis: Lickometer TTL are read by the same DAQ and computer interface and therefore come as a time series array synchronized with the fluorescence trace. To identify feeding bouts, we first trimmed the TTL data to eliminate all the TTL signals that have any other TTL signal preceding within 20s. As a result, the TTL signals remaining will indicate the initiation of each feeding bout. We then isolated the fluorescence intensity data 10s flanking each side of the trimmed TTL signal, normalized to the median signal in that bout, and defined each as a PSTH for initiation of each licking bout. We then averaged all the PSTH bouts of each individual mice (17 +/- 2 bouts/mouse). We calculated the mean and standard error using a sample size corresponding to the number of different mice (not the number of trials)

For the shuffled control, we generated a random TTL array that had the same number of feeding initiation bouts within the same feeding period for each mouse. Then these TTL were used to calculate the PSTH in the same way as we did for lickometer data analysis. This process is repeated for 100 times and then averaged for each mouse to minimize variation from trial to trial.

Cross-correlation analysis was done using the MATLAB Function `xcorr` and data were further normalized by subtracting 1 (the median) prior to analysis. As the two wave forms we are analyzing were not recorded simultaneously but rather time stamped to each other through lickometer TTL, we did cross-correlation analysis of the averaged lickometer PSTH data across all different pairs of AgRP and POMC mice used in this experiment (7 AgRP mice x 4 POMC mice = 28 pairs).

Behavior Video Analysis: Video was made with a customized program using MATLAB Image Processing Toolbox. Video was time stamped to the data by aligning the flashes in the video recording to the TTL inputs. All videos were taken at a 5 Hz frame rate with 160x120 resolution.

Statistics: Values are reported as mean +/- SEM in the figures and text. P values for pairwise comparison were performed using a two-tailed Student's t-test. p values for comparisons across multiple groups were corrected using the Holm-Sidak method in Prism. * $p < 0.05$. ** $p < 0.01$, *** $p < 0.001$, **** $p < 0.0001$.

SUPPLEMENTARY FIGURES

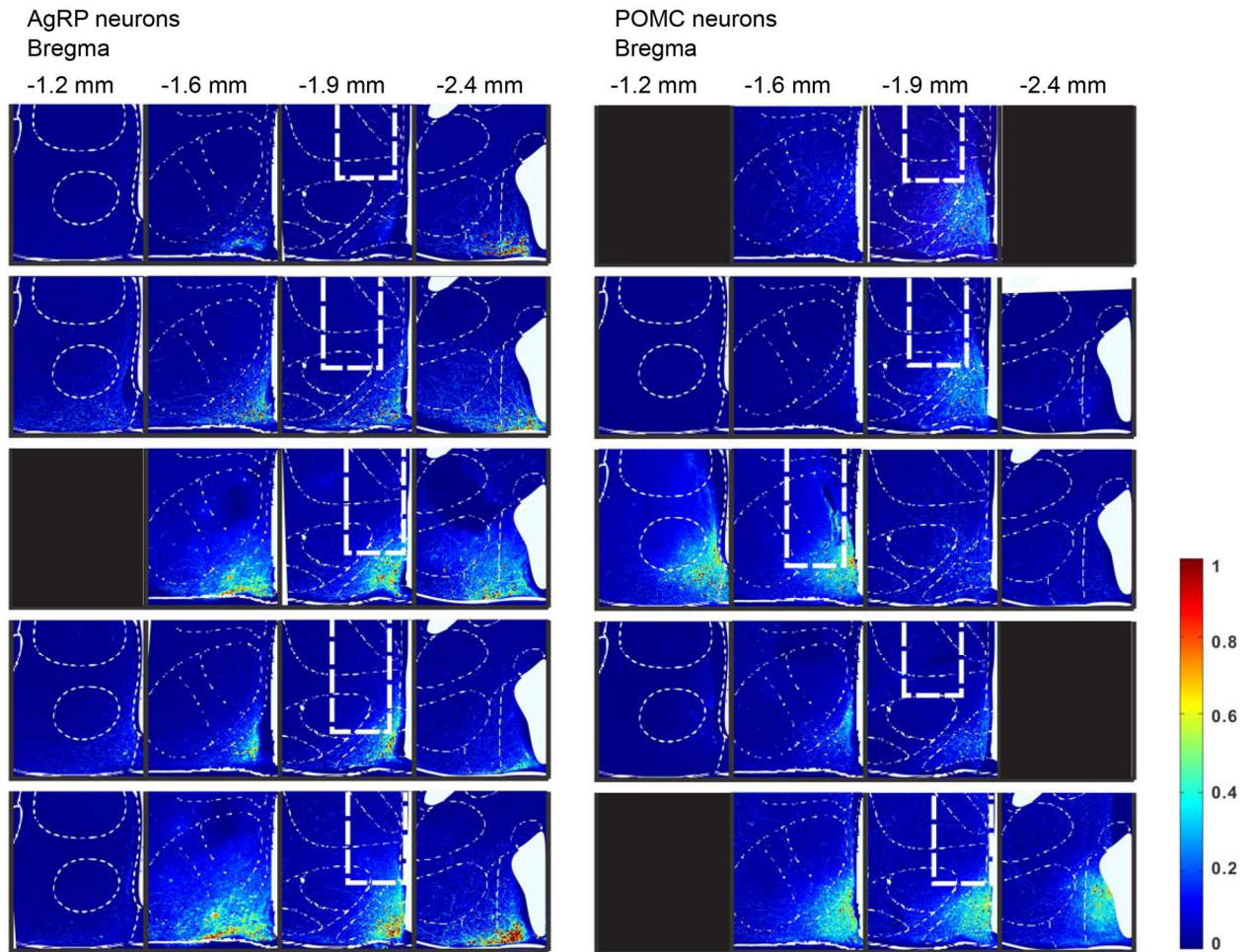


Figure 2.8 - Related to Figure 2.1. Location of viral infection and cannula placement for five AgRP and five POMC mice. Coronal sections showing GCaMP6s expression in five AgRP and five POMC mice, with distance from bregma indicated. Scale bar indicates fluorescence intensity for GCaMP6. Cannula location was estimated based on slices containing fiber tract. Black squares indicate sections that were damaged during staining.

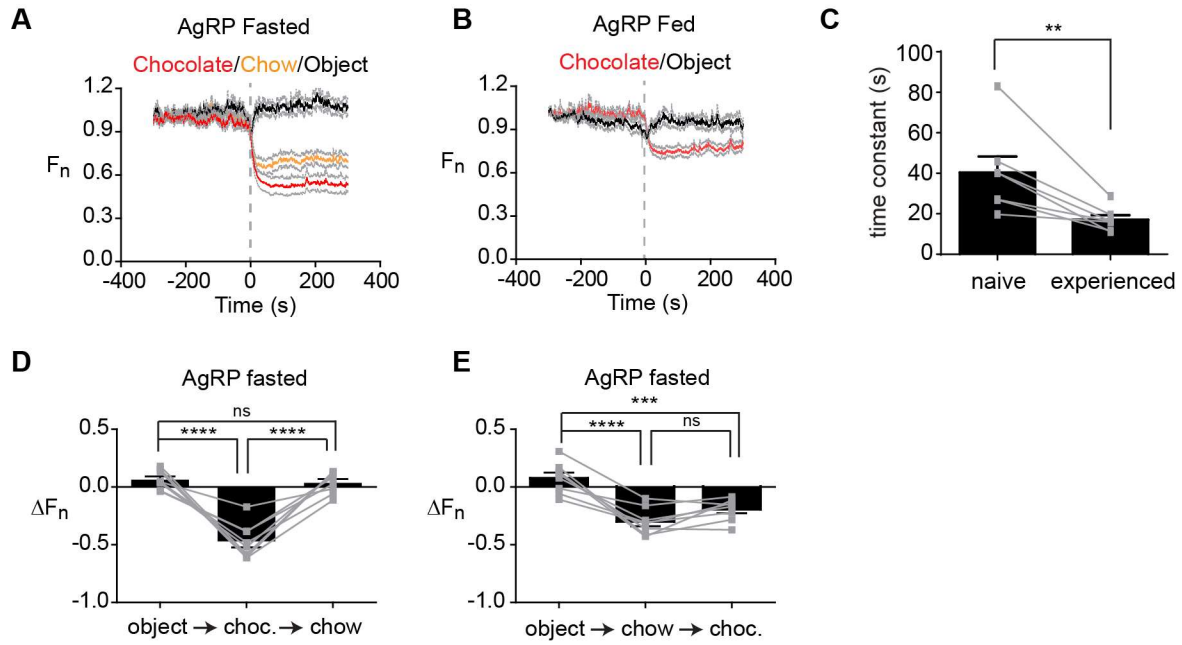


Figure 2.9. - Related to Figure 2.4. Response of AgRP neurons to chocolate.
(A and B) Calcium signals aligned to the presentation of chocolate, chow, or object in fasted and fed mice. **(C)** Time constant (τ) for the response chocolate presentation in the first trial (naïve) and in the fourth trial (experienced). **(D and E)** Quantification of response to sequential presentation of object, chow, and chocolate.

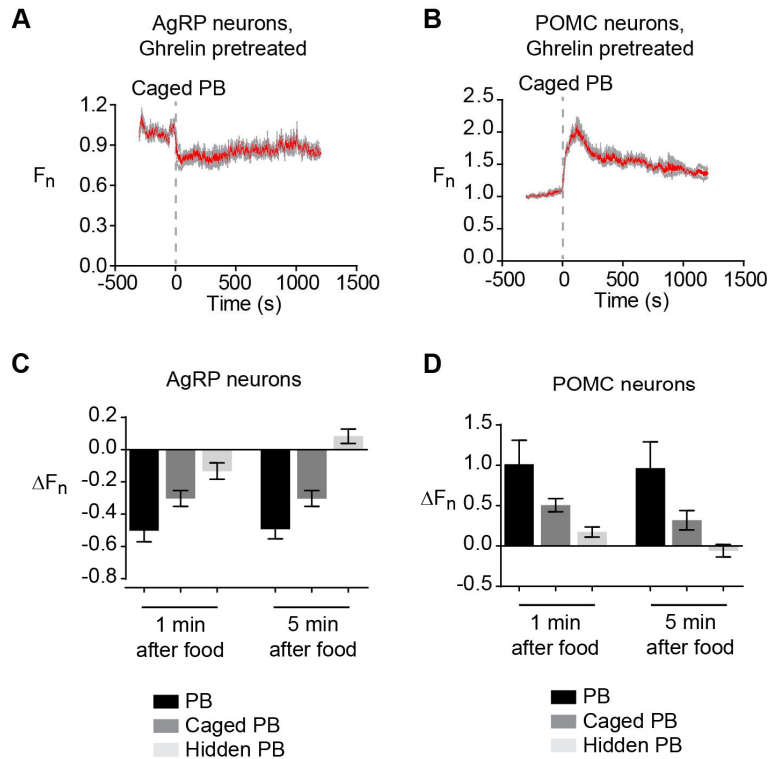


Figure 2.10 - Related to Figure 2.5. Peanut butter accessibility.

(A and B) Effect of caged peanut butter in mice pretreated with ghrelin. **(C and D)** Comparison of effects of presentation of peanut butter that was either accessible, caged, or hidden to fasted mice. Data for one and five minutes are shown.

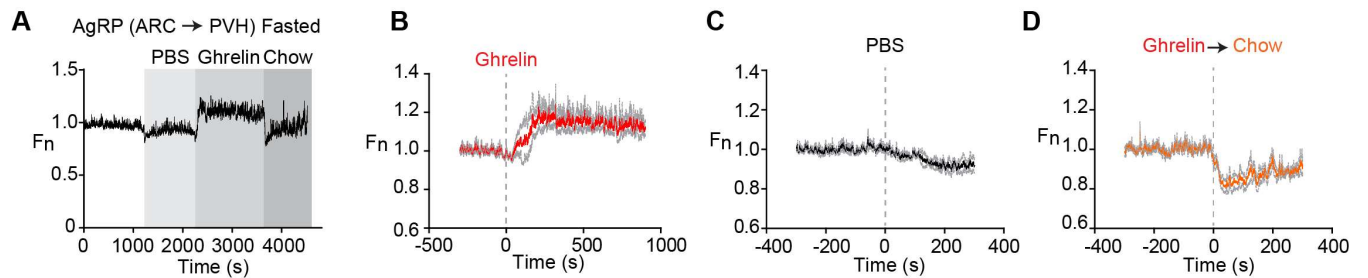


Figure 2.11. - Related to Figure 2.7. Effect of ghrelin on AgRP (ARC → PVH) projections. (A) AgRP calcium dynamics from one mouse given sequential PBS and ghrelin injection followed by chow presentation. **(B-D)** Average calcium dynamics for ghrelin, PBS, and ghrelin injection followed by chow presentation.

Chapter 3: Extended Discussion: making sense of the sensory regulation of hunger neurons

SUMMARY

AgRP and POMC neurons are two key cell types that regulate feeding in response to hormones and nutrients. Recently, it was discovered that these neurons are also rapidly modulated by the mere sight and smell of food. This rapid sensory regulation “resets” the activity of AgRP and POMC neurons before a single bite of food has been consumed. This surprising and counterintuitive discovery challenges longstanding assumptions about the function and regulation of these cells. Here we review these recent findings and discuss their implications for our understanding of feeding behavior. We propose several alternative hypotheses for how these new observations might be integrated into a revised model of the feeding circuit, and also highlight some of the key questions that remain to be answered.

MAIN CONTENT

The body weight of most animals is remarkably stable over time, suggesting that a homeostatic system balances food intake and energy expenditure over the long-term (Weigle, 1994). Two neural cell types in the hypothalamus, termed Agouti-related protein (AgRP) and Proopiomelanocortin (POMC) neurons, are thought to be critical components of this homeostatic system (**Figure 3.1A**). AgRP neurons are activated by energy deficit (Hahn et al., 1998) and their activity promotes food seeking and consumption (Aponte et al., 2011; Gropp et al., 2005; Krashes et al., 2011; Luquet et al., 2005). POMC neurons, in contrast, are activated by energy surfeit, and their activity promotes fasting and weight loss (Aponte et al., 2011; Zhan et al., 2013). These two cell types are often described as the “gas pedal” and the “brake” for the neural control of feeding. Together, they have been studied in far greater depth than any other neurons in the brain that have a specialized role in energy balance.

AgRP and POMC neurons are regulated by circulating signals of nutritional state, which modulate these cells in opposite directions consistent with their function. For example, the hormone leptin, which signals energy availability, activates POMC neurons and inhibits AgRP neurons (Cowley et al., 2001; Pinto et al., 2004). The hormone ghrelin, which signals energy scarcity, has the opposite effect (Cowley et al., 2003; Nakazato et al., 2001) (**Figure 3.1B**). Based on these observations, an intuitive and widely accepted model has emerged for how these two cell types control feeding. According to this model, food deprivation decreases the level of hormones that inhibit feeding, such as leptin, and increases the level of hormones that promote feeding, such as ghrelin. This hormonal switch activates AgRP neurons and inhibits POMC neurons, creating a “hunger drive” that motivates animals to find and consume food, and that persists until food intake replenishes the body of nutrients. In this way, a simple negative feedback loop is thought to explain the remarkable coordination of feeding behavior with physiologic need.

While this homeostatic model is widely accepted, one key piece of data has been missing: information about the activity dynamics of these neurons in vivo. In the past year, this gap has been closed, as three groups have reported measurements of AgRP and POMC neuron dynamics in awake, behaving mice (Betley et al., 2015; Chen et al., 2015; Mandelblat-Cerf et al., 2015). Contrary to expectations, these experiments revealed that AgRP and POMC neurons are rapidly modulated by the mere sight and smell of food, in a way that “resets” their activity before any food is consumed. This paradoxical discovery has prompted reassessment of the regulation and function of these long-studied cells (Betley et al., 2015; Chen et al., 2015; Mandelblat-Cerf et al., 2015; Seeley and Berridge, 2015). In this essay, we summarize these recent findings and discuss their implications for our understanding of the neural regulation of feeding.

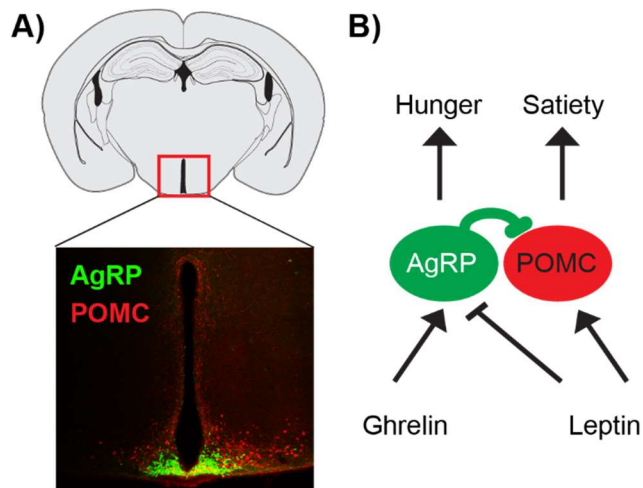


Figure 3.1. AgRP and POMC neurons regulate feeding in response to nutritional signals.

(A) AgRP and POMC neurons are intermingled in the arcuate nucleus of the hypothalamus. **(B)** The anorexigenic hormone leptin and the orexigenic hormone ghrelin regulate AgRP/POMC neurons in opposite directions. ‘

The sensory detection of food rapidly resets AgRP and POMC neurons

AgRP and POMC neurons were first implicated in the control of feeding almost 20 years ago (Fan et al., 1997; Hahn et al., 1998; Huszar et al., 1997; Lu et al., 1994; Ollmann et al., 1997; Seeley et al., 1997), yet their in vivo dynamics were only described in the past year (Betley et al., 2015; Chen et al., 2015; Mandelblat-Cerf et al., 2015). This long delay was due to technical challenges associated with recording neural activity from the arcuate nucleus (ARC) of the hypothalamus, which is located at the base of the forebrain and contains a diversity of intermingled neural cell types. To overcome these obstacles, it was necessary to develop new methods that enable optical (Gunaydin et al., 2014; Ziv et al., 2013) or electrophysiological (Lima et al., 2009) recordings from genetically defined cell types at deep brain sites and in freely behaving animals. Three such methods have now been developed and applied to investigate the dynamics of AgRP and POMC neurons (**Figure 3.2**).

The first study used an approach called fiber photometry, which utilizes an optical fiber to record fluorescence signals from a genetically encoded calcium reporter (e.g. GCaMP6s) targeted to a specific cell type (Gunaydin et al., 2014). This approach measures population-level calcium dynamics but does not resolve single cells (**Figure 3.2**). In the key experiment in this study, mice were fasted overnight and then presented with a piece of food, and during this time the calcium dynamics of AgRP and POMC neurons were optically recorded (Chen et al., 2015).

Contrary to the predictions of homeostatic models, it was found that food presentation alone rapidly inhibited AgRP neurons and activated POMC neurons. This response began the moment that food was presented and was complete within seconds, often before a single bite of food could be consumed. Thus sensory cues associated with food, rather than the post-ingestive effects of feeding, are primarily responsible for resetting the activity of these cells (Chen et al., 2015). This finding was counterintuitive in part because it revealed that AgRP neurons, which promote food intake, are actually less active when a mouse is eating, and conversely that POMC neurons, which inhibit food intake, are more active during feeding. This paradoxical activity pattern creates a puzzle for explaining how these neurons are able to perform their presumed functions.

Further characterization of the rapid sensory modulation of these neurons revealed five important properties (Chen et al., 2015). (1) The response depends on nutritional state, since neurons from fasted mice respond more strongly to food cues than neurons from fed mice. (2) It depends on food palatability, since energy dense foods such as peanut butter induce a stronger response than energy poor foods such as chow. (3) It depends on food accessibility, since food that is hidden or inaccessible induces a weaker and less durable response. (4) It is contingent on eventual food consumption, since removal of food before it can be consumed causes reversion of neural activity back to its prior state. (5) It is integrative, because these factors interact with each other to determine the magnitude of the response. As an example of this last property, presentation of a palatable food such as peanut butter was shown to modulate these neurons even in fed mice, which were otherwise insensitive to presentation of chow (Chen et al., 2015). Taken together, these findings reveal that AgRP and POMC neurons are regulated in a way that anticipates the nutritional or incentive value of a forthcoming meal (Chen et al., 2015; Seeley and Berridge, 2015). This anticipatory regulation resembles an expected value calculation, in which the brain weighs factors such as the need for food, the energy density or palatability of the food, and the likelihood that it is obtainable (Chen et al., 2015).

These findings were extended by a second study that used fluorescence microendoscopy to analyze calcium dynamics of AgRP neurons in freely behaving mice (Betley et al., 2015). An important advantage of this approach is that it provides single cell resolution and therefore can reveal heterogeneity in responses within a genetically defined population of neurons (**Figure 3.2**). This study added two additional important pieces of information. First, it showed that essentially every AgRP neuron is rapidly inhibited by food presentation, at least at the level of calcium dynamics (106/110 cells) (Betley et al., 2015). Thus AgRP neurons, despite having diverse projection patterns, appear to be subject to remarkably homogeneous regulation by sensory cues. Second, it showed that AgRP neurons can be modulated by an arbitrary cue, such as a light or sound, that animals have been trained to associate with food (Betley et al., 2015). This indicates that the response to food cues is, at least in part, learned. This finding is consistent with the fact that response of these neurons to novel foods accelerates upon repeated exposure, which also indicates learning (Chen et al., 2015).

A third study reported optrode recordings of AgRP and POMC neuron activity in head fixed mice (Mandelblat-Cerf et al., 2015). Optrodes enable the use of channelrhodopsin (ChR2) to identify cells from electrode recordings based on their light sensitivity (Lima et al., 2009) and, unlike calcium imaging, provide reliable measurement of single action potentials (**Figure 3.2**). In this study ChR2 was targeted to AgRP neurons, so that AgRP neurons could be identified as light-activated units and putative POMC neurons could be identified as light-inhibited units. Using this approach AgRP neuron firing rates were found to gradually increase throughout the course of the light phase, consistent with the slow development of energy deficit that occurs during the day (Mandelblat-Cerf et al., 2015). Subsequent food presentation rapidly inhibited AgRP neurons and activated POMC neurons, similar to the findings from calcium imaging. One important difference between these studies, however, was that AgRP neuron activity was shown to remain somewhat elevated following food presentation in the optrode experiment (Mandelblat-Cerf et al., 2015). This persistent elevated activity was interpreted to represent a

residual “hunger drive” that is responsible for promoting subsequent food consumption. We discuss this observation and its possible implications later in the text.

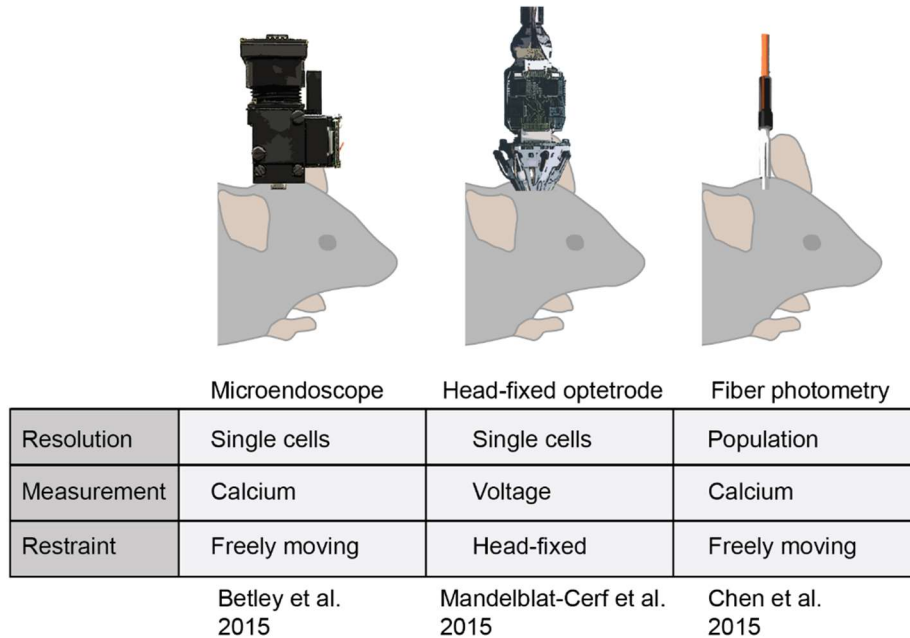


Figure 3.2. Techniques for cell-type-specific recording of deep brain neural activity.

(Left) Microendoscopic calcium imaging utilizes a head-mounted, miniaturized microscope to record fluorescence signals from a genetically encoded calcium indicator targeted to a specific cell type. This method can be used to probe deep brain structures by coupling the microscope to a gradient refractive index (GRIN) lens of appropriate length. **(Middle)** Optrode recordings utilize an electrode array paired with an optical fiber to perform extracellular recordings. The optical fiber enables cells expressing channelrhodopsin to be identified by their short latency responses to light stimulation. **(Right)** Fiber photometry uses a single optical fiber to both excite and record fluorescence from a population of neurons expressing a calcium reporter. The publications that used each of these approaches to investigate AgRP/POMC neurons are listed below.

Feeding is regulated by both homeostatic and anticipatory mechanisms

The rapid sensory modulation of AgRP and POMC neurons was unexpected in part because thinking about these cells has been dominated by the concept of homeostasis. A homeostatic mechanism is one in which a deviation from a physiologic set-point triggers a counterregulatory response (Berridge, 2004; Cannon, 1929). For example, a decline in plasma leptin activates AgRP neurons to induce feeding. The sensory modulation of AgRP and POMC

neurons by contrast is not homeostatic, because it occurs before any physiologic change has taken place. This response is instead “anticipatory,” because it predicts the nutritional changes that will occur in the future after the food has been consumed (**Figure 3.3**).

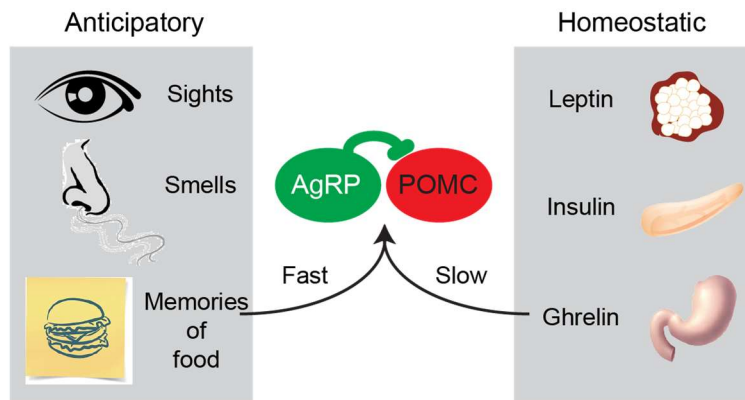


Figure 3.3. Fast and slow regulation of AgRP and POMC neurons by anticipatory and homeostatic signals.

(Right) Circulating hormonal signals such as leptin, ghrelin, and insulin have traditionally been thought to play a primary role in the regulation of AgRP and POMC neurons. The levels of these signals fluctuate slowly over minutes to hours in accordance with changes in nutritional state.

(Left) In vivo recordings however revealed a dominant role for anticipatory signals in the regulation of AgRP and POMC neurons. These anticipatory signals are triggered by sensory cues from the outside world and communicated by neural input, and therefore develop much faster than hormonal changes. In addition, these anticipatory signals precede rather than respond to changes in the nutritional state of the body.

Anticipatory mechanisms are widespread in neurobiology (Berridge, 2004; Stricker and Hoffmann, 2007; Woods and Ramsay, 2007), but are often overlooked in discussions of feeding behavior. The classic example of anticipatory regulation is Pavlov’s dogs, which salivate following ringing of a bell that predicts food availability (Pavlov, 1902). The anticipatory response in this case is the secretion of saliva containing digestive enzymes, which functions to prepare the oral cavity for food ingestion just moments before the food arrives. By contrast, the function of the anticipatory regulation of AgRP and POMC neurons is less clear. We consider below five alternatives.

Hypothesis #1: Sensory feedback gates cephalic phase responses

Food consumption is necessary for survival but also represents an acute threat, since it floods the body with nutrients that can disrupt physiologic balance (Woods, 1991). To deal with this challenge, animals have developed a large class of peripheral adaptations that are triggered by the sight, smell and taste of food and function to prepare the body to metabolize and absorb nutrients (Power and Schulkin, 2008; Zafra et al., 2006). These anticipatory responses, which Pavlov called “psychic secretions,” are now known as cephalic phase responses because they are controlled by the brain. In addition to salivation, cephalic phase responses include the secretion of gastric acid, bile, and digestive enzymes into the stomach and intestines; the release of hormones such as insulin, cholecystinin, and pancreatic polypeptide into the bloodstream; and an increase in body temperature (Power and Schulkin, 2008; Zafra et al., 2006). Most of these responses can be triggered by both food cues and food absorption. For example, the cephalic phase of insulin release is triggered by sensory cues that occur at the onset of feeding and precedes changes in blood glucose (Steffens, 1976; Strubbe and Steffens, 1975). Later, a second phase of insulin release occurs following food absorption in response to hyperglycemia.

Similarities between the sensory regulation of AgRP and POMC neurons and the activation of cephalic phase responses suggest these neurons could be part of the upstream pathway. For example, cephalic phases responses are triggered more strongly by palatable foods (Brand et al., 1982; Janowitz et al., 1950; Klajner et al., 1981; Powley, 1977), by multisensory compared to unisensory food cues (Feldman and Richardson, 1986), and following food deprivation (Klajner et al., 1981). The sensory regulation of AgRP/POMC neurons shares all of these properties (Chen et al., 2015). Cephalic phase responses can also be learned by Pavlovian conditioning (Pavlov, 1902; Powley, 1977; Woods and Kuskosky, 1976; Woods et al., 1977), similar to the sensory modulation of AgRP/POMC neurons (Betley et al., 2015). While the forebrain circuitry that controls cephalic phase responses is largely unknown, manipulations

of the paraventricular, ventromedial and lateral hypothalamus can trigger gastric acid release and other gastrointestinal responses, indicating a role for the hypothalamus (Kermani and Eliassi, 2012; Powley, 1977; Takahashi et al., 1999). There is also some evidence that chemogenetic modulation of AgRP neurons can rapidly alter peripheral metabolism (Krashes et al., 2011), although this has not been explored in detail. In future studies it will be important to measure the effects of cell-type-specific manipulations of AgRP and POMC neurons on cephalic phase responses in peripheral tissues, in order to understand the role of these neurons in gating this response.

Hypothesis #2: Sensory feedback induces anticipatory satiety

AgRP neurons are thought to promote hunger, and thus their rapid inhibition by food cues would be predicted to result in “anticipatory satiety” – satiety that occurs before the food is consumed. While this seems paradoxical, there is evidence that learned associations with sensory cues contribute to the termination of feeding (Smith, 2000). The most compelling data come from sham feeding experiments, performed primarily in rats, which used a gastric fistula to drain the ingested food from the stomach (Davis and Campbell, 1973; Young et al., 1974). This preparation enables disconnection of the effects of gastrointestinal signals from external sensory cues on feeding behavior. These studies showed, first, that rats consume much more food during sham feeding compared to real feeding (Davis and Campbell, 1973; Young et al., 1974), confirming the importance of post-ingestive negative feedback signals such as gastric distension in meal termination. However, it was found that during repeated sham feeding trials the amount of food these animals consumed increased even further (Davis and Campbell, 1973; Young et al., 1974). This progressive increase in sham food consumption was shown to reflect the extinction of a learned association between the sensory properties of specific foods (the conditioned stimulus) and their post-ingestive consequences (the unconditioned stimulus). This learned association functions to reduce the rate of food intake at the beginning of a meal (Davis

and Smith, 1990; Weingarten and Kulikovsky, 1989), perhaps so that animals can anticipate at the outset of a meal some of its physiologic effects and thereby calibrate their food intake more precisely.

An implication of this finding is that food delivered directly to the stomach, thereby bypassing sensory cues, should be experienced as less satiating than food consumed orally. This prediction has been confirmed by experiments showing that enteral feeding in humans fails to fully suppress appetite (Cecil et al., 1998; Stratton and Elia, 1999; Stratton et al., 2003, 2008). This failure does not appear to reflect decreased production of gastrointestinal satiation signals (LeGall-Salmon et al., 1999; Stratton et al., 2003), suggesting it involves the absence of a cognitive signal triggered by sensory cues. Consistent with this, some enteral fed human subjects report that simply chewing food decreases their residual hunger, even though the food cannot be swallowed (Stratton and Elia, 1999; Wolf and Wolff, 1943).

The rapid inhibition of AgRP neurons by food cues could contribute to this phenomenon of anticipatory satiety. The fact that these neurons are more strongly inhibited by energy dense foods (Chen et al., 2015) and respond to Pavlovian conditioning (Betley et al., 2015) are both consistent with this possibility. One way to test this model would be to determine whether AgRP neurons can be conditioned by gastrointestinal negative feedback signals. For example, would an arbitrary cue that predicts the infusion of nutrients into the stomach attain the ability to inhibit AgRP neurons following training? Conversely, would the response of AgRP neurons to a food cue undergo extinction if the ingested food was drained from the stomach each time the cue was presented? These types of experiments would clarify the nature of the unconditioned stimulus that trains AgRP neurons to respond to food cues, and in doing so provide insight into the function of this anticipatory modulation.

Hypothesis #3: Sensory feedback suppresses appetitive behaviors

AgRP neurons regulate not only food intake but also appetitive behaviors that promote food obtainment. For example, optogenetic or chemogenetic activation of AgRP neurons motivates animals to engage in vigorous lever pressing or nose poking for a food reward (Atasoy et al., 2012; Krashes et al., 2011). AgRP neuron activation also stimulates locomotor activity specifically in the absence of food, which has been interpreted as representing foraging (Jerlhag et al., 2006; Krashes et al., 2011). Pharmacologic experiments have shown that delivery of AgRP or NPY into the brain can preferentially promote appetitive rather than consummatory behaviors under some conditions (Ammar et al., 2005; Day et al., 2005; Sederholm et al., 2002; Woods et al., 1998). Together, these observations highlight the importance of AgRP neurons for promoting behaviors that lead to food discovery, and raise the question of how the transition from appetitive to consummatory behaviors is controlled.

The discovery that AgRP neurons are rapidly inhibited by food cues suggested that this inhibition may gate the transition from foraging to feeding (Chen et al., 2015; Mandelblat-Cerf et al., 2015). Indeed, the response properties of AgRP neurons to sensory cues appear almost perfectly designed to serve this function. As described above, food cues modulate AgRP neurons in a way that resembles an expected value calculation, in which the animal weighs factors such as the accessibility of the food, the energy density of the food, and its own need for nutrition. This integration would enable animals to make foraging decisions that are adaptive in the face of changing internal and external circumstances. For example, discovery of a suboptimal source of nutrition by a starving animal would nonetheless inhibit AgRP neurons, thereby ensuring that foraging is blocked when food is of greatest value (Betley et al., 2015; Chen et al., 2015; Mandelblat-Cerf et al., 2015). By contrast AgRP neurons from a well-fed animal would be insensitive to food cues unless the food was particularly palatable (Chen et al., 2015).

While this model is appealing, it is inconsistent in its simplest form with all of the available evidence. One problem is that if AgRP neuron inhibition is required for the transition from foraging to feeding, then continuous optogenetic stimulation of AgRP neurons should result in animals that perpetually forage and as a result do not eat. However this is not the case (Aponte et al., 2011). One way to explain this discrepancy might be that AgRP neuron inhibition promotes, but is not required, for the transition from foraging to feeding. Alternatively, it is possible that food presentation sends a sufficiently strong inhibitory signal to AgRP neurons that they become silenced even in the presence of continuous optogenetic stimulation. Consistent with this second possibility, it has been shown that AgRP activation induced by high-dose ghrelin treatment can be largely reversed by presentation of a single piece of chow (Chen et al., 2015), highlighting the potency of this inhibitory sensory input.

An important unresolved question is whether AgRP neurons are required for appetitive behaviors in food deprived mice. One study found that neonatal ablation of AgRP neurons reduced food anticipatory activity (FAA), which is an increase in locomotor activity that occurs before food availability and resembles foraging in mice subjected to scheduled feeding protocols (Tan et al., 2014). By contrast, adult ablation of AgRP neurons reduced food intake primarily due to “visceral malaise,” a defect that is consummatory in nature since AgRP neuron ablated mice will reject food delivered directly into their mouths (Wu et al., 2008). However, this nausea may be specific to the extreme case of acute AgRP neuron ablation in adults, since otherwise the mere sight and smell of food would trigger sickness and eating would be impossible.

Experiments that test the requirement for AgRP neurons in specific appetitive behaviors will be important in order to clarify how the sensory modulation of these cells influences the transition from foraging to feeding. While AgRP neuron dynamics appear well-suited to serve this function, it is possible that these anticipatory dynamics are merely a consequence of this behavioral transition rather than its cause, as has been proposed for other cell types (Berridge, 2007).

Hypothesis #4: Sensory feedback acts as a teaching signal

Hunger is an unpleasant state, and one reason animals eat is to eliminate this negative feeling. Recently, it was shown that AgRP neuron activity has negative valence, meaning that mice find it aversive and therefore learn to avoid places and flavors that are associated with elevated AgRP neuron activity (Betley et al., 2015). It has been proposed that, by alleviating this negative state, the rapid sensory inhibition of AgRP neurons may function as a teaching signal that trains animals to search for and consume food (Betley et al., 2015). This mechanism for encouraging a behavior by linking it to the removal of an aversive stimulus is known as negative reinforcement (Skinner, 1938).

A prediction of this negative reinforcement model is that mice should learn to perform instrumental responses that lead to a reduction in AgRP neuron activity. However this is not the case (Betley et al., 2015), as it has been shown that mice fail to execute simple operant tasks that have been experimentally paired with AgRP neuron inactivation. For example, fed mice will neither lever press nor nose poke in order to pause optogenetic stimulation of AgRP neurons (Betley et al., 2015). Similarly, fasted mice fail to nose poke in order to induce optogenetic silencing of naturally elevated AgRP neuron activity (Betley et al., 2015). This indifference to AgRP neuron silencing is in stark contrast to the dramatic lever pressing and nose poking that AgRP neuron stimulated animals will perform for an actual food reward (Atasoy et al., 2012; Krashes et al., 2011). Therefore negative reinforcement is not the primary motivational mechanism that AgRP neurons utilize to achieve their remarkable behavioral effects.

An alternative possibility is that AgRP neurons function by increasing the positively rewarding properties of food, such as its sight, smell, and taste (Seeley and Berridge, 2015). It is well known that food deprivation makes food more appealing, a concept known as alliesthesia (Cabanac, 1971), and that this enhanced palatability and incentive salience can promote food seeking and consumption (Seeley and Berridge, 2015). Consistent with this, palatable foods

have enhanced ability to modulate AgRP neurons (Chen et al., 2015; Seeley and Berridge, 2015). At present, however, there is little data that directly addresses this hypothesis.

Hypothesis #5: Sensory feedback connects the present to the future

It is possible that the rapid sensory modulation of AgRP and POMC neurons may not trigger any immediate behavioral transition, motivational change, or physiologic response. Instead, this sensory modulation could function primarily to synchronize rapid feeding behavior with slower nutritional changes. To illustrate why this may be necessary, consider three types of signals that could communicate ongoing meal status to AgRP and POMC neurons (**Figure 3.4**). The first is post-absorptive signals, such as leptin, that report on the nutritional state of the body. These signals have been the focus of most studies of the regulation of AgRP and POMC neurons, yet they act too slowly to control behavior directly (**Figure 3.4A**). For example, changes in plasma leptin require metabolic and transcriptional responses in adipocytes which develop over hours, and therefore leptin could not directly terminate a “hunger drive” following feeding. A second candidate is post-ingestive signals that arise from the stomach and intestine following feeding, including gastric distension and gut derived satiation peptides such as cholecystokinin. These signals have the right kinetics for controlling feeding behavior (**Figure 3.4B**), but there is little evidence that they actually regulate AgRP and POMC neurons, with the possible exception of peptide YY ((Batterham et al., 2002; Parkinson et al., 2008) but see also (Halatchev et al., 2004)).

In the absence of post-absorptive and post-ingestive signals, external sensory cues are the primary remaining type of information that AgRP and POMC neurons could use to learn about the status of an ongoing meal (**Figure 3.4C**). Because these sensory cues are detected before food has been consumed, they can most easily be used to make predictions about impending food consumption, which is how they are utilized in practice (Chen et al., 2015). Thus the anticipatory regulation of AgRP and POMC neurons may have evolved primarily as a facile

mechanism for the brain to coordinate rapid food ingestion with much slower homeostatic changes, rather than as a way to trigger a specific behavioral or metabolic transition upon the discovery of food.

Whatever the reason, it is clear that AgRP and POMC neurons are rapidly modulated by food associated sensory cues. This raises another question: if these neurons are “reset” by the sight and smell of food, then how do they control feeding at all?

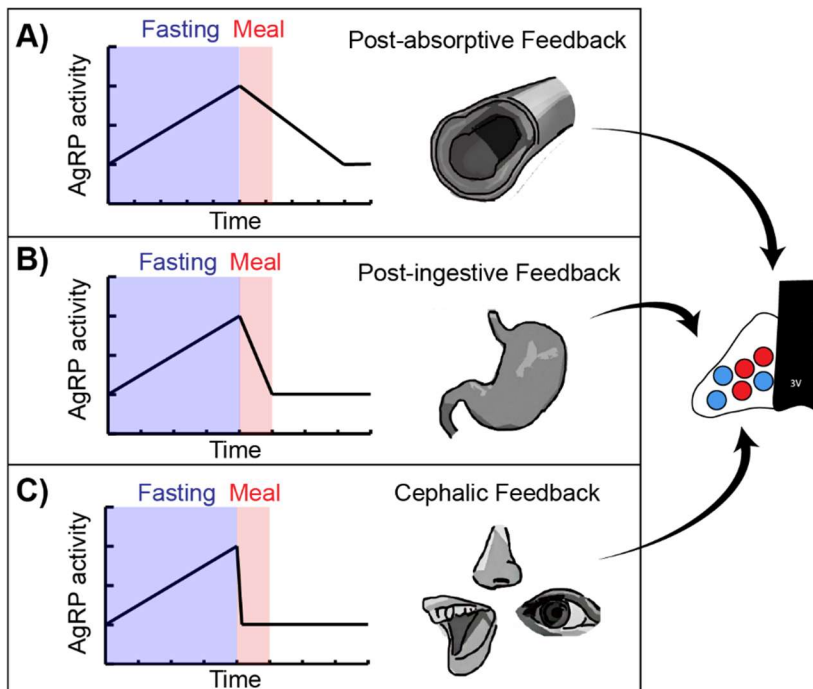


Figure 3.4. Three models for the inactivation of AgRP neurons by feeding.

(A) Post-absorptive feedback reports on the nutritional state of the body and includes circulating signals such as leptin. These signals evolve over hours and therefore are too slow to explain the rapid suppression of hunger by food intake. (B) Post-ingestive signals arise from the stomach and intestine immediately following food intake, and including gastric distension as well as gut-derived satiation peptides. These signals directly control meal termination, and therefore would be well-suited to inactivate AgRP neurons after feeding. However current data does not support a prominent role for these gastrointestinal signals in the actual regulation of AgRP neuron activity. (C) Cephalic feedback involves sight, smell, taste, and possibly other external sensory cues. In vivo recordings reveal that this is the major mechanism for the regulation of AgRP and POMC neurons during meals.

How do AgRP and POMC neurons control feeding?

A vast body of evidence shows that AgRP and POMC neurons control food intake. This includes the results of optogenetic, chemogenetic, and cell ablation studies in mice demonstrating that bidirectional manipulation of these cells alters feeding (Aponte et al., 2011; Gropp et al., 2005; Krashes et al., 2011; Luquet et al., 2005; Zhan et al., 2013), as well as pharmacologic and genetic studies showing that the neurotransmitters produced by these cells (gamma-aminobutyric acid (GABA), neuropeptide Y (NPY), AgRP, and POMC) modulate feeding in ways consistent with their putative functions (Clark et al., 1985; Fan et al., 1997; Krashes et al., 2013; Ollmann et al., 1997; Poggioli et al., 1986; Seeley et al., 1997; Tong et al., 2008). These findings have been extended to humans by the discovery that loss-of-function mutations in the melanocortin 4-receptor (MC4R) are a common cause of extreme obesity (Farooqi et al., 2003; Farooqi et al., 2000; Hinney et al., 1999; Vaisse et al., 2000). Thus a mechanism must exist by which the activity of these neurons is translated into changes in food consumption.

Nonetheless, the natural activity patterns of these neurons are difficult to reconcile with their presumed functions. It is generally assumed that, if a neuron drives a behavior, then the neuron should be more active during or immediately preceding the behavior's execution. Yet this is not the case for AgRP and POMC neurons. AgRP neurons, which are thought to drive food intake, are much less active during feeding compared to minutes before. POMC neurons, which are thought to inhibit food intake, are more active during the act of feeding itself. These counterintuitive trends apply to even the small fluctuations in AgRP and POMC neuron activity that surround individual bouts of eating, which often have the opposite sign relative to what would be predicted based on the known functions of these cells (Chen et al., 2015; Mandelblat-Cerf et al., 2015).

How can we explain these paradoxical findings? We consider below two hypotheses, which are not mutually exclusive, for how these cells may regulate feeding.

Mechanism #1: Residual AgRP neuron activation persists after food presentation and drives feeding

An important question is whether food presentation completely resets the activity of AgRP and POMC neurons to baseline, or whether a residual orexigenic activity pattern persists in these cells. Microendoscopic calcium imaging found that essentially all AgRP neurons were rapidly inhibited by food presentation (106/110 cells inhibited versus 1/110 cells activated) (Betley et al., 2015). By contrast, optrode recordings found that only 64% of AgRP neurons were inhibited by food presentation (14/22 cells), whereas 23% of AgRP neurons were activated (5/22 cells) (Mandelblat-Cerf et al., 2015). Consistent with this mixed response, optrode recordings showed that food presentation to food restricted mice in the dark phase did not reduce the firing rate of AgRP neurons all the way to the level of fed mice at the start of the light phase, a time that mice generally do not eat. This residual activity of AgRP neurons was proposed to represent a hunger drive that persists after food discovery (Mandelblat-Cerf et al., 2015).

Why would optrode recordings reveal residual AgRP activity that was not detected by calcium imaging? One possibility is that the difference is technical. Calcium dynamics are only a surrogate for neural firing and provide relative, not absolute, measurements of neural activity. Calcium sensors can also display non-linearity in their response properties outside a certain range. By contrast, electrophysiologic recordings provide data on absolute firing rates by measuring individual spikes. Thus it is possible that a residual activation of AgRP neurons following food presentation was simply not detected in the calcium imaging experiments due to a technical limitation of the approach.

However there are reasons to suspect this is not the whole story. One reason is that technical differences would not obviously explain why the two studies found a different direction of modulation for a significant subset of AgRP neurons; i.e. why would calcium imaging show that 96% of AgRP neurons were inhibited by food cues if 23% were actually activated? In

response to other stimuli, AgRP activation was robustly detected by calcium imaging (Betley et al., 2015). Second, photometry recordings showed that presentation of palatable food to fed mice can reduce calcium signals considerably below the ad libitum fed baseline (Chen et al., 2015). Therefore calcium imaging is not inherently limited by linear range or sensitivity in its ability to detect activity reductions below the baseline level of fed animals.

An alternative possibility is that these discrepancies reflect differences in experimental paradigm. One important difference is that the optrode study used head-fixed mice presented with a liquid diet (Mandelblat-Cerf et al., 2015), whereas the calcium imaging studies used freely behaving mice presented with solid food (Betley et al., 2015; Chen et al., 2015). It has been shown that the magnitude and durability of the response of AgRP and POMC neurons to food cues is very sensitive to factors such as the accessibility and palatability of the food (Chen et al., 2015). Thus it may be that the use of a head-fixed preparation or liquid diet reduces the anticipatory response of these neurons, either due to stress or some change in the animal's expectation of food availability or value. This would explain why the calcium imaging and electrophysiologic measurements showed different percentages of AgRP neurons that were inhibited by food cues.

To clarify these issues, it will be important to perform optrode recordings from AgRP neurons in freely behaving mice and measure whether any residual activation persists after food presentation. In addition, it will be important to test the functional importance of any residual AgRP activity by using methods with high temporal control, such as optogenetic silencers, to selectively inhibit AgRP neurons after food presentation and measure the kinetics of the cessation of feeding. These experiments will enable dissection of the contribution of residual AgRP neuron activity to subsequent food consumption.

Mechanism #2: AgRP neurons transmit a sustained hunger signal

An alternative hypothesis is that AgRP neurons act through a sustained or persistent mechanism that enables the activity of these neurons before food presentation to “spill over” and influence the food intake that occurs later. There have been hints that such a sustained mechanism might operate. One clue is that feeding following optogenetic stimulation of AgRP neurons has an unusually long latency (six minutes) (Aponte et al., 2011). By contrast, optogenetic stimulation of inputs to the lateral hypothalamus can induce feeding within ten seconds (Jennings et al., 2013). This suggests that AgRP neurons do not control the food intake machinery directly, but rather produce some factor that must “build up” in the downstream circuit before feeding is triggered.

How could such a mechanism operate? It has been shown that a single injection of the AgRP neuropeptide into the brain can increase feeding for up to one week, indicating that the effects of AgRP peptide release can extend far beyond the duration of AgRP neuron activation (Hagan et al., 2000). Similarly, activation of POMC neurons inhibits feeding on a time-scale of hours to days (Aponte et al., 2011; Zhan et al., 2013). Thus modulation of the melanocortin system can have delayed and chronic effects on feeding. However this mechanism cannot explain feeding that results from release of NPY and GABA, which in many contexts are more important than release of AgRP itself (Aponte et al., 2011; Atasoy et al., 2012; Krashes et al., 2013; Qian et al., 2002; Tong et al., 2008; Wu et al., 2008). In this regard, activation of AgRP neurons lacking both GABA and NPY does not promote feeding in the first two hours after stimulation (Krashes et al., 2013). This implies that any mechanism that regulates acute feeding would necessarily be mediated by a melanocortin independent signal (either GABA or NPY).

A prediction of this model is that there should exist a population of feeding-regulatory neurons that serve as the substrate for this sustained response. These neurons would be located downstream of AgRP neurons in the feeding circuit and integrate AgRP neuron activity over time, so that their response to sudden changes in AgRP neuron firing rate was delayed. As

a result, these downstream cells would appear to “remember” the history of AgRP neuron activity, enabling them to promote feeding even after AgRP neurons have been silenced by sensory cues. If such neurons exist, their dynamics would correlate more closely with the subjective notion of hunger than AgRP neurons themselves.

CONCLUSION AND OUTLOOK

Over the past year we have witnessed some of the first glimpses into the dynamics of the key neural cell types that control feeding, including AgRP and POMC neurons. This has revealed that these cell types, long regarded as merely sensors of the internal state of the body, in fact respond rapidly to sensory cues from the outside world. They use this sensory information to predict nutritional changes that will occur in the future, revealing anticipatory dynamics that are both remarkable and puzzling, since they confound traditional explanations for how these neurons control behavior. An important challenge for the field will be to integrate these new observations into a revised model of the feeding circuit, and we have highlighted here some of the key questions that remain to be answered. As AgRP and POMC neurons represent only a small piece of the neural network that controls feeding, it is likely that additional surprises lie ahead as we uncover the dynamics of this circuitry.

Chapter 4: Hormonal and intragastric modulation of arcuate feeding circuit

SUMMARY

Communication between the gut and brain is critical for homeostasis, but how this communication is represented in the dynamics of feeding circuits is unknown. Here we describe nutritional regulation of key neurons that control hunger *in vivo*. We show that intragastric nutrient infusion rapidly and durably inhibits hunger-promoting AgRP neurons in awake, behaving mice. This inhibition is proportional to the number of calories infused but surprisingly independent of macronutrient identity or nutritional state. We show that three gastrointestinal signals – serotonin, CCK, and PYY – are necessary or sufficient for these effects. In contrast, the hormone leptin has no acute effect on dynamics of these circuits or their sensory regulation, but instead induces a slow modulation that develops over hours and is required for inhibition of feeding. These findings reveal how layers of visceral signals operating on distinct timescales converge on hypothalamic feeding circuits to generate a central representation of energy balance.

INTRODUCTION

Energy homeostasis requires communication between the body and brain. This communication is mediated by a web of hormones, metabolites, and ascending neural signals that report on the nutritional state of the body (Cummings and Overduin, 2007). The targets of these signals are neurons in the hypothalamus and related structures that integrate this information in order to generate a central representation of physiologic state (Clemmensen et al., 2017). While this gut-brain communication has been studied for decades by manipulating the signals and sensors that comprise the afferent pathways (Sohn et al., 2013), we still know remarkably little about how interoception is represented in the dynamics of the target neural

circuits. Indeed, it remains a mystery how even basic visceral events, such as nutrient detection in the gut, are encoded by feeding circuits in a living animal.

AgRP and POMC neurons are the two most widely-studied cell types that control feeding. AgRP neurons are activated by fasting and promote food seeking and consumption, whereas POMC neurons are inhibited by food deprivation and promote satiety (reviewed in (Andermann and Lowell, 2017)). These two sets of neurons are intermingled in the arcuate nucleus of the hypothalamus and project broadly to a common set of subcortical structures, where they have opposing effects on food intake and other autonomic and behavioral outputs modulated by energy balance.

Due to their robust regulation by nutritional state, AgRP and POMC neurons provide a unique entry point into the study of mechanisms of interoception. Traditionally, the nutritional regulation of these cells has been investigated in two ways: by using slice physiology to measure the direct effects of hormones and nutrients on these cells *in vitro* (Cowley et al., 2001; Cowley et al., 2003; Pinto et al., 2004; van den Top et al., 2004) and by using mouse genetics to perturb these nutrient-sensing pathways and then measure the effect on physiology and behavior (reviewed in (Sohn et al., 2013)). While much has been learned using these approaches, they do not provide information about neural activity *in vivo*, and consequently cannot reveal the natural dynamics of these cells or their modulation by physiologic signals that are absent from *ex vivo* preparations.

To bridge this gap, we and others recently recorded the dynamics of AgRP and POMC neurons in awake, behaving mice (Betley et al., 2015; Chen et al., 2015; Mandelblat-Cerf et al., 2015). However the unexpected finding from these studies was that AgRP and POMC neuron activity *in vivo* is dominated by external sensory cues associated with food: when a hungry mouse detects food, or conditioned cues that predict food availability, AgRP neurons become inhibited and POMC neurons become activated within seconds. As a result, the functional state of the arcuate feeding circuit is effectively “reset” by the sensory detection of food, in a way that

predicts the nutritional content of a meal before it begins. While this discovery raised a host of new questions about the neural regulation of feeding (Chen and Knight, 2016), it also complicated our ability to probe the underlying nutritional regulation of these cells, because it revealed that the direct effects of nutrients are masked by faster, anticipatory responses.

To overcome this obstacle, we have developed a protocol for recording neural dynamics while feeding mice by intragastric infusion, thereby bypassing sensory cues associated with food. We describe here the application of this approach to dissect mechanisms of gut-brain communication underlying hunger. We show that intragastric nutrients rapidly and durably inhibit AgRP neurons in a way that is proportional to the total number of calories delivered but independent of macronutrient composition or nutritional state of the animal. We further show that three satiation signals – serotonin (5HT), cholecystokinin (CCK), and peptide YY (PYY) – are necessary or sufficient for the inhibition of AgRP neurons by intragastric nutrients. In contrast, we find that the widely-studied hormone leptin only modulates AgRP and POMC neuron dynamics on a timescale of hours, and that this slow modulation is required for leptin's effects on feeding. These findings reveal for the first time how diverse nutritional inputs are integrated in the arcuate nucleus of awake mice to enable the neural control of feeding.

RESULTS

Sustained inhibition of AgRP neurons requires food consumption

The sensory detection of food inhibits AgRP neurons within seconds, but this inhibition is transient unless the food is subsequently consumed (Betley et al., 2015; Chen et al., 2015). To illustrate this phenomenon, we analyzed the response of AgRP neurons to presentation of inaccessible food (**Figure 1A**). Mice were equipped for recording calcium dynamics in AgRP neurons by fiber photometry (Chen et al., 2015) and then fasted overnight. Presentation of 'caged' chocolate that mice could see and

smell but not consume resulted in a rapid inhibition of AgRP neurons ($\Delta F/F -20.1 \pm 5.1\%$ from baseline at 5 min; **Figure 4.1B, C**). However, despite continued presence of the caged chocolate, this inhibition was reversed within 20 minutes ($\Delta F/F -7.1 \pm 3.1\%$ from baseline at 20 min; **Figure 4.1B,C**).

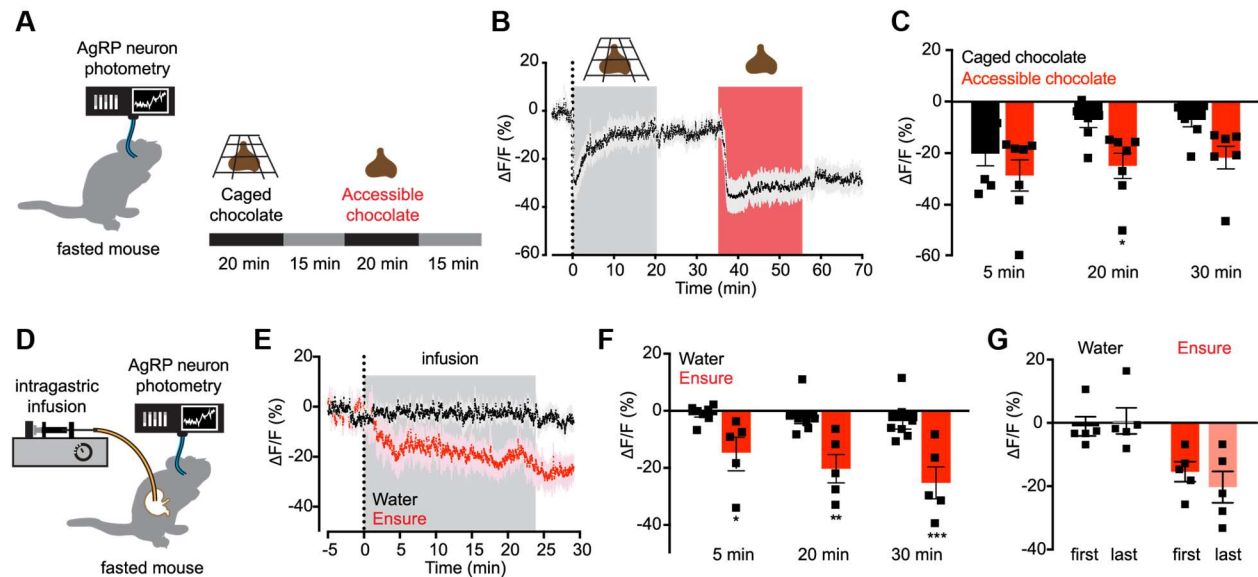


Figure 4.1. Nutrient intake is necessary and sufficient for sustained AgRP neuron inhibition

(A) Schematic of experiment in (B-C). Fasted mice were presented with caged chocolate and then available chocolate during photometry recording from AgRP neurons. **(B)** Calcium signal from AgRP neurons in fasted mice presented first with caged chocolate (gray) and then available chocolate (red) ($n=7$ mice). **(C)** Quantification of $\Delta F/F$ from (B). Times shown are 5-min windows immediately after chocolate presentation (5 min), immediately prior to chocolate removal (20 min), and 10 min following chocolate removal (30 min). * $P = 0.02$ compared to caged chocolate (Holm-Sidak's multiple comparisons test adjusted p-value) **(D)** Schematic of the experimental set-up for AgRP photometry recording during intragastric nutrient infusion for 24 min. **(E)** Calcium signal from AgRP neurons in fasted mice during intragastric infusion with water (black) or Ensure liquid diet (red). Gray denotes infusion ($n = 7$ mice for water; $n = 5$ mice for Ensure). **(F)** Quantification of $\Delta F/F$ from (E). Times shown are 5-min windows from the early part of infusion (5 min), the end of infusion (20 min), and 10 min following the end of infusion (30 min). * $P < 0.05$, ** $P < 0.01$, *** $P < 10^{-3}$ compared to water infusion at the indicated time point (Holm-Sidak's multiple comparisons test, adjusted p-value). **(G)** Quantification of $\Delta F/F$ at the end of infusion following the first and last intragastric exposures to water (black) and Ensure (red). Infusions were separated by approximately 7 weeks. **(B and E)** Traces represent mean \pm SEM

(C,F,G) ■ denotes individual mice. Bars represent mean \pm SEM

Subsequent presentation of accessible chocolate that mice could eat resulted again in a rapid inhibition of AgRP neuron activity ($\Delta F/F$ $-28.7\% \pm 6.6\%$ from baseline at 5 min), but in this case AgRP neuron inhibition was sustained for the duration of the experiment ($\Delta F/F$ $-24.9\% \pm 5.3\%$ from baseline at 20 min), persisting even after the chocolate was removed ($-21.7 \pm 4.7\%$ 10 min after chocolate removal **Figure 4.1B,C**). Thus food consumption is required for long-lasting inhibition of AgRP neuron activity.

Intragastric nutrients rapidly and durably inhibit AgRP neuron activity

The mechanism by which food intake stabilizes the rapid sensory inhibition of AgRP neurons is unknown. One possibility is that AgRP neurons are inhibited by an oropharyngeal signal generated during the act of eating, analogous to how thirst neurons are inhibited by the sensation of water in the oral cavity (Zimmerman et al., 2016). Alternatively, AgRP neurons could be inhibited as a consequence of nutrient detection in the gut (Tellez et al., 2013; Tolhurst et al., 2012). To distinguish between these possibilities, we equipped mice with an intragastric catheter for direct infusion of nutrients into the stomach as well as an optical fiber for photometry recordings from AgRP neurons (**Figure 4.1D**). This preparation enables direct observation AgRP neuron responses to internal nutritional changes while bypassing exterosensory and oropharyngeal cues associated with feeding.

Mice were fasted overnight and then received an intragastric infusion of different solutions while AgRP neuron dynamics were monitored by photometry. Infusion of the liquid diet Ensure caused a rapid and progressive decrease in AgRP neuron activity ($\Delta F/F$ $-14.7 \pm 6.1\%$ from baseline at 5 min, $-20.2 \pm 5.5\%$ at the end of infusion; **Figure 4.1E,F**). This inhibition persisted following the end of infusion ($\Delta F/F$ $-25.2 \pm 6.3\%$ from baseline 10 min after the end of infusion; **Figure 4.1E,F**), demonstrating that intragastric nutrients can durably inhibit AgRP neuron activity. In contrast, water infusion had no effect on AgRP neuron dynamics ($\Delta F/F$ $-2.2 \pm$

2.5% from baseline at the end of infusion; **Figure 4.1E,F**), indicating that gastric distension is insufficient to inhibit these cells (**Figure 4.9**). These neural responses were not secondary to learning, because we observed a robust reduction of AgRP neuron activity during the first infusion of Ensure in each animal (**Figure 4.1G**, right), whereas the lack of response to water was maintained following months of intermittent testing (**Figure 4.1G**, left). Thus gastrointestinal nutrients are sufficient to rapidly and durably inhibit AgRP neuron activity.

AgRP neuron inhibition is proportional to the number of calories infused, but independent of macronutrient identity or nutritional state

Ensure is a complex mixture of sugars, fats, and protein. To determine which of these components mediates the inhibition of AgRP neurons, we measured the neural response to intragastric infusion of isovolemic and isocaloric solutions of glucose, lipid, or peptide (**Figure 4.2A-F**). Surprisingly, intragastric infusion of each of these individual macronutrients to fasted mice caused a similar reduction in AgRP neuron activity ($\Delta F/F$ $-26.5 \pm 5.5\%$ for glucose, $-25.7 \pm 5.0\%$ for lipid, $-16.8 \pm 3.8\%$ for peptide at the end of infusion, $P < 0.01$ compared to water). These responses were sustained following the completion of infusion (**Figure 4.2A-C**), indicating that individual macronutrients are sufficient to durably reset AgRP neuron activity. To explore further the role of nutrient identity in AgRP neuron regulation, we compared the response to infusion of three additional sugars: fructose, galactose, and sucrose (**Figure 4.2J**). Remarkably, infusion of isocaloric solutions of each of these mono- and disaccharides caused a similar inhibition of AgRP neurons, whereas infusion of the non-caloric but structurally similar sweetener sucralose had no effect on AgRP neuron activity ($\Delta F/F$ $-2.1 \pm 0.7\%$ at the end of infusion; $p=0.99$ compared to water; **Figure 4.2J**). Thus AgRP neurons are inhibited by intragastric delivery of a broad range of nutrients, but not by chemically related, non-nutritive substances.

The observation that any macronutrient can inhibit AgRP neuron activity (**Figure 4.2A-C**) suggests that the calorie content of the infusate may be the primary determinant of the neural response. To test this possibility, we infused glucose solutions of equal volume but different concentrations (6% to 45%) into the stomach of fasted mice. This resulted in a striking dose-dependent inhibition of AgRP neuron activity (two-way ANOVA dose effect $P < 10^{-3}$; **Figure 4.2D, G**). We observed a similar dose-dependent inhibition following infusion of solutions of lipid (**Figure 4.2E, H**) and protein (**Figure 4.2F, I**). Thus the degree of inhibition of AgRP neurons by intragastric nutrients is proportional to the number of calories delivered.

We next asked how the response to nutrient infusion would be modulated by changes in nutritional state. Previously, we showed that the sensory detection of food inhibits AgRP neurons in fasted but not fed mice (Chen et al., 2015). To test whether fasting also gates the response of AgRP neurons to nutrient delivery, we infused Ensure into the stomach of fed mice while recording AgRP neuron dynamics (**Figure 4.2K**). Surprisingly, we found that AgRP neuron activity was further reduced by intragastric Ensure even in fed animals ($\Delta F/F -21.3 \pm 7.2\%$ in fed mice infused with Ensure versus $-4.6\% \pm 3.6\%$ for water, $P = 0.012$). We observed a similar reduction of AgRP neuron activity in fed mice that received intragastric glucose or lipid (**Figure 4.2K**). Thus, in contrast to their regulation by external sensory cues, AgRP neurons in fed mice can be further inhibited by delivery of intragastric nutrients. This discrepancy has implications for our understanding of how AgRP neuron activity encodes changes in energy balance.

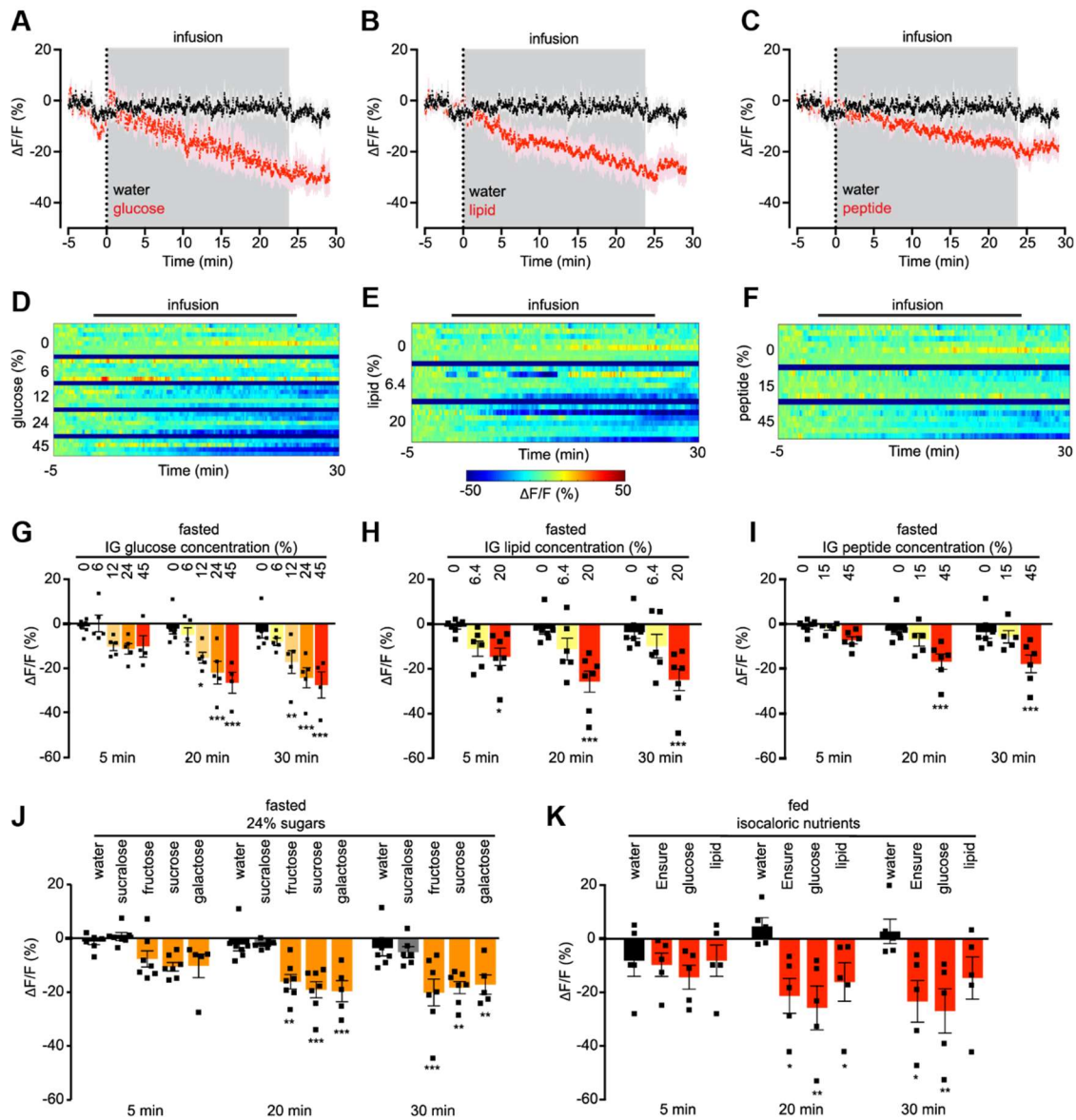


Figure 4.2. Inhibition of AgRP neurons by nutrients is independent of macronutrient composition or nutritional state and is proportional to calorie ingestion.

(A-C) Calcium signal from AgRP neurons in fasted mice during intragastric infusion with water (black) or isocaloric and isovolemic quantities of 45% glucose (A), 20% lipid (B), or 45% peptide (C) solutions (red). Traces represent mean \pm SEM. Gray denotes infusion. (n = 4-7 mice per group) (D-F) Peri-infusion heat maps depicting $\Delta F/F$ during photometry recording in fasted mice receiving intragastric infusion of the indicated concentrations of glucose (D), lipid (E), or peptide (F). Each row represents the average of 1-3 trials of an individual mouse. (n = 4-7 mice per group). (G-I) Quantification of $\Delta F/F$ from (D-F). (J) Quantification of $\Delta F/F$ during photometry recording in fasted mice receiving intragastric infusion of the indicated 24% mono- and disaccharide solutions or the non-caloric sweetener sucralose. (K) Quantification of $\Delta F/F$ during photometry recording from AgRP neurons in *ad libitum* fed mice receiving intragastric infusion of the indicated isocaloric solutions. (n = 5 mice per group).

(G-K) ■ denotes individual mice. Times shown are 5-min windows from the early part of infusion (5 min), the end of infusion (20 min), and 10 min following the end of infusion (30 min). Bars represent mean \pm SEM. * $P < 0.05$, ** $P < 0.01$, *** $P < 10^{-3}$ compared to H₂O infusion at the indicated time point (Holm-Sidak multiple comparisons test, adjusted p-value).

Intragastric nutrients diminish the sensory response of AgRP neurons to subsequently presented food

We next investigated how intragastric feeding influences the response of AgRP neurons to the sensory detection of food. Animals were fasted overnight and then infused with intragastric nutrients or water. Following infusion, animals were presented with a piece of chow and the response of AgRP neurons was measured. In mice infused with water, food presentation rapidly and robustly inhibited AgRP neuron activity (**Figure 4.3A**), whereas intragastric infusion of Ensure significantly attenuated this sensory response ($\Delta F/F$ $-31.6 \pm 5.6\%$ after water versus $-15.6 \pm 5.8\%$ after Ensure, $P = 0.01$; **Figure 4.3A**). Infusion of isocaloric solutions of glucose, lipid, or protein each caused a similar or stronger attenuation of the sensory response (**Figure 4.3A**). This effect was dose-dependent, with infusion of increasing concentrations of glucose resulting in a progressive decrease in the inhibition of AgRP neurons by chow presentation (**Figure 4.3C**). Thus intragastric nutrients are sufficient to block the response of AgRP neurons to external sensory cues associated with food.

The inhibition of AgRP neurons by the sensory detection of food has been proposed to represent a prediction of the number of calories that will be consumed in a forthcoming meal (Chen and Knight, 2016; Chen et al., 2015). To test this idea, we measured food intake in the first 20 minutes after presentation of chow in the experiments above (**Figure 4.3B, D**), and then correlated this food intake with the prior response of AgRP neurons to the sensory detection of food (**Figure 4.3E**). This revealed a striking correlation between these two parameters: the greater the reduction in AgRP neuron activity that occurred upon food detection, the more food the mouse subsequently consumed ($R^2 = 0.36$, $P = 0.02$, **Figure 4.3E**).

To test whether this correlation between AgRP neuron sensory response and subsequent food intake extends to other conditions, we investigated the effect of treatment with lipopolysaccharide (LPS), a bacterial toxin that causes visceral malaise and inhibits food intake. We found that treatment of fasted mice with LPS significantly reduced both the inhibition of AgRP neurons by food presentation ($\Delta F/F$ $-35.1 \pm 4.1\%$ after vehicle versus $-13.1 \pm 3.1\%$ after LPS, $P < 10^{-4}$) and subsequent food intake (0.57 g after vehicle versus 0.10 g after LPS, $P < 10^{-4}$) (Figure 4.10A-C). Analysis of individual LPS-treated animals revealed a clear correlation between these two parameters: animals that consumed no food showed essentially no sensory inhibition of AgRP neurons, whereas animals that consumed some food had a diminished but measurable response (Figure 4.10D). These findings further support a model in which the sensory regulation of AgRP neurons encodes a prediction of imminent food consumption (Chen and Knight, 2016; Chen et al., 2015).

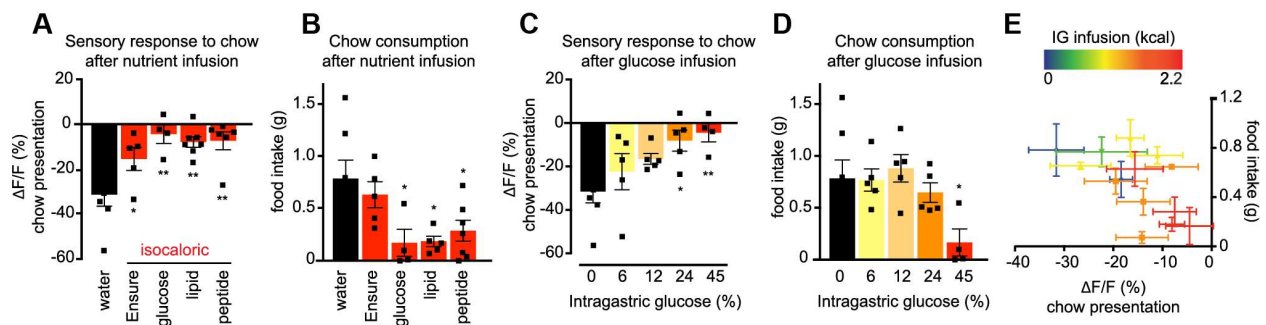


Figure 4.3. AgRP neuron inhibition in response to the sensory detection of food is inversely related to intragastric calorie infusion and predicts subsequent chow consumption.

(A and C) Quantification of $\Delta F/F$ during photometry recording from AgRP neurons in fasted mice for 5 min following chow presentation. Chow was presented 15 min after the end of intragastric infusion of the indicated nutrients. ($n = 4-7$ mice per group). (B and D) Food intake was recorded for the first 20 minutes of re-feeding during the experiment described in (A and C). (E) Correlation of $\Delta F/F$ following chow presentation with food intake during the first 20 minutes of re-feeding for all intragastric infusions in fasted animals shown in Figure 2. Points on the scatter plot represent mean \pm SEM. Color gradient represents caloric content of the infusates. (A-D) ■ denotes individual mice. Bars represent mean \pm SEM. $*P < 0.05$, $**P < 0.01$ compared to H_2O infusion (Holm-Sidak multiple comparisons test, adjusted p-value).

The inhibition of AgRP neurons during nutrient infusion does not require changes in blood glucose

Intragastric nutrients begin to inhibit AgRP neuron activity within five minutes of the start of infusion (**Figure 4.1E**). This timing suggests that a signal triggered by nutrient detection in the gut likely mediates the inhibition of AgRP neurons, but it does not rule out a role for a change in the level of a circulating metabolite.

To distinguish between these mechanisms, we first analyzed the role of blood glucose, since glucose has been proposed to inhibit AgRP neurons directly (Becskei et al., 2008). We observed no change in blood glucose following intragastric infusion of fat or protein (**Figure 4.11A**), indicating that the inhibition of AgRP neurons by those macronutrients is glucose-independent. In contrast and as expected, intragastric infusion of glucose caused a dose-dependent rise in blood glucose measured at the completion of infusion (**Figure 4.11B**). To assess whether this rise in blood glucose was sufficient to explain the concomitant inhibition of AgRP neurons, we measured the neural response to an equivalent parenteral glucose dose. We found that intraperitoneal (IP) glucose (4.5 g/kg) caused only a transient reduction of AgRP neuron activity ($\Delta F/F$ $-10.8 \pm 1.4\%$ at 5 min versus $-1.7 \pm 1.8\%$ at 30 min, **Figure 4.11D, E**). In contrast, a similar dose of glucose delivered intragastrically (12% glucose) resulted in a stronger and sustained inhibition ($\Delta F/F$ $-10.1 \pm 2.1\%$ at 5 min and $-17.1 \pm 5.7\%$ at 30 min, **Figure 4.11D,E**). This was true even though animals that received IP glucose exhibited a robust increase in circulating glucose levels that persisted for at least 30 minutes (**Figure 4.11C**). Thus, changes in blood glucose levels are not correlated with the inhibition of AgRP neurons following administration of glucose or other nutrients, and therefore blood glucose cannot explain the inhibition of AgRP neurons by intragastric nutrient infusion.

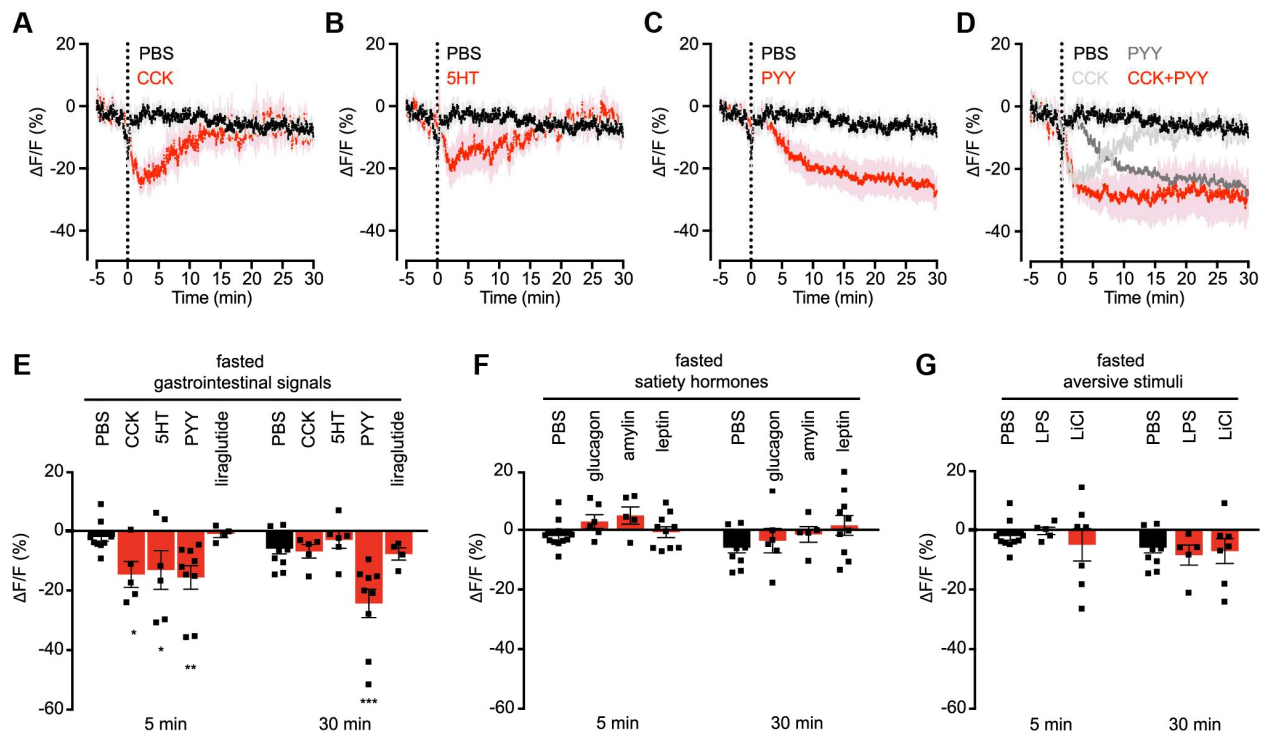


Figure 4.4. CCK, PYY, and 5HT are sufficient to inhibit AgRP neuron activity

(A-D) Calcium signal from AgRP neurons in fasted mice after IP injection with PBS (black) or CCK (A), 5HT (B), PYY(C), or a combination of CCK and PYY (D) (red). Traces represent mean \pm SEM. Traces showing $\Delta F/F$ for individual injections of CCK and PYY are also shown in (D) (gray). (n=5-11 mice per group). (E) Quantification of $\Delta F/F$ from (A-C). Quantification of $\Delta F/F$ following liraglutide injection is also shown. (F and G) Quantification of $\Delta F/F$ during photometry recording in fasted mice following IP injection of the indicated compounds.

(E-G) ■ denotes individual mice. Times shown are 5-min windows 5 and 30 min after injection. Bars represent mean \pm SEM. * $P < 0.05$, ** $P < 0.01$, *** $P < 10^{-3}$ compared to PBS injection at the indicated time point (Holm-Sidak multiple comparisons test, adjusted p-value).

The gut-secreted hormones 5HT, CCK, and PYY are sufficient for the inhibition of AgRP neurons

Nutrient detection in the gut triggers the release of many hormones that inhibit food intake (Clemmensen et al., 2017; Tolhurst et al., 2012). To investigate whether these satiation signals are able to regulate AgRP neuron activity, we fasted mice overnight, challenged them with IP injection of a panel of candidate hormones, and then measured the response by photometry.

Three gastrointestinal hormones were sufficient to reduce AgRP neuron activity following peripheral injection: 5HT, CCK, and PYY (**Figure 4.4A-C**). Among these, PYY has previously been proposed to regulate AgRP neuron activity (Acuna-Goycolea and van den Pol, 2005; Riediger et al., 2004), whereas a role for peripheral 5HT and CCK has not been described. Interestingly, these three signals showed different kinetics of AgRP neuron inhibition *in vivo* (**Figure 4.4A-C**). 5HT and CCK caused a rapid but transient reduction in AgRP neuron activity (T_{\max} inhibition CCK = $186 \pm 1s$, 5HT = $446 \pm 113s$), whereas PYY induced a slower, more sustained response (T_{\max} inhibition $1409 \pm 196s$). Since these hormones are co-released from the gut following food ingestion, we challenged fasted mice with injection of combinations of these signals. Co-injection of CCK and PYY resulted in a rapid and sustained inhibition of AgRP neurons that matched the linear superposition of the response to the individual hormones (**Figure 4.4D; Figure 4.12A, D**). In contrast, co-injection of CCK and 5HT had no additive effect (**Figure 4.12B, D**). The responses to individual hormones were unaffected by whether the mice were fasted or fed (**Figure 4.12E**), consistent with the ability of intragastric nutrients to reduce AgRP neuron activity even in fed animals (**Figure 4.2K**).

We observed no response of baseline AgRP neuron activity to peripheral injection of lithium chloride or LPS (**Figure 4.4G**), two agents that are commonly used to induce nausea. Thus visceral malaise is unlikely to contribute to the inhibition of AgRP neurons following administration of 5HT, CCK, or PYY. We also found that a number of hormones implicated in the control of food intake had no acute effect on AgRP neuron dynamics (**Figure 4.4E, F**), including amylin, glucagon, glucagon-like peptide-1 (GLP-1), and, surprisingly, leptin (**Figure 4.4F, 4.12**). Thus AgRP neurons are rapidly modulated by a subset of peripheral signals involved in energy homeostasis.

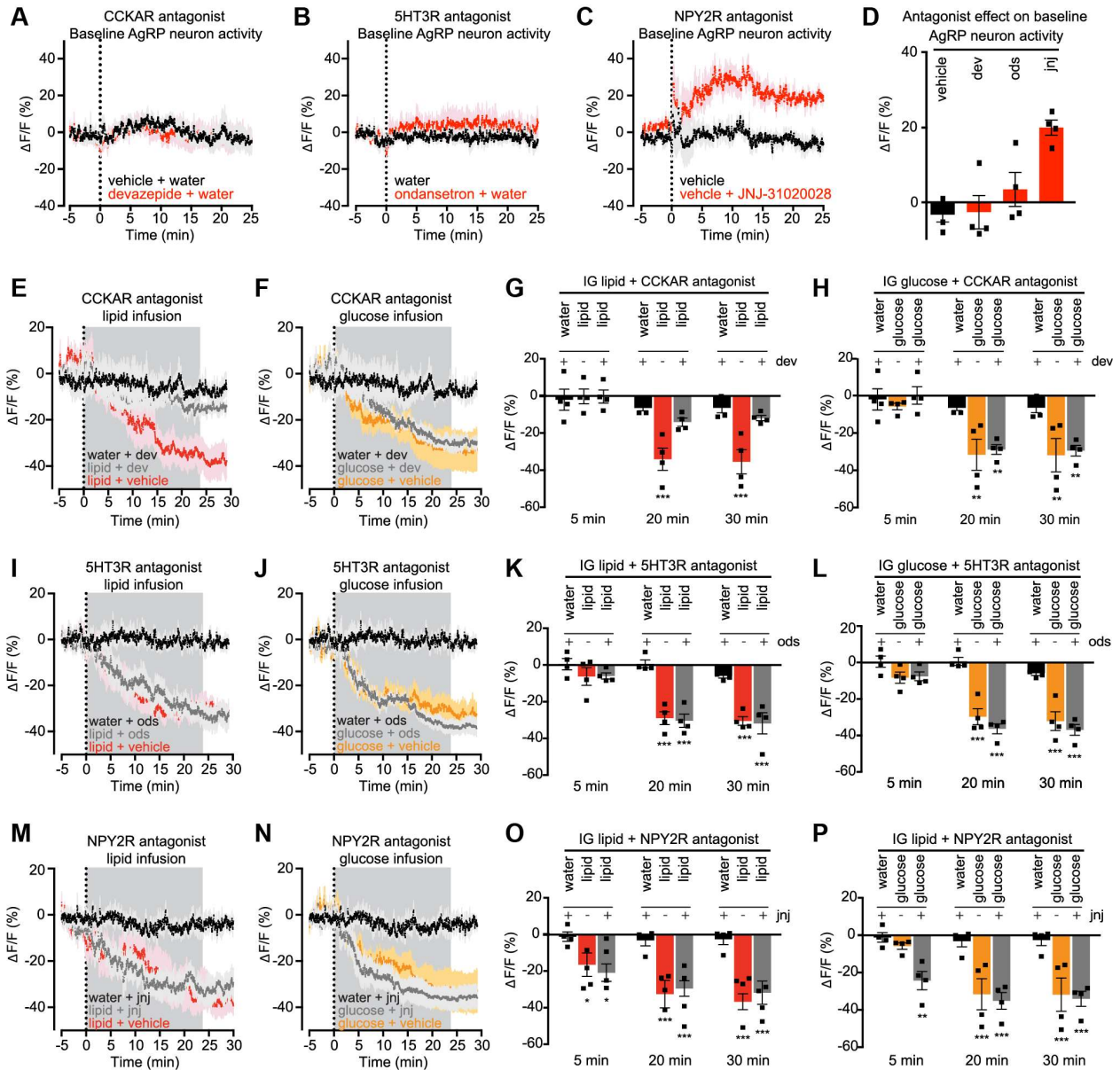


Figure 4.5. PYY is necessary for inhibiting the basal firing rate of AgRP neurons. CCK is necessary for AgRP neuron inhibition caused by lipid.

(A-C) Calcium signal from AgRP neurons in fasted mice in response to vehicle (black) or devazepide (dev, A), ondansetron (ods, B), or JNJ-31020028 (jnj, C) (red). (D) Quantification of $\Delta F/F$ from (A-C). Time shown is a 5-min time window 25 min after antagonist administration. (E and F) Calcium signal in fasted mice after intragastric injection of dev or vehicle followed by intragastric infusion of lipid (E) or glucose (F). (G and H) Quantification of $\Delta F/F$ from (E and F). $n = 4$ mice per group. (I and J) Calcium signal from AgRP neurons in fasted mice after intragastric injection of ods or vehicle followed by intragastric infusion of lipid (I) or glucose (J). (K and L) Quantification of $\Delta F/F$ from (I and J). $n = 4$ mice per group. (M and N) Calcium signal from AgRP neurons in fasted mice after subcutaneous injection of jnj or vehicle followed by intragastric infusion of lipid (M) or glucose (N). (O and P) Quantification of $\Delta F/F$ from (M and N). $n = 4$ mice per group.

(A-C, E, F, I, J, M, N) Traces represent mean \pm SEM

(G, H, K, L, O, P) Times shown are 5-min windows from the early part of infusion (5 min), the end of infusion (20 min), and 10 min following the end of infusion (30 min).

■ denotes individual mice. Bars represent mean \pm SEM. * $P < 0.05$, *** $P < 10^{-3}$ compared to vehicle at the indicated time point.

Gastrointestinal satiation signals are differentially required for the regulation of AgRP neurons

The preceding data demonstrate that peripheral 5HT, CCK, and PYY are sufficient to inhibit AgRP neurons. To test whether these hormones are necessary, we treated mice with antagonists of their receptors and then recorded AgRP neuron calcium dynamics, both at baseline and in response to infusion of specific nutrients.

CCK inhibits food intake by binding to CCK-A receptors (CCKARs) in the periphery and brain (Reidelberger, 1994). Treatment of mice with a selective CCKAR antagonist (devazepide) had no effect on the baseline activity of AgRP neurons in fasted mice (**Figure 4.5A,D**), but dramatically attenuated the lipid-mediated inhibition of AgRP neurons ($\Delta F/F -35.5 \pm 3.5\%$ after vehicle + lipid versus $-11.9 \pm 1.7\%$ after devazepide + lipid infusion, $P = <0.001$, **Figure 4.5E,G**). In contrast, devazepide pretreatment had no effect on the response of AgRP neurons to intragastric glucose infusion (**Figure 4.5F,H**). This indicates that CCK is required for the inhibition of AgRP neurons by fat but not glucose, which is consistent with the observation that fat is the most potent stimulus for CCK secretion *in vivo* (Berthoud, 2008; Tolhurst et al., 2012).

Analysis of 5HT signaling is complicated by the presence of 14 different receptors. Among these, the 5HT 3A receptor (5HTR3A) is highly expressed in vagal afferents and has been implicated in nutrient sensing (Berthoud, 2008). However, we found that treatment with a 5HTR3A antagonist (ondansetron) had no effect on the baseline activity of AgRP neurons in fasted mice (**Figure 4.5B,D**) or their inhibition by intragastric lipid or glucose infusion (**Figure 4.5I-L**). Thus HTR3A signaling is individually dispensable for the regulation of AgRP neurons, but may modulate these cells in concert with other 5HT receptors.

PYY acts through NPY2 receptors (NPY2Rs) expressed in both the periphery and brain (Broberger et al., 1997). Unexpectedly, we found that treatment of fasted mice with an NPY2R antagonist (JNJ-31020028) caused a rapid increase in the activity of AgRP neurons at baseline ($\Delta F/F$ $-5.0 \pm 3.2\%$ after vehicle versus $19.8 \pm 2.3\%$, $P = 0.006$ **Figure 4.5C, E**). In contrast JNJ-31020028 had no effect on the inhibition of AgRP neurons by infusion of intragastric lipid or glucose (**Figure 4.5M-P**). This indicates that AgRP neurons are under tonic inhibition by an NPY2R-mediated signal in fasted mice, but that PYY is dispensable for their nutritional regulation by fat or sugar consumption.

Leptin has no acute effect on calcium dynamics in AgRP and POMC neurons measured by photometry

Leptin is a critical regulator of arcuate feeding circuits, but we observed no acute effect of leptin on AgRP neuron activity in fasted mice, either when leptin was injected alone (**Figure 4.5F and 4.13**) or in combination with CCK (**Figure 4.12C**). This was unexpected because leptin has been reported to rapidly inhibit AgRP neuron activity *in vitro* ((Takahashi and Cone, 2005; van den Top et al., 2004) but see also (Claret et al., 2007)) and to synergistically inhibit food intake when co-administered with CCK (Barrachina et al., 1997). We therefore investigated in more detail how leptin modulates arcuate feeding circuits *in vivo*.

We first extended our analysis to include POMC neurons, which are activated by leptin *in vitro* (Cowley et al., 2001), and also to test the role of nutritional state. We observed no acute effect of leptin administration on the dynamics of either AgRP (**Figure 4.13A-D**) or POMC neurons (**Figure 4.13I-L**) in either fasted or fed animals. To increase the sensitivity of our assay, we repeated these experiments in knockout mice that have no endogenous leptin and thus are hypersensitive to exogenous leptin (AgRP^{Cre} ob/ob and POMC^{Cre} ob/ob). Remarkably, we failed to observe any rapid leptin-induced change in AgRP (**Figure 4.13E-H**) or POMC neuron (**Figure 4.13M-P**) dynamics even in an ob/ob background and even after increasing the dose of

leptin to supraphysiologic levels (**Figure 4.13Q,R**). We confirmed the bioactivity of our leptin by showing that it induced pSTAT3 in the arcuate nucleus after peripheral injection (**Figure 4.13U-X**), and further that it reduced food intake and body weight in *ob/ob* mice (**Figure 4.6L,M** and **Figure 4.8F**). We also confirmed the functionality of our photometry assay by validating that each mouse showed a robust response to two positive control stimuli: ghrelin administration to fed mice (**Figure 4.13S, T**), and food presentation to fasted mice (**Figure 4.7**). Thus, despite *in vitro* data suggesting that leptin rapidly modulates the electrical activity of AgRP and POMC neurons, we find that leptin has no acute effect on the calcium dynamics of these cells *in vivo*.

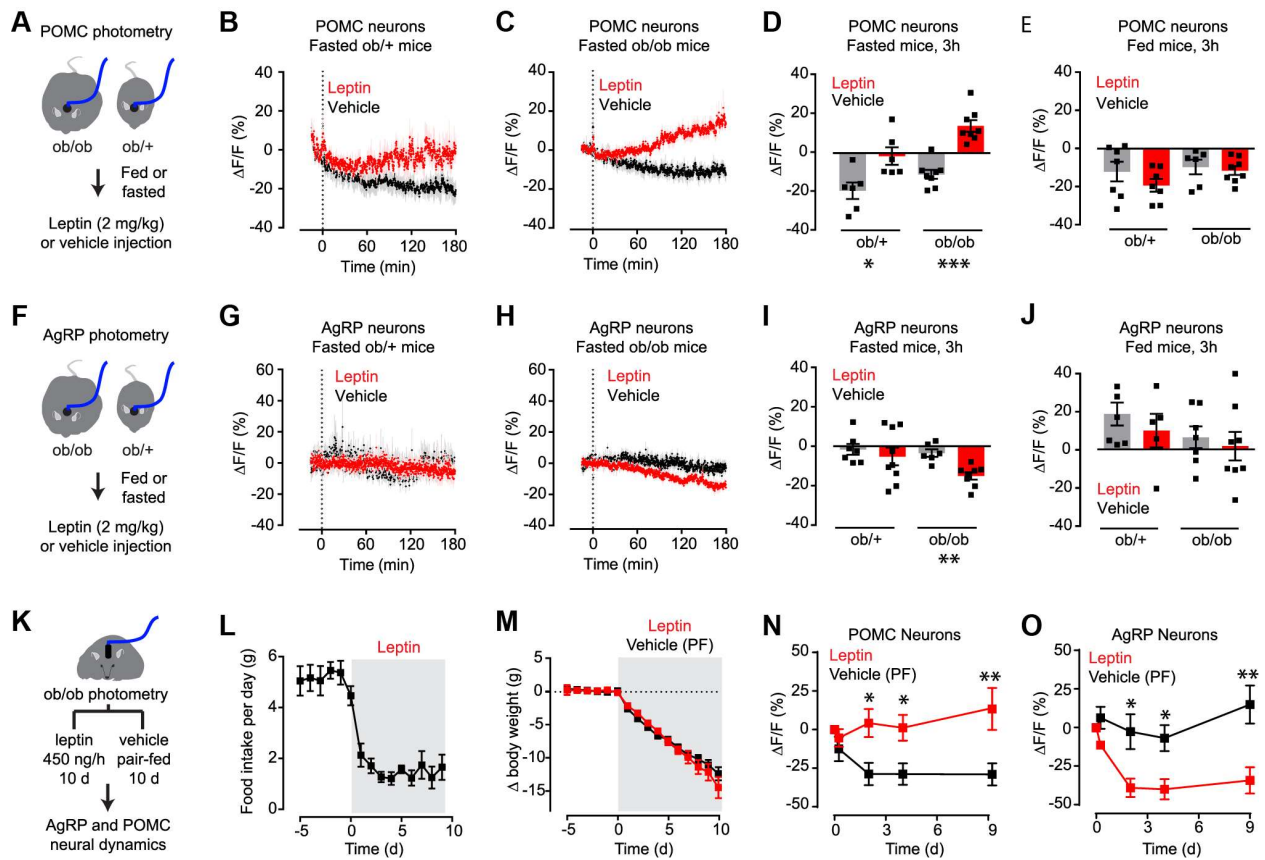


Figure 4.6. Leptin gradually modulates the activity of AgRP and POMC neurons in fasted animals.

(A) Schematic of experiments in (B-E). 3 hour photometry recording from POMC neurons in fasted or fed *ob/ob* and *ob/+* mice injected with leptin. (B and C) Calcium signal from POMC neurons in fasted *ob/+* (B) and *ob/ob* (C) mice after vehicle (black) or leptin (red) injection. (n = 6-8 mice per group). (D and E) Quantification of $\Delta F/F$ of POMC neurons after prolonged photometry recording following IP injection of vehicle or leptin in fasted (D) and fed (E) states. (F) Schematic of experiments in (G-J). 3 hour photometry recording from AgRP neurons in

fasted or fed ob/ob and ob/+ mice injected with leptin. **(G and H)** Calcium signal from AgRP neurons in fasted ob/+ (G) and ob/ob (H) mice after vehicle (black) or leptin (red) injection. (n = 7-8 mice per group) **(I and J)** Quantification of $\Delta F/F$ of AgRP neurons after prolonged photometry recording following IP injection of vehicle or leptin in fasted (I) and fed (J) states. **(K)** Schematic of experiments in (L-O). Body weight, food intake, and photometry signals from AgRP and POMC neurons were measured in ob/ob mice during chronic leptin or vehicle infusion by mini-osmotic pumps. Vehicle treated animals were pair-fed (PF) to leptin treated animals. Mini-osmotic pump was implanted at day 0 **(L and M)** Food intake (L) and change in body weight (M) following vehicle or leptin infusion. (n = 9 mice per group). **(N and O)** Quantification of $\Delta F/F$ following vehicle (black) or leptin (red) infusion by mini-osmotic pump in POMC (N) and AgRP (O) neurons. (n = 4 mice).

(B, C, G, H, L, M, N, O) Traces represent mean \pm SEM

(D,E,I,J) \square \blacksquare denotes individual mice. Bars represent mean $\Delta F/F \pm$ SEM over a 15-min window 3 hours after injection.

* $P < 0.05$, ** $P < 0.01$, *** $P < 10^{-3}$

See also Figure 4.13.

Leptin gradually inhibits AgRP neurons and activates POMC neurons on a timescale of hours

In addition to rapid modulation of ionic currents, leptin can also induce changes in gene expression that develop over hours and have long-term effects on synaptic plasticity (Pinto et al., 2004). To investigate these slower responses *in vivo*, we administered leptin by IP injection to fasted ob/ob mice as well as ob/+ littermates, and then recorded the photometry response of AgRP and POMC neurons for three hours in the absence of food (**Figure 4.6**). This revealed a slow onset activation of POMC neurons ($\Delta F/F = 13.8 \pm 2.3$ for leptin versus -10.7 ± 2.3 for vehicle $P < 0.0001$; **Figure 4.6C, D**) and inhibition of AgRP neurons ($\Delta F/F = -15.0 \pm 1.9$ for leptin versus -3.4 ± 2.0 for vehicle, $P = 0.0018$; **Figure 4.6H, I**). As expected, this modulatory effect was smaller in ob/+ animals that have endogenous leptin (**Figure 4.6B,G**). In fed animals leptin failed to induce any change in AgRP or POMC neuron dynamics after three hours, even in ob/ob mice (**Figure 4.6E,J** and **Figure 4.13**). Thus, leptin induces a reciprocal activation of POMC neurons and inhibition of AgRP neurons that develops on a timescale of hours, is enhanced in leptin-deficient animals, and is only evident in a state of food deprivation.

To explore further these long-term effects, we measured the neural response to leptin infusion (**Figure 4.6K**). *ob/ob* mice were equipped for photometry measurements of AgRP or POMC neurons and then implanted with subcutaneous mini-osmotic pumps dispensing leptin or vehicle. Following pump implantation, vehicle-treated animals were pair-fed to leptin-treated animals to eliminate any effects of differential food intake. As expected, leptin treatment caused a precipitous decrease in food intake and body weight (**Figure 4.6L, M**). Periodic photometry measurements in these mice revealed that, relative to vehicle-treated controls, leptin induced activation of POMC neurons and inhibition of AgRP neurons (**Figure 4.6N, O**). This modulation reached a maximum within three days and persisted through the termination of the experiment ($\Delta F/F = -38.9 \pm 6.0\%$ for AgRP-leptin versus $-2.5 \pm 11.3\%$ for AgRP-vehicle, $P = 0.017$; $\Delta F/F = 4.2 \pm 9.1\%$ for POMC-leptin versus $-28.8 \pm 7.2\%$ for POMC-vehicle, $P = 0.015$; **Figure 4.6N, O**). Thus chronic leptin infusion induces a durable modulation of AgRP and POMC neuron activity *in vivo*, consistent with the effects of this hormone on feeding.

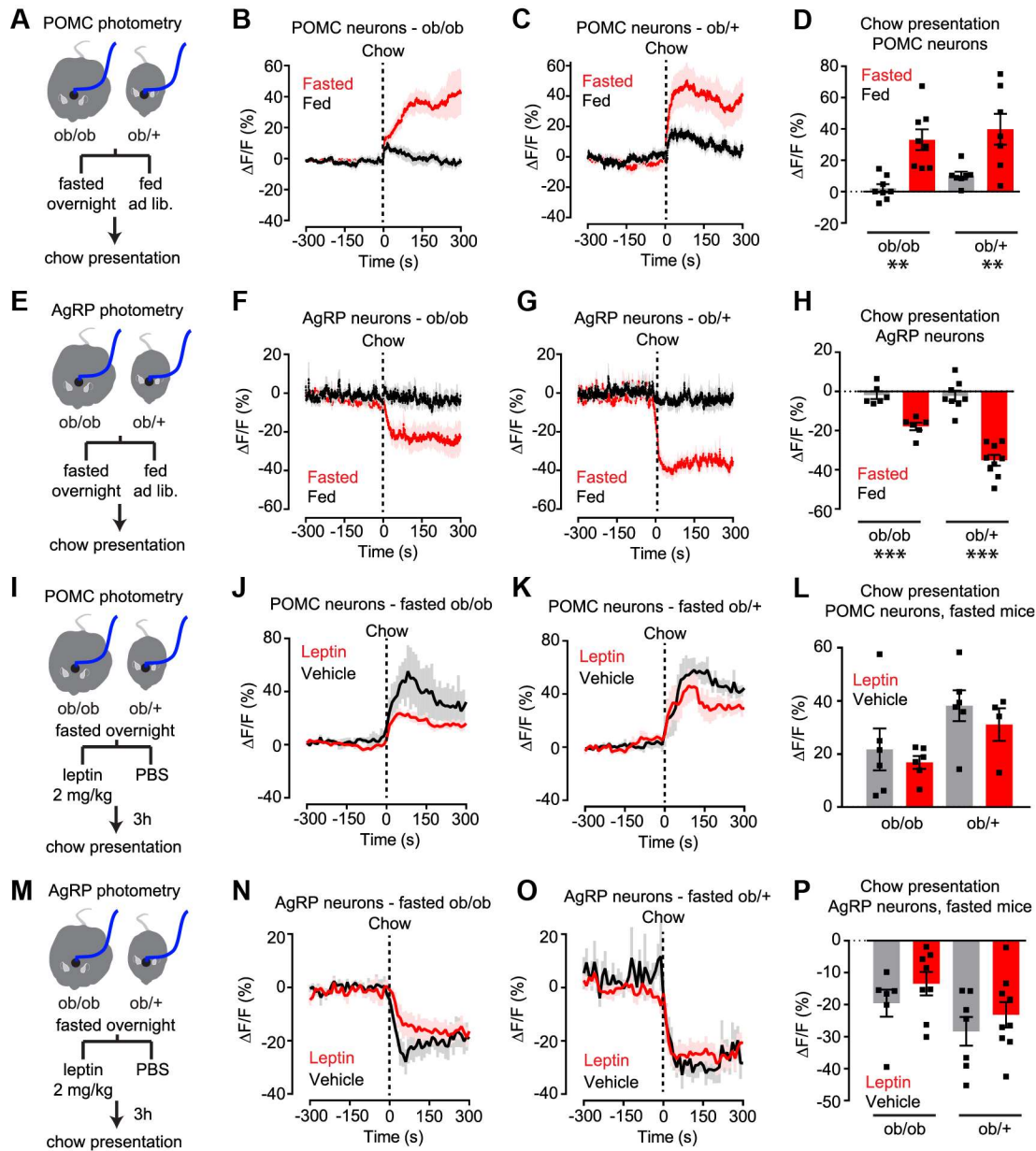


Figure 4.7. Leptin is neither necessary nor sufficient for gating the sensory regulation of AgRP and POMC neurons.

(A) Schematic of experiments in (B-D). Photometry recording from POMC neurons in fasted and fed ob/ob and ob/+ mice in response to chow presentation. (B and C) Calcium signal from POMC neurons in ob/ob (B) and ob/+ (C) mice in response to chow presentation in the fed (black) or fasted (red) state. (n = 7-8 mice per group). (D) Quantification of $\Delta F/F$ from (B, C). (E) Schematic of experiments in (F-H). Photometry recording from AgRP neurons in fasted and fed ob/ob and ob/+ mice in response to chow presentation (F and G) Calcium signal from AgRP neurons in ob/ob (F) and ob/+ (G) mice in response to chow presentation in the fed (black) or fasted (red) state (n = 6-9 mice per group). (H) Quantification of $\Delta F/F$ from (F, G). (I) Schematic of experiments in (J-L). Photometry recording from POMC neurons in fasted ob/ob and ob/+ mice in response to chow presentation after vehicle or leptin injection. (J and K) Calcium signal from POMC neurons in ob/ob (J) and ob/+ (K) mice in response to chow presentation after

vehicle (black) or leptin (red) injection. (n = 4-6 mice per group). **(L)** Quantification of $\Delta F/F$ from (J, K). **(M)** Schematic of experiments in (N-P). Photometry recording from AgRP neurons in fasted ob/ob and ob/+ mice in response to chow presentation after vehicle or leptin injection. **(N and O)** Calcium signal from AgRP neurons in ob/ob (N) and ob/+ (O) mice in response to chow presentation after vehicle (black) or leptin (red) injection (n= 6-9 mice per group). **(P)** Quantification of $\Delta F/F$ from (N,O).

(B, C, F, G, J, K, N, O) Traces represent mean \pm SEM

(D,H,L,P) ■ denotes individual mice. Bars represent mean $\Delta F/F \pm$ SEM over a 5-min window following chow presentation. * $P < 0.05$, ** $P < 0.01$, *** $P < 10^{-3}$

Leptin is neither necessary nor sufficient for gating the sensory regulation of AgRP and POMC neurons

In addition to regulating the baseline activity of AgRP and POMC neurons, leptin could also modulate their sensitivity to other signals, including the sensory detection of food (Betley et al., 2015; Chen et al., 2015; Mandelblat-Cerf et al., 2015). We therefore investigated how leptin might alter the responsiveness of these neurons to food cues.

We first compared the neural response to food presentation in ob/ob and ob/+ mice (**Figure 4.7**). As expected, presentation of chow to fasted ob/+ mice rapidly activated POMC neurons and inhibited AgRP neurons, whereas presentation of chow to fed mice had little effect (**Figure 4.7C, G**). Unexpectedly, the response of ob/ob mice to chow presentation was also strictly dependent on nutritional state, with responses in fasted but not fed animals ($\Delta F/F = 33.1 \pm 6.6\%$ for fasted versus $2.1 \pm 2.6\%$ for fed POMC, $P = 0.0019$; $\Delta F/F = -17.9 \pm 1.9\%$ for fasted versus -1.9 ± 2.0 for fed AgRP, $P = 0.0005$; **Figure 4.7B,F**). We extended this analysis by measuring the neural responses to presentation of peanut butter, an energy rich food that modulates AgRP and POMC neurons even in fed animals (Chen et al., 2015). Again, the neural response of ob/ob mice to food presentation was indistinguishable from ob/+ littermates (**Figure 4.14**). Thus, although ob/ob mice are hyperphagic, the regulation of their AgRP and POMC neurons by food cues remains dependent on whether the animal is fasted or fed.

Given that leptin is not necessary for regulation of AgRP or POMC neurons by food cues (**Figure 4.7A-H**), we tested whether it is sufficient. Fasted mice were challenged with peripheral

leptin injection and the neural response to chow presentation measured three hours later. We chose this time point because three hours is required to observe robust changes in AgRP and POMC neuron activity after leptin injection (**Figure 4.6**). In animals pre-treated with leptin, we observed a trend toward reduced activation of POMC neurons (**Figure 4.7I-L**) and reduced inhibition of AgRP neurons (**Figure 4.7M-P**) in response to food presentation in both *ob/ob* and *ob/+* genetic backgrounds. However none of these effects reached significance when compared to vehicle-treated controls (**Figure 4.7L, P**). Taken together, these data demonstrate that changes in plasma leptin concentrations across a wide range have little to no effect on the nutritional gating of the sensory regulation of AgRP and POMC neurons. Thus, other nutritional signals must play a dominant role in regulating the sensitivity of these neurons to sensory cues.

AgRP neurons are epistatic to leptin's effects on food intake

Leptin administration profoundly inhibits food intake in *ob/ob* mice, but the identity of the key neural targets remains unresolved (Myers et al., 2009). We therefore investigated how AgRP neuron activity functionally interacts with leptin in the control of feeding behavior (**Figure 4.8**).

To enable manipulation of AgRP neuron activity, we generated mice that express channelrhodopsin-2 (ChR2) in AgRP neurons in either wild-type ($\text{AgRP}^{\text{ChR2}}$) or leptin-deficient ($\text{AgRP}^{\text{ChR2}} \text{ ob/ob}$) genetic backgrounds, and then equipped these mice with an optical fiber positioned above the arcuate nucleus (**Figure 4.8A**). In the absence of photostimulation, *ad libitum* fed mice ate little during a 60-minute trial (0.21 ± 0.05 g for wild-type versus 0.33 ± 0.05 g for *ob/ob*; **Figure 4.8B-D**). Stimulation of AgRP neurons for 60 minutes prior to food availability (Chen et al., 2016) resulted in a significant increase in subsequent food intake that was similar between groups (0.74 ± 0.07 g for wild-type versus 0.76 ± 0.10 g for *ob/ob*; two way ANOVA effect of stimulation, $P < 10^{-3}$). The striking similarity in food intake between wild-type and *ob/ob* mice was not due to a ceiling effect, because both genotypes consumed more food

during an alternative costimulation protocol (1.2 ± 0.1 g for wild-type versus 1.1 ± 0.1 g for ob/ob). The fact that ob/ob mice do not consume more food than wild-type animals following AgRP neuron stimulation is consistent with a model in which leptin deficiency increases food intake by acting at or upstream of AgRP neuron activity.

To test this a different way, we investigated the interaction between leptin treatment and AgRP neuron stimulation. AgRP^{ChR2} ob/ob mice were treated with leptin or vehicle by continuous subcutaneous infusion (**Figure 4.8E**). Leptin treatment resulted in a significant reduction in body weight over the first three days of infusion (**Figure 4.8F**) and leptin-treated animals ate less food than vehicle-treated controls in a 60-minute trial conducted without photostimulation (0.05 ± 0.02 g for leptin-treated versus 0.32 ± 0.04 g for vehicle-treated; **Figure 4.8G, H**). However, prestimulation of AgRP neurons for 60 minutes prior to food availability resulted in increased food intake that was similar between groups (0.47 ± 0.07 g for leptin-treated versus 0.60 ± 0.08 g for vehicle-treated; **Figure 4.8G,H**). This similarity in food intake between leptin and vehicle-treated animals was again not due to a ceiling effect, because both cohorts consumed more food during a costimulation protocol (0.89 ± 0.22 g for leptin-treated versus 0.76 ± 0.15 g for vehicle-treated; **Figure 4.8G, H**). Thus AgRP neuron photostimulation can bypass the ability of leptin to block food intake, suggesting that inhibition of AgRP neurons is required for leptin's effects on feeding.

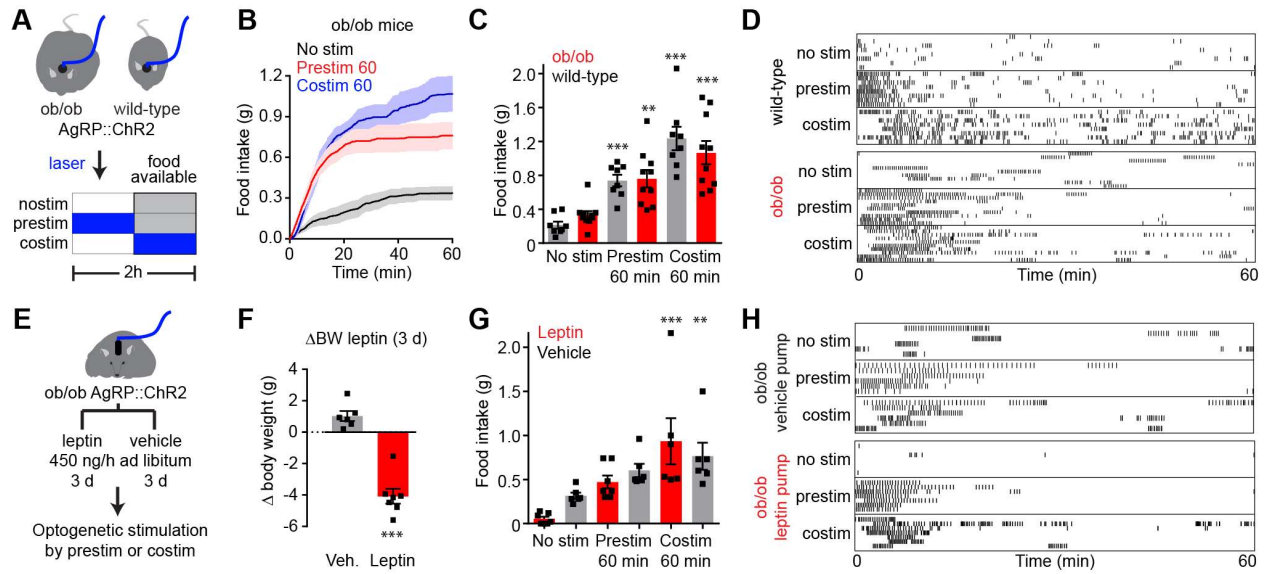


Figure 4.8. AgRP neurons are epistatic to leptin's effect on food intake.

(A) Schematic of experiments in (B-D). Optogenetic stimulation of AgRP neurons in *ad libitum* fed WT and *ob/ob* mice prior to (prestim) or during (costim) food availability. Blue indicates the timing of laser stimulation. (B) Cumulative food intake by *ob/ob* mice after no stimulation (black), 60 min pre-stimulation (red), or during 60 min co-stimulation (blue). Traces represent mean \pm SEM ($n = 6-10$ mice per group). (C) Quantification of food intake from (B). (D) Raster plots showing feeding pattern in individual mice from (B and C). (E) Schematic of experiments in (F-H). Optogenetic stimulation of AgRP neurons in *ad libitum* fed, *ob/ob* mice during chronic vehicle or leptin infusion by mini-osmotic pumps. Stimulation occurred prior to (prestim) or during (costim) food availability as in (A). (F) Bodyweight change in *ob/ob* mice 3 days after implantation of a mini-osmotic pump infusing vehicle (gray, $n = 4$ mice) or leptin (red, $n = 5$ mice) (G) Quantification of food intake by *ad libitum* fed *ob/ob* mice from (F) receiving chronic vehicle (gray) or leptin (red) infusion after no stimulation, 60 min pre-stimulation, or during 60 min co-stimulation. (H) Raster plots showing feeding pattern in individual mice from (G). (C, F, G) ■ denotes individual mice. Bars represent mean \pm SEM. * $P < 0.05$, ** $P < 0.01$, *** $P < 10^{-3}$. (D and H) Each row represents a single trial from a different animal and each point indicates consumption of a 0.02 g pellet.

DISCUSSION

Feeding is regulated by communication between the gut and brain. For decades, this process has been studied by manipulating hormones and other peripheral signals and then measuring the effect on behavior (Richter, 1942). While much has been learned from this effort, it has left unresolved the question of how this gut-brain communication is represented in the activity of specific neural circuits. Indeed, we know remarkably little about how any nutritional signal influences the dynamics of feeding circuits in an awake, behaving animal.

To observe this gut-brain communication directly, we developed a preparation that combines intragastric nutrient infusion with optical recording of AgRP neuron dynamics in awake, behaving mice. This preparation separates the hard-wired regulation of AgRP neurons by nutrients from their learned regulation by sensory cues. Using this approach, we have discovered layers of previously unsuspected regulation of these cells. We have found that AgRP neurons are inhibited by gastrointestinal nutrients on a timescale of minutes, in a way that is proportional to the number of calories infused but independent of macronutrient identity or nutritional state. We have further shown that this negative feedback loop involves a combination of gut hormones that are differentially required for the response to different nutrients. Conversely, we have shown that leptin, the most widely-studied hormone that regulates feeding, modulates circuit dynamics only on a timescale of hours. These findings reveal fundamental mechanisms that govern hunger and satiety, while also demonstrating a generally applicable strategy for dissecting gut-brain communication.

AgRP neurons are inhibited by gastrointestinal nutrients during satiation

Studies of the regulation of AgRP neurons have traditionally focused on a small set of hormones, including most prominently leptin and ghrelin (Cowley et al., 2001; Cowley et al., 2003; Nakazato et al., 2001; Pinto et al., 2004). While these hormones provide one mechanism for coupling AgRP neuron activity to nutritional state, their circulating levels are thought to reflect primarily long-term changes in energy balance, not acute fluctuations in nutrients caused by food consumption. Acute responses to food intake are instead mediated by gastric distension and the release of “gut peptides” which trigger satiation and meal termination (Cummings and Overduin, 2007). Satiation is predominantly a brainstem phenomenon (Grill and Norgren, 1978), which is modulated by but does not require input from the forebrain. Consequently it has remained unclear whether hypothalamic feeding circuits are informed of satiation in real-time and, if so, what signals are involved and what specific information is communicated.

We have shown here that AgRP neurons are inhibited by intragastric nutrients with kinetics that mirror the process of satiation, strongly suggesting that some of the same signals that govern meal termination regulate these cells. Consistent with this, we have demonstrated that three well-established satiation signals are sufficient to inhibit AgRP neuron activity *in vivo*: PYY, CCK, and 5HT. Interestingly, we have found that CCK is necessary for the inhibition of AgRP neurons by intragastric lipid, but dispensable for their regulation by glucose (**Figure 4.5**), indicating that information about food intake is communicated to AgRP neurons in a nutrient-specific way. This implies that AgRP neurons are able to monitor the complex hormonal milieu that develops following consumption of different foods and extract information about their caloric content.

While CCK is necessary for the inhibition of AgRP neurons by intragastric lipid, the identity of the signals that are required for the response to intragastric protein and glucose remain unknown. We have shown that blood glucose levels do not correlate with AgRP neuron inhibition when glucose is delivered by different routes, indicating that circulating glucose is not the sole signal that communicates glucose ingestion to arcuate feeding circuits. We have also shown that GLP-1, the most prominent gastrointestinal peptide released following glucose ingestion, is not sufficient to inhibit AgRP neurons *in vivo*. However we cannot rule out more complex mechanisms involving interactions between glucose and hormones, nor can we exclude a role for intracellular glucose in regulating AgRP neuron activity directly (Andrews et al., 2008).

A second important question regards the pathway by which CCK and other signals communicate nutritional information to AgRP neurons *in vivo*. Receptors for CCK and PYY are expressed on vagal afferents that innervate the gastrointestinal tract (Berthoud, 2008), and abdominal vagotomy reduces the anorectic effect of both hormones (Koda et al., 2005; Reidelberger, 1994). Thus it is possible that these hormones communicate with AgRP neurons via an ascending neural pathway that includes vagal afferents. On the other hand, AgRP

neurons express the PYY receptor (Broberger et al., 1997), and PYY can directly inhibit AgRP neuron firing in slice (Acuna-Goycolea and van den Pol, 2005), suggesting that circulating PYY may act directly on these cells. Combining the experimental preparation described here with systematic manipulation of the afferent pathways will enable these mechanisms to be distinguished

Leptin induces a slow modulation of AgRP and POMC neurons that is required for its ability to inhibit feeding

Leptin is a critical regulator of food intake thought to modulate its targets by two distinct mechanisms: gating of ion channels, resulting in rapid modulation of neural firing (Cowley et al., 2001; van den Top et al., 2004) and changes in gene expression, resulting in slower alterations in neural excitability (Pinto et al., 2004) and neurotransmitter levels (Schwartz et al., 1996; Stephens et al., 1995). While both of these mechanisms have been studied extensively using indirect and *ex vivo* approaches (Sohn et al., 2013), neither has yet been investigated by monitoring directly how leptin modulates the dynamics of feeding circuits *in vivo*.

To address this question, we measured how leptin administration modulates the activity of AgRP and POMC neurons in awake, behaving mice. To obtain a complete picture of this hormone's effects, we recorded calcium dynamics while systematically varying the leptin dose, route of delivery (injection versus infusion), timescale (minutes to days), genetic background (*ob/ob* versus wild-type), nutritional state (fasted versus fed) and measured readout (baseline activity versus sensory regulation). The unanimous finding from these experiments was that leptin has no acute effect on calcium dynamics in AgRP or POMC neurons, but instead induces a slow modulation that develops over hours and persists as long as leptin is continually delivered. This change in baseline activity correlated with changes in food intake but surprisingly was neither necessary nor sufficient for the nutritional gating of the response of AgRP and POMC neurons to sensory cues. Complementary optogenetic manipulations demonstrated that

AgRP neuron activation could bypass leptin's effects on feeding, suggesting that the slow inhibition of AgRP neurons is required for leptin's anorectic effects. Together, these findings reveal how leptin modulates its key neural targets *in vivo*.

In contrast to our findings, prior studies have reported rapid effects of leptin on AgRP and POMC neurons in slice (Claret et al., 2007; Cowley et al., 2001; Takahashi and Cone, 2005; van den Top et al., 2004). One possible explanation for this discrepancy is that fiber photometry measures population calcium dynamics and therefore may fail to detect changes in activity that occur in a small subset of cells. However the fact that we observe dramatic modulation of AgRP and POMC neurons in response to many other stimuli places an upper bound on the magnitude of any rapid leptin-mediated effect. Of note, this lack of a rapid response to leptin is consistent with the kinetics of the behavioral and autonomic responses to this hormone, which develop over hours (Pinto et al., 2004). Thus we propose that leptin's effects on feeding are mediated primarily by long-term changes in neural activity, probably involving transcription-dependent synaptic plasticity (Horvath, 2005; Horvath and Diano, 2004). This conclusion reemphasizes the importance of identifying the transcriptional targets of leptin, which remain poorly defined, in order to understand this hormone's biological effects.

AgRP neuron activity encodes an integrated estimate of energy balance

AgRP neurons are commonly described as "hunger neurons," but recent *in vivo* recording experiments have called into question what exactly is encoded in the activity of these cells (Betley et al., 2015; Chen et al., 2015; Mandelblat-Cerf et al., 2015). The rapid inhibition of AgRP neurons by the sight and smell of food suggests that they do not control hunger or food intake directly (Chen and Knight, 2016), although they powerfully modulate these processes by indirect means (Chen et al., 2016). In the present study, we have described how AgRP neurons are regulated by visceral signals, which has revealed previously unknown layers of interactions

between nutrients, hormones, nutritional state, and sensory cues. How do these observations fit together to explain the biological function of these cells?

The data presented here demonstrate that AgRP neurons receive three streams of information, each of which evolves on a different timescale (**Figure 4.15**). The first stream consists of homeostatic signals, such as leptin, that report on energy reserves within the body and fluctuate over hours (**Figure 4.6**). The second consists of signals triggered by nutrient detection in the gut that report on calories ingested over the past few minutes (**Figure 4.2**). The third stream consists of sensory cues from the outside world that report on the moment-by-moment availability of food (Betley et al., 2015; Chen et al., 2015; Chen et al., 2016; Mandelblat-Cerf et al., 2015) and predict imminent food consumption (**Figure 4.3 and 4.10**). We propose that the function of AgRP neurons is to integrate these three streams of information to generate a coherent estimate of the animal's energy needs. Importantly, this process takes into account not only current energy reserves, but also predicted changes in energy balance due to ongoing or impending food intake. Such an integration of feedforward and feedback signals would enable the most accurate estimate of energy balance, which would have obvious survival benefit. We believe that accumulating evidence supports this model of AgRP neurons as “energy calculators” that continually estimate nutritional state and then broadcast this information to downstream circuits, rather than as neurons that directly control behavioral output. An important challenge for the future will be to clarify further how AgRP neurons perform this energy calculation, since this is likely a major determinant of body weight in mammals.

METHODS

Stereotaxic surgery

For photometry experiments, recombinant AAV expressing cre-dependent GCaMP6s (AAV1.CAG.Flex.GCaMP6s) was purchased from the Penn Vector Core. AAV was stereotaxically injected unilaterally above the arcuate nucleus of AgRP-IRES-Cre mice. In the

same surgery a custom-made photometry cannula (Doric Lenses; MFC_400/430-0.48_6.1mm_MF2.5_FLT) was implanted unilaterally in the ARC at the coordinates $x=-0.3\text{mm}$, $y=-1.85\text{mm}$, $z=-5.8\text{mm}$ from bregma. Mice were allowed 2–4 weeks for viral expression and recovery from surgery before photometry recording, mini-osmotic pump implantation or intragastric catheter implantation.

For optogenetic experiments, custom-made fiberoptic implants (Thorlabs ; 0.39 NA $\text{\O}200$ mm core FT200UMT and CFLC230-10) were placed unilaterally above the arcuate nucleus of AgRP-IRES-Cre; ROSA-loxStoplox-ChR2-eYFP mice at the coordinates $x=-0.25$ from bregma, $y=-1.7$ from bregma, $z=-5.6$ to -5.7 from dorsal skull surface. Mice were allowed 2–3 weeks recovery from surgery before behavior experiments or mini-osmotic pump implantation.

Intragastric catheter implantation

Intragastric catheters were made and implanted as described in detail previously (ref). AgRP-IRES-Cre mice with functional photometry implants were anesthetized with ketamine/xylazine and the surgical areas shaved and scrubbed with betadine and alcohol. A skin incision of about 1 cm was made between the scapula and the skin dissected from the subcutaneous tissue toward the left flank. A midline abdominal skin incision about 1.5 cm was made extending from the xyphoid process caudally and the skin was dissected from the subcutaneous tissue toward the left flank to complete a subcutaneous tunnel between the two incisions. A hemostat was used to pull the ethylene oxide-sterilized catheter through the tunnel. The linea alba was incised and the abdominal cavity entered. A small incision was made in the left lateral abdominal wall through which the intragastric catheter was passed into the abdominal cavity. The stomach was externalized and a small puncture made using a jeweler's forcep. The tip of the catheter was immediately placed into this punctured area and sutured into place with polypropylene suture

(CP medical 8695P). Saline injection into catheter confirmed absence of leakage. The stomach was placed back in the abdominal cavity. The abdominal muscle was sutured and the skin incision closed in two layers. Next, the catheter was secured at its interscapular site with sutures into surrounding muscle. Finally, the interscapular skin incision was closed. Post-operatively, mice were treated with enrofloxacin, normal saline, and buprenorphine and allowed 7-10 days to recover prior to infusion and photometry experiments.

Mini-osmotic Pump Implantation

Mini-osmotic pumps with a release rate of about 0.5ul/hr (Alzet, Model 2002) were filled with vehicle or leptin to achieve release of 450 ng leptin per hour. These pumps were implanted subcutaneously into the dorsum of mice. An incision was made and a subcutaneous pocket created by tissue spreading. The pump was placed in this pocket and the skin wound closed with sutures. Animals were allowed to recover for 3 days prior to photometry or optogenetic experiments. This delay also ensured the pumps were primed..

Fiber photometry

Two rigs for performing fiber photometry recordings were constructed following basic specifications previously described. Laser and chopper were shared between two rigs with beam splitter (Thorlabs CM1-BS013) and BNC signal splitter respectively. To reduce photobleaching during recordings that exceeded 3 hours, the laser was modulated as 1 second every 10 seconds by a TTL signal (Graphic State software). Each pulse was then extrapolated into a single data point by calculating the median of the center 50%. All experiments were performed in sound-proof behavioral chambers (Coulbourn H10-11M-TC). Experiments were performed during the dark cycle in a dark environment.

Intragastric infusions.

Nutrients or water were infused via intragastric catheters using a syringe pump (Harvard Apparatus, 70-2001). All infusions were delivered at 50 microliters per minute with a total infusion volume of 1.2 mL. All photometry experiments involving intragastric infusion were performed in fasted animals unless otherwise specified. Animals were habituated to behavioral chambers for 20 min during photometry recording. During this time, the intragastric catheter was attached to the syringe pump using plastic tubing and adapters (Tygon, AAD04119; Instech, LS20). Total infusion time was 24 min for all experiments. After infusion, photometry recording was allowed to continue for 15 min before animals were presented with chow (PicoLab 5058). Photometry recording continued for 20 min following chow presentation. One to three trials of the same experiment for each mouse were combined, averaged, and treated as a single replicate. Vanilla Ensure powder was dissolved in deionized water (diH₂O) fresh for each experiment at a concentration of 0.42 grams/mL of solution. Other infused nutrients were also made fresh for each experiment as follows: 20% intralipid (Sigma-Aldrich) both undiluted and diluted to 6.4% with diH₂O; premium collagen peptides (Sports Research) diluted in diH₂O at concentrations of 0.45 grams/mL and 0.15 grams/mL; glucose diluted in diH₂O at concentrations of 0.45 g, 0.24 g, 0.12 g, and 0.06 g per mL; sucrose, fructose and galactose in diH₂O at 0.24 g/mL; and sucralose diluted in diH₂O at 8mg/mL. For peristimulus plots time zero was defined as the moment that the infusion pump was started

Drug and hormone injections

For photometry experiments, the following hormones and small molecules were injected at the indicated concentrations and routes during recording. All compounds were injected at a volume of 10 ul/g body weight. Animals were habituated to the recording chambers for 20 minutes prior to injection. Following hormone injection, photometry recording continued for 35 min or longer as indicated. For the combination injection of leptin and CCK, leptin was injected 2 hours prior

to the start of recording, and then animals were habituated and injected with CCK as described for other experiments. For other hormone combinations, both hormones were injected simultaneously after habituation to the recording chamber. One to three trials of the same experiment for each mouse were combined, averaged, and treated as a single replicate. For peristimulus plots time zero was defined as the moment that the behavior chamber is opened by the investigator.

We used the following doses, which are based on previously published reports, unless otherwise specified. Glucose 4.5 g/kg IP (Sigma), CCK octapeptide 10 ug/kg IP (Bachem), serotonin hydrochloride 2 mg/kg IP (Sigma-Aldrich), PYY 0.1 mg/kg IP (Tocris), leptin 2 mg/kg IP (R&D Systems), liraglutide 0.4 mg/kg IP (Novo Nordisk; generous gift from Dr. Randy Seeley), amylin 10 ug/kg IP (Tocris), glucagon 2 mg/kg SQ (Bachem), lithium chloride 84 mg/kg IP (Acros), LPS 100 ug/kg (Sigma), and ghrelin 2mg/kg IP (R&D Systems).

Food and Object Presentation

To eliminate any effects of novelty mice were exposed prior to testing to peanut butter, chocolate, and “cages” as described in the main text. Mice were either fasted overnight (16 h) or fed *ad libitum*, acclimated to the behavioral chamber, and then presented with chow, peanut butter, caged chocolate, or available chocolate as indicated in the main text. For peristimulus plots time zero was defined as the moment that the behavior chamber is opened by the investigator.

Optogenetic Feeding Behavior

Optogenetic stimulation was performed as previously described. A 473 nm laser was modulated by Coulbourn Graphic State software through a TTL signal generator (Coulbourn H03-14) and synchronized with behavior experiments. The laser was split through a 4- way splitter (Fibersense and Signals) or passed through a single patch cable (Doric Lenses). The laser was

then passed to custom-made fiber optic patch cables (Thorlabs FT200UMT, CFLC230-10; Fiber Instrument Sales F12774) through a rotary joint (Doric Lens FRJ 1x1). Patch cables were connected to the implants on mice through a zirconia mating sleeve (Thorlabs ADAL1). For opto-stimulation protocols, laser was modulated at 20 Hz on a 2 s ON and 3 s OFF cycle with 1 ms pulse width. Laser power was set between 15–20 mW at the terminal of patch cable. We estimated the light power at the ARC to be 4.02 mW/mm². Effective power is likely lower due to loss at the cable-implant connection.

Feeding behavior experiments were performed as previously described (Chen et al. 2016). Mice were allowed to recover for seven days after optogenetic implant surgery before experiments. During this time, in addition to regular chow, mice were given *ad libitum* access to the food pellets used during behavioral testing (20 mg Bio-Serv F0163) in their home cage unless otherwise specified. Mice were habituated to the behavioral chambers (Coulbourn H10-11M-TC with H10-11M-TC-NSF) and pellet dispensing systems (Coulbourn H14-01M-SP04 and H14-23M) for three days before the first experiment. Mice were provided *ad libitum* access to food and water unless otherwise specified. Experiments were run during the early phase of the light cycle.

All pre-stimulation food intake experiments follow this general structure: 70 min habituation/pre-stimulation period with no food access followed by 60 min food access. Pellet removal from the pellet dispensing system was detected using a built-in photo-sensor (Coulbourn H20-93). Food pellets left on the ground after each session were counted and deducted from the total food consumed.

Quantification and Statistical Analysis

Photometry analysis

Data were analyzed using a custom MatLab script. In intragastric infusion and IP hormone injection experiments, background fluorescence was corrected by subtracting the photometry

signal in the absence of mice from total signal. For peri-stimulus time plots, unless otherwise specified, the median value of data points within a 2 min window flanking the -5 min time point before each treatment was used as the normalization factor (F_0) to calculate $\Delta F(t)/F_0 = (F(t) - F_0)/F_0$. For experiments where recording data was sampled from pulsed lasers (1 second per 10 seconds), the median of all data points 15min before each treatment was used as the normalization factor to ensure reliable representation of the activity state. For experiments that track fluorescence signal strength across different days, the median of data points measured 20-30min after the start of the photometry recording session on day 0 were used as the normalization factor (F_0). The median of the fluorescent signal 20-30min after the start of recording on each of the subsequent days was defined as $F(t)$ and used to estimate $\Delta F(t)/F_0 = (F(t) - F_0)/F_0$.

For all experiments correction for photobleaching was not necessary due to the low laser power used during photometry recordings (~ 0.07 mW), the short time windows for most experiments (around 60 min), pulsed laser used for long-term experiments and the fact that all experimental groups had control groups treated with identical laser powers. To calculate the change of fluorescent signal at indicated time points after treatment, all data points $F(t)$ over the indicated time range were averaged as F_a to estimate $\Delta F_a/F_0 = (F_a - F_0)/F_0$.

Behavior Data Analysis

Data were analyzed using a custom MatLab script. Consumption of each pellet was defined as the first pellet removal event after each food pellet delivery. Total food consumption was estimated by subtracting the pellets found dropped after each experiment from the total number of food removal events. Multiple trials of the same experiment for each mouse were combined, averaged, and treated as a single replicate.

Statistical analysis

Fiber photometry data were subjected to analysis as described above. In figures 1-5, 7, and S1-S4, $\Delta F/F(\%)$ represents the mean $\Delta F(t)/F_0 \times 100$. Bar graphs depicting photometry data in these figures show the mean $\Delta F/F(\%)$ over a 5 minute time window as indicated in the figure legends. For the 3h photometry recordings shown in figure 4.6, bar graphs depict the mean $\Delta F/F(\%)$ over a 15-min window from 165-180 min after injection. For photometry signal comparisons across days shown in figure 4.6, $\Delta F/F(\%)$ represents $\Delta F(t)/F_0 \times 100$ as described in photometry analysis.

The effects of different intragastric infusates or hormone injections on fluorescence changes in photometry experiments as well as changes in blood glucose following intragastric infusion were analyzed using two-way, repeated-measures ANOVA. Changes in fluorescence in response to chow presentation and quantity of chow consumption after intragastric infusion were compared using one-way ANOVA. The effects of leptin administration and presentation of food on fluorescence changes in photometry experiments as well as changes in food intake following mini-osmotic pump delivery of leptin were analyzed using two-way ANOVA. The effects of optogenetic stimulation on food intake were compared using two-way, repeated-measures ANOVA. Holm-Sidak's multiple comparisons test was used in conjunction with ANOVA. All statistical analysis was performed using Prism. Statistics and numbers of animals are included in the figure legends. Significance was defined as $P < 0.05$ and is indicated on figures and in figure legends.

SUPPLEMENTARY FIGURES



Figure 4.9. - related to Figure 4.1. Intragastric infusion of water causes stomach distension (A-D) Photographs of the stomach of an anesthetized, intragastric catheterized mouse before (A and B) and after (C and D) infusion of 1.2 mL of deionized water over 24 minutes

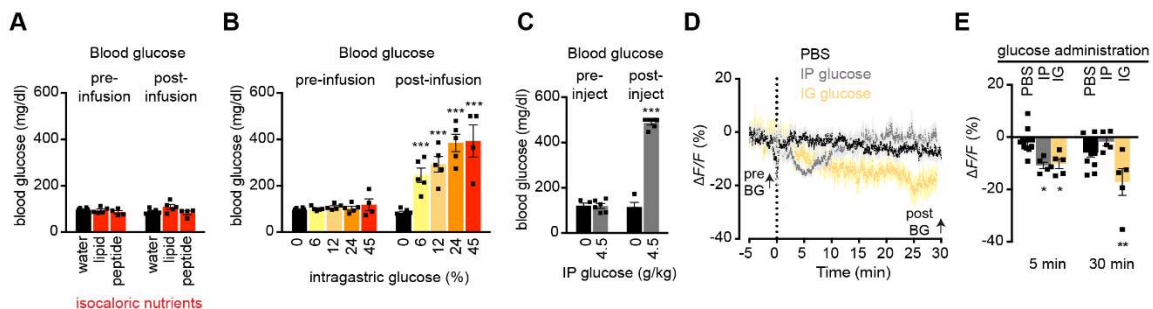


Figure 4.10. - related to Figure 4.2. AgRP neuron inhibition in response to intragastric and systematic administration of glucose

(A) Blood glucose in fasted mice immediately before and after intragastric infusion of water, lipid, or peptide. (n = 6-7 mice per group). (B) Blood glucose in fasted mice immediately before and after intragastric infusion of the indicated concentrations of glucose (n = 4-7 mice per group). ***P < 0.001 compared to pre-infusion blood glucose (Holm-Sidak multiple comparisons test, adjusted p-value). (C) Blood glucose in fasted mice immediately before and 35 minutes after IP administration of glucose 4.5 g/kg or PBS (n = 4 mice for PBS; n = 6 mice for glucose). ***P < 0.001 compared to pre-injection blood glucose (Holm-Sidak multiple comparisons test, adjusted p-value). (D) Calcium signal from AgRP neurons in fasted mice after IP injection with PBS (black) or glucose 4.5 g/kg (gray), or during intragastric infusion with 12% glucose (yellow). Traces represent mean ± SEM. Time points at which blood glucose was checked are indicated.

(E) $\Delta F/F$ from (D). Times shown are 5-min windows 5 and 30 min after injection or the start of infusion ($n = 5-11$ mice per group). $*P < 0.05$, $**P < 0.01$ compared to PBS injection at the indicated time point (Holm-Sidak multiple comparisons test, adjusted p-value). Bars represent mean \pm SEM

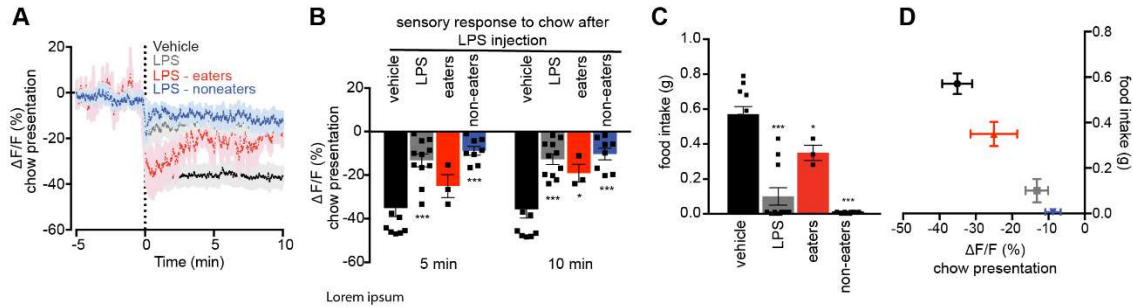


Figure 4.11. - related to Figure 4.3. AgRP neuron inhibition in response to the sensory detection of food and subsequent chow intake are attenuated by LPS injection.

(A) Calcium signal from AgRP neurons in fasted mice presented with chow 4 hours after LPS (gray) or vehicle (black) injection. Also shown are the subsets of LPS-injected animals that ate no chow (blue) and those that consumed some amount of chow (red). Traces represent mean \pm SEM **(B)** Quantification of $\Delta F/F$ from (A). Times shown are 5-min windows 5 and 10 min after chow presentation ($n = 11$ mice per group; for subgroups, $n = 3$ for eaters and $n = 8$ for non-eaters) **(C)** Food intake was recorded for the first 20 minutes of re-feeding during the experiment described in (A and B). **(D)** Correlation of $\Delta F/F$ following chow presentation with food intake during the first 20 minutes of re-feeding for the experiment in (A-C). Points on the scatter plot represent mean \pm SEM. There was a significant correlation between $\Delta F/F$ and food intake ($R^2 = 0.99$, $P < 10^{-4}$; Pearson correlation) (B and C) ■ denotes individual mice. Bars represent mean \pm SEM. $*P < 0.05$, $***P < 10^{-3}$ compared to vehicle injection at the indicated time point.

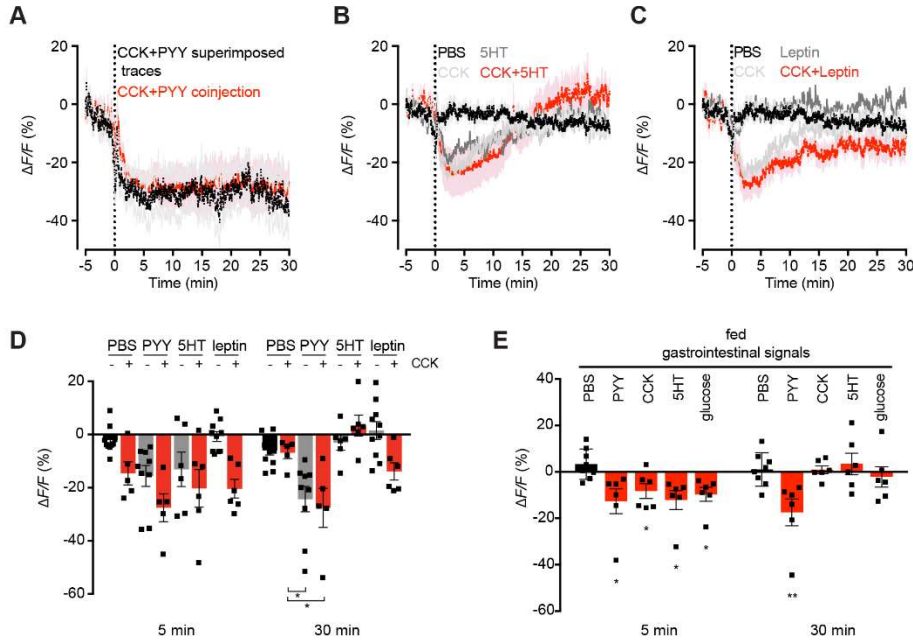


Figure 4.12. - related to Figure 4.4. Systemic hormones can have additive effects on AgRP neuron activity, and are effective in both fed and fasted mice.

(A) Calcium signal from AgRP neurons in fasted mice after co-injection of CCK and PYY (red) compared to the sum of the effect of individual injections of CCK and PYY (black). (n=5 mice per group). **(B and C)** Calcium signal from AgRP neurons in fasted mice after intraperitoneal injection with PBS (black) or combinations of CCK and serotonin (B) or CCK and leptin (C) (red). Traces showing $\Delta F/F$ for individual injections of CCK, serotonin, and leptin are also shown (gray traces) (n=5-11 mice per group). **(D)** Quantification of $\Delta F/F$ from (B and C, and from Figure 4.5D). *P < 0.05 compared to CCK injection at the indicated time point (Holm-Sidak multiple comparisons test, adjusted p-value). **(E)** Quantification of $\Delta F/F$ during photometry recording from AgRP neurons in ad libitum fed mice following IP injection of the indicated compounds. (n = 6-8 mice per group). *P < 0.05, **P < 0.01 compared to PBS injection at the indicated time point (Holm-Sidak multiple comparisons test, adjusted p-value).

(A-C) Traces represent mean \pm SEM.

(D and E) Times shown are 5-min windows 5 and 30 min after injection. Bars represent mean \pm SEM

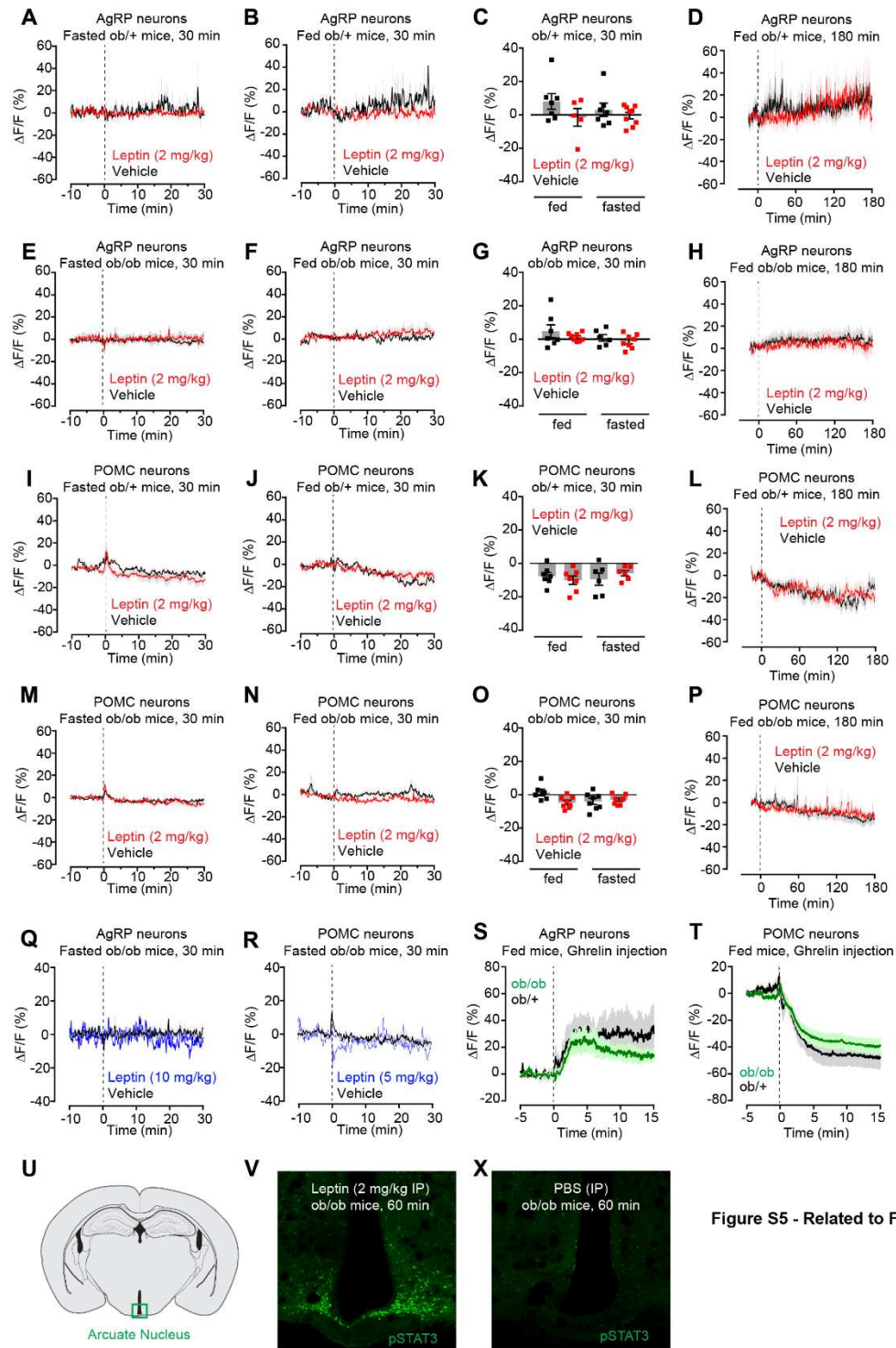


Figure S5 - Related to Figure 6

Figure 4.13. – Related to Figure 4.6. Leptin has no acute effect on the calcium dynamics of AgRP and POMC neurons.

(A and B) Calcium signal from AgRP neurons during photometry recording in fasted (A) and ad libitum fed (B) ob/+ mice after IP injection with vehicle (black traces) or leptin (red traces) (n = 5-9 mice per group). **(C)** Quantification of $\Delta F/F$ from (A, B) **(D)** Calcium signal from AgRP neurons in ad libitum fed ob/+ mice during 3 hours of photometry recording after intraperitoneal injection with vehicle (black trace) or leptin (red trace). (n = 5 mice for leptin; n = 7 mice for vehicle). **(E and F)** Calcium signal from AgRP neurons during photometry recording in fasted (E) and ad libitum fed (F) ob/ob mice after IP injection with vehicle (black traces) or leptin (red traces). (n = 6-8 mice per group). **(G)** Quantification of $\Delta F/F$ from (E, F). **(H)** Calcium signal from AgRP neurons in ad libitum fed ob/ob mice during 3 hours of photometry recording after intraperitoneal injection with vehicle (black trace) or leptin (red trace). (n = 8 mice for leptin; n = 7 mice for vehicle). **(I and J)** Calcium signal from POMC neurons during photometry recording in fasted (I) and ad libitum fed (J) ob/+ mice after IP injection with vehicle (black traces) or leptin (red traces) (n = 6-7 mice per group). **(K)** Quantification of $\Delta F/F$ from (I, J). **(L)** Calcium signal from POMC neurons in ad libitum fed ob/+ mice during 3 hours of photometry recording after intraperitoneal injection with vehicle (black trace) or leptin (red trace). (n = 7 mice for leptin; n = 7 mice for vehicle). **(M and N)** Calcium signal from POMC neurons during photometry recording in fasted (M) and ad libitum fed (N) ob/ob mice after IP injection with vehicle (black traces) or leptin (red traces) (n = 6-8 mice per group). **(O)** Quantification of $\Delta F/F$ from (M, N). **(P)** Calcium signal from POMC neurons in ad libitum fed ob/ob mice during 3 hours of photometry recording after intraperitoneal injection with vehicle (black trace) or leptin (red trace). (n = 8 mice for leptin; n = 6 mice for vehicle). **(Q and R)** Calcium signal during photometry recording from AgRP (Q) and POMC (R) neurons in fasted ob/ob mice after IP injection with vehicle (black traces) or high dose leptin (blue traces). (n=2 mice per group). **(S and T)** Calcium signal during photometry recording from AgRP (S) and POMC (T) neurons in ad libitum fed ob/ob (green traces) and ob/+ (black traces) mice after ghrelin injection (n = 5-8 mice per group). **(U-X)** pSTAT3 immunostaining in the arcuate nucleus 60 min after leptin (V) or vehicle (W) injection. **(A, B, D, E, F, H, I, J, L, M, N, P, Q, R, S, T)** Traces represent mean \pm SEM. Bars represent mean $\Delta F/F \pm$ SEM over a 5-min window 30 min after injection. *P < 0.05, **P < 0.01, ***P < 10⁻³

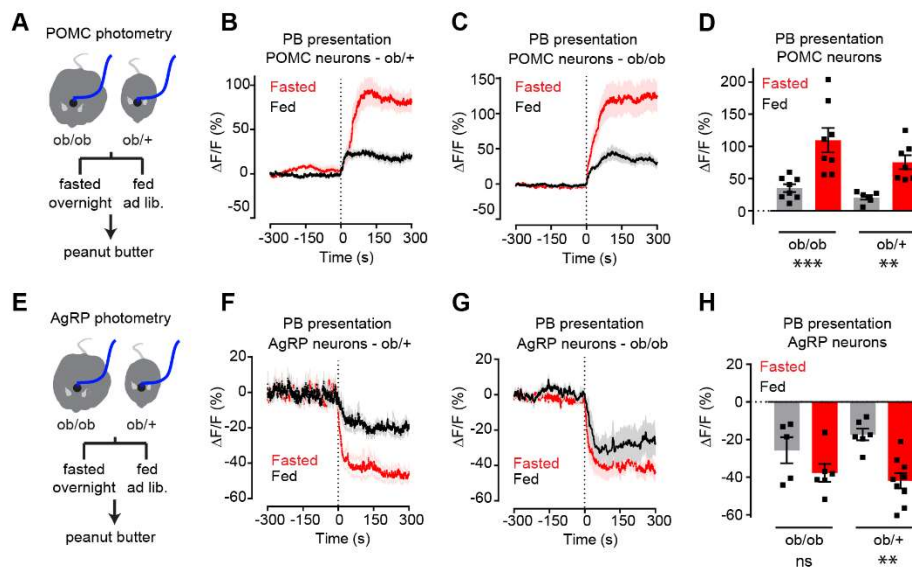


Figure 4.14. – Related to Figure 4.7. Leptin is not necessary for gating the sensory regulation of AgRP and POMC neurons by palatable food.

(A) Schematic of experiments in (B-D) Photometry recording from POMC neurons in fasted and fed *ob/ob* and *ob/+* mice in response to peanut butter presentation. (B and C) Calcium signal from POMC neurons in *ob/+* (B) and *ob/ob* (C) mice in response to peanut butter presentation in the ad libitum fed (black traces) or fasted (red traces) state (n = 6-8 mice per group). (D) Quantification of $\Delta F/F$ from (B,C). (E) Schematic of experiments in (F-H) Photometry recording from AgRP neurons in fasted and fed *ob/ob* and *ob/+* mice in response to peanut butter presentation. (F and G) Calcium signal from AgRP neurons in *ob/+* (F) and *ob/ob* (G) mice in response to peanut butter presentation in the ad libitum fed (black traces) or fasted (red traces) state (n = 5-9 mice per group). (H) Quantification of $\Delta F/F$ from (F,G). (B, C, F, G) Traces represent mean \pm SEM. Bars represent mean $\Delta F/F \pm$ SEM over a 5-min window 5 min after peanut butter presentation. *P < 0.05, **P < 0.01, ***P < 10⁻³

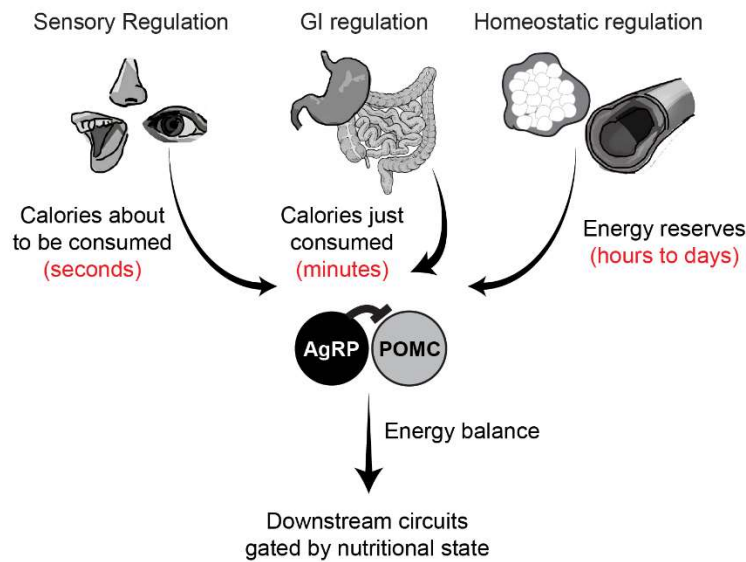


Figure 4.15. Model for how AgRP neurons calculate energy balance by integrating three streams of information that develop on different timescales.

Chapter 5: A sustained valence signal from AgRP neurons that drives feeding

SUMMARY

The neural mechanisms underlying hunger are poorly understood. AgRP neurons are activated by energy deficit and promote voracious food consumption, suggesting these cells may supply the fundamental hunger drive that motivates feeding. However recent in vivo recording experiments revealed that AgRP neurons are inhibited within seconds by the sensory detection of food, raising the question of how these cells can promote feeding at all. Here we resolve this paradox by showing that brief optogenetic stimulation of AgRP neurons before food availability promotes intense appetitive and consummatory behaviors that persist for tens of minutes in the absence of continued AgRP neuron activation. We show that these sustained behavioral responses are mediated by a long-lasting potentiation of the rewarding properties of food and that AgRP neuron activity is positively reinforcing. These findings reveal that hunger neurons drive feeding by transmitting a positive valence signal that triggers a stable transition between behavioral states.

INTRODUCTION

Food deprivation motivates animals to find and consume food. This implies that the brain can transform nutritional signals into the desire to eat, but how this transformation is performed remains unclear. Agouti-related protein (AgRP) neurons within the arcuate nucleus (ARC) of the hypothalamus are a molecularly-defined cell type that is particularly important for the control of feeding. AgRP neurons are regulated by hormones that report on the nutritional state of the body (Cowley et al., 2001; Cowley et al., 2003; Gao and Horvath, 2007; Nakazato et al., 2001; Pinto et al., 2004) and their activity is strongly increased by food deprivation (Hahn et al., 1998; Mandelblat-Cerf et al., 2015). Optogenetic or chemogenetic stimulation of AgRP neurons

promotes intense food consumption as well as appetitive behaviors that lead to food discovery (Aponte et al., 2011; Krashes et al., 2011), whereas inhibition of these neurons leads to aphagia (Gropp et al., 2005; Krashes et al., 2011; Luquet et al., 2005). Thus AgRP neurons are poised to connect nutritional signals with the motivational processes that govern feeding.

Traditionally, AgRP neurons were thought to be regulated primarily by nutritional cues that circulate in the blood (Gao and Horvath, 2007; Luo, 2015). According to this model, AgRP neurons are activated by gradual changes in the concentrations of hormones such as leptin and ghrelin that develop during food deprivation. This generates a “hunger drive” that motivates animals to find and consume food and persists until food consumption restores these hormones to their previous level, thereby inhibiting AgRP neurons and quelling the desire to eat.

Recently, this textbook model was challenged by experiments that recorded for the first time the activity of AgRP neurons in awake, behaving mice (Betley et al., 2015; Chen et al., 2015; Mandelblat-Cerf et al., 2015). These experiments unexpectedly revealed that AgRP neurons are inhibited within seconds by the mere sight and smell of food, or by conditioned cues that predict food availability. These responses were much too fast to be mediated by a hormonal signal, implying that they arise from changes in neural input. Paradoxically, this rapid inhibition was often complete before a single bite of food could be consumed, such that AgRP neuron activity was greatly reduced prior to the onset of feeding. This observation raises the question of how AgRP neurons are able to drive feeding at all.

Several hypotheses have been advanced to explain these counterintuitive findings (Chen and Knight, 2016; Seeley and Berridge, 2015). An important unresolved question regards when AgRP neuron activity must occur in order to influence feeding behavior. While it has long been assumed that AgRP neurons promote feeding primarily through firing that occurs during the act of food intake (Aponte et al., 2011), an alternative possibility is that AgRP neuron activity before food obtainment could be sufficient to elicit the voracious feeding that occurs later (Chen and Knight, 2016). If such a mechanism were operational, then it would explain how AgRP

neurons could promote food intake despite being silenced at the beginning of a meal by sensory cues.

Here we investigate this question by using optogenetics to stimulate AgRP neurons selectively before food availability, thereby “replaying” the natural regulation of these cells that occurs during fasting and refeeding. We find that this preparatory photostimulation is sufficient to elicit voracious food consumption and vigorous operant responding for food in well-fed animals. These sustained behavioral effects develop rapidly, persist for tens of minutes, and can be triggered by stimulation of several distinct anatomic pathways. We show that these long-lasting behavioral changes are mediated by a motivational switch that magnifies the positively rewarding properties of food, and furthermore that AgRP neuron activity is positively reinforcing. These findings reconcile the function of AgRP neurons with their paradoxical natural dynamics, and in doing so reveal the motivational mechanism by which these cells drive food consumption.

RESULTS

AgRP neurons transmit a sustained hunger signal

To test the hypothesis that AgRP neurons drive feeding through a sustained mechanism, we used optogenetics to manipulate AgRP neuron activity before food presentation and then measured the effect on subsequent feeding behavior (**Figure 5.1B**). Ad libitum fed mice expressing channelrhodopsin in AgRP neurons (AgRP-ChR2; **Figure 5.1C**) were acclimated to a behavioral chamber early in the light phase, a time when mice ordinarily eat little, and photostimulated for one hour in the absence of food. Photostimulation was then terminated and food was made available (**Figure 5.1B**). Strikingly, we found that this preparatory photostimulation triggered intense feeding upon subsequent food presentation (**Figure 5.1D-G**). This voracious feeding approached the level of food consumption observed following an overnight fast (**Figure 5.1E**); it did not require learning, as it was observed in the first trial of every mouse (**Figure 5.7**); and it was absent from control mice that lacked ChR2 expression

(Figure 5.7). Thus stimulation of AgRP neurons in the absence of food is sufficient to elicit intense food consumption at a later time when food is made available. Importantly, this observation provides an explanation for how AgRP neurons can promote feeding despite being inhibited at a meal's outset by the sensory detection of food (**Figure 5.1A**).

We investigated the properties of this sustained feeding response. Prestimulation of AgRP neurons for as little one minute was sufficient to increase food intake above the baseline level of unstimulated mice (0.34 ± 0.03 vs 0.14 ± 0.03 g, $p < 0.01$), indicating that the response begins to develop rapidly. Increasing the duration of prestimulation progressively increased the amount of food consumed, reaching a plateau at approximately 30 minutes (**Figure 5.1F**). This relationship between prestimulation duration and subsequent food intake displayed first order association kinetics (**Figure 5.1G**; $R^2 = 0.96$), suggesting that AgRP neuron activity transmits a saturable signal that “builds up” in a downstream circuit element. Consistent with this model, the sustained effects of AgRP neuron activity did not require a specific sequence of light pulses (**Figure 5.7**), although intermittent, high frequency stimulation (20 Hz) was slightly more effective than tonic lower frequency stimulation (10 Hz) at eliciting feeding when the total number of light pulses was held constant. These sustained effects were long-lasting, as introduction of a delay of 30 minutes between the offset of AgRP neuron stimulation and onset of food availability only modestly decreased subsequent food consumption (**Figure 5.1H**). Analysis of the microstructure of feeding revealed that these long-lasting effects were manifest primarily as an increase in bout size, rather than bout number (**Figure 5.1I, J**). Thus AgRP neuron activity transmits a hunger signal that accumulates in a downstream circuit element on a timescale of approximately 30 minutes, resulting in a sustained potentiation of feeding that persists even after AgRP neurons have been silenced.

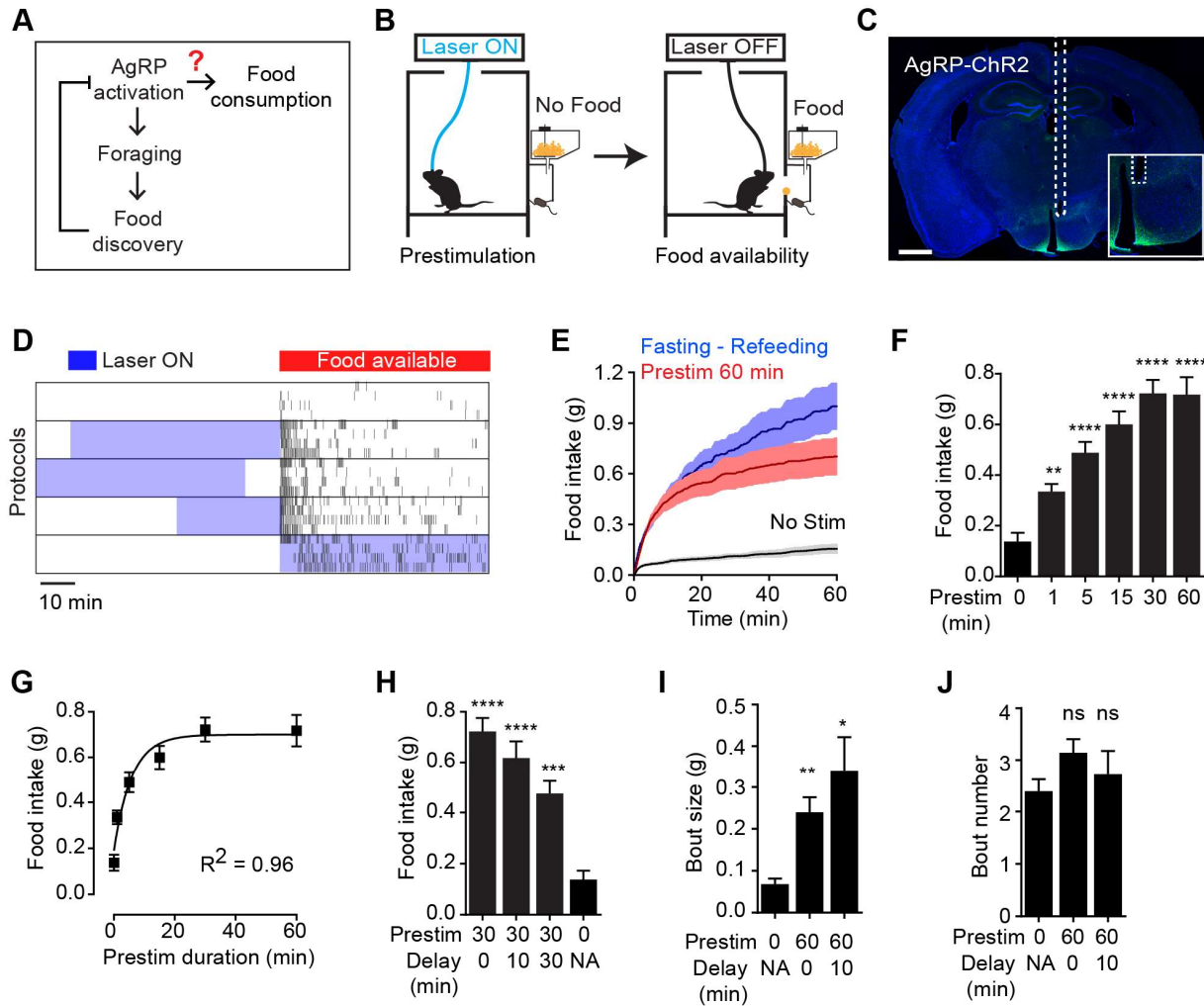


Figure 5.1. Prestimulation of AgRP neurons promotes sustained consummatory behavior.

(A) Current model of feeding control by AgRP neurons illustrating the disconnect between the natural dynamics and orexigenic function of these cells. (B) Schematic of the prestimulation experiment. (C) Expression of ChR2-eYFP in AgRP neurons and optical fiber placement above arcuate nucleus. (D-J) Prestimulating ARC^{AgRP} neurons evokes food consumption in fed mice. (D) Raster plots showing temporal relationship between food pellet consumption events (black vertical bars) and opto-stimulation patterns (blue boxes). (E) Plots of cumulative food intake by mice after 0 min prestim (black $n=7$), 60 min prestim (red $n=7$) and overnight fasting (blue $n=6$). Filled areas indicate S.E.M. (F) Food intake evoked by prestimulation with varied duration ($n=8$). (G) First order association between average total food intake and prestimulation durations (Equation: $Y=Y_0 + (Plateau-Y_0) \cdot (1 - \exp(-K \cdot x))$). (H) Food intake evoked by protocols with different duration of delay between prestimulation and food availability ($n=8$). (I) Bout size analysis of different prestimulation protocols ($n=7$). (J) Bout number analysis of prestimulation protocols ($n=7$). Asterisks on top of bar plots indicate significance levels compared to no stimulation control and asterisks on top of brackets indicate significance levels for comparisons with the respective protocols, using one-way-ANOVA with Holm-Sidak's correction for multiple comparisons (**** $p \leq 0.0001$, *** $0.0001 < p \leq 0.001$, ** $0.001 < p \leq 0.01$, * $0.01 < p \leq 0.05$, ns $p > 0.05$).

Prestimulation of thirst neurons does not have a sustained effect on drinking

We wondered whether this unusual persistent mechanism utilized by AgRP neurons to drive feeding is a general feature of neurons that control ingestive behavior. To test this, we examined thirst-promoting neurons in the subfornical organ that express Nos1 (SFO^{Nos1} neurons). SFO^{Nos1} neurons are activated by circulating signals of fluid balance, and their artificial stimulation is sufficient to drive voracious drinking even in water sated animals (Betley et al., 2015; Oka et al., 2015; Zimmerman et al., 2016). We delivered ChR2 to SFO^{Nos1} neurons by stereotaxic injection of a Cre dependent AAV into the SFO of Nos1-IRES-Cre mice (**Figure 5.2A**), and then measured the effects of optogenetic stimulation of these cells on water consumption (**Figure 5.2B**). As previously reported, photostimulation of SFO^{Nos1} neurons resulted in rapid and intense drinking (508 ± 68 licks for stimulated animals versus 3 ± 1 licks for controls, $p < 0.001$ **Figure 5.2C, D**). However, unlike AgRP neurons, prestimulation of SFO^{Nos1} neurons for one hour prior to water access had no effect on subsequent water intake (**Figure 5.2C, D**). We confirmed that this was not due to a technical problem associated with chronic photostimulation of these cells, because 30 minutes of prestimulation did not impair the ability of subsequent co-stimulation in the presence of water to drive drinking (**Figure 5.2D, column 3**). Thus the persistent mechanism utilized by AgRP neurons to promote feeding does not generalize to related ingestive circuits.

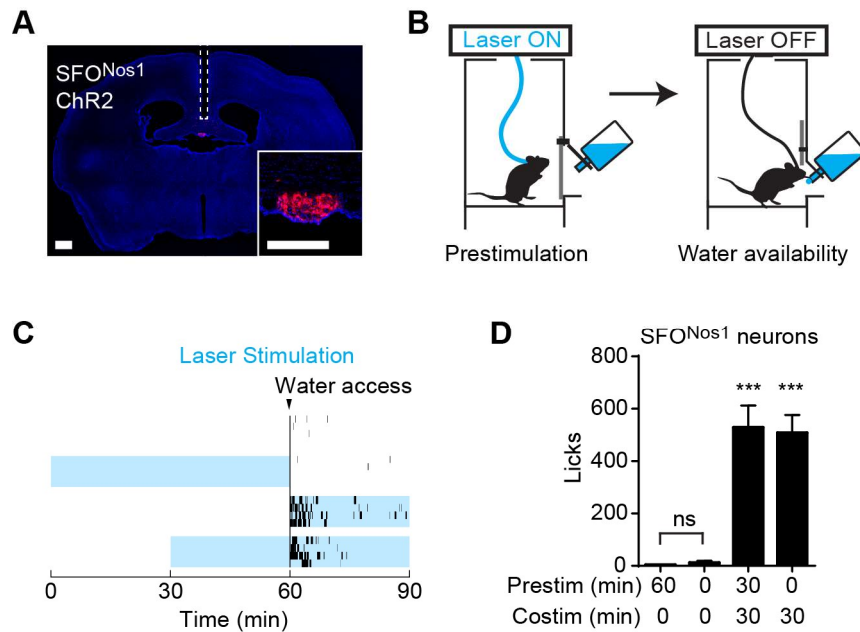


Figure 5.2. Prestimulation of SFO^{Nos1} neurons does not prime drinking behavior.

(A) Expression of ChR2-mCherry in SFO^{Nos1} neurons and optical fiber placement above SFO. (B) Schematic of the prestimulation experiment. (C-D) Drinking evoked by different protocols stimulating SFO^{Nos1} neurons (n=4). (C) Raster plots showing temporal relationship between licking (black vertical lines) and opto-stimulation pattern (blue boxes). (D) Comparison of total licking events. Co-stimulation data are a reanalysis of experiments described in (Zimmerman et al., 2016). Asterisks on top of bar plots indicate significance levels compared to no stimulation control and asterisks on top of brackets indicate significance levels for comparisons with the respective protocols, using one-way-ANOVA with Holm-Sidak's correction for multiple comparisons (****p<0.0001, ***0.0001<p<0.001, **0.001<p<0.01, *0.01<p<0.05, ns p>0.05).

Prestimulation of AgRP neurons results in sustained motivation to work for food

AgRP neurons promote not only food intake but also appetitive behaviors that lead to food obtainment. For example, optogenetic or chemogenetic stimulation of AgRP neurons motivates animals to perform instrumental responses such as lever pressing in order to obtain a food reward (Atasoy et al., 2012; Krashes et al., 2011). It has been hypothesized that the rapid inhibition of AgRP neurons by the sensory detection of food may serve as a signal that inhibits these appetitive behaviors, thereby enabling the transition from foraging to feeding (Chen and Knight, 2016). However this possibility has never been directly tested.

To investigate this question, we tested whether prestimulation of AgRP neurons would alter animals' subsequent motivation to work for food. We trained AgRP-ChR2 mice to lever

press for food pellets and then tested them in a progressive ratio 3 (PR3) reinforcement schedule (**Figure 5.3A**), in which an increasing number of lever presses are required to obtain each successive food reward (Hodos, 1961). In the absence of prior photostimulation, AgRP-ChR2 mice engaged in a low level of operant responding (**Figure 5.3CD**), consistent with the fact that ad libitum fed mice have little motivation to work for food. In contrast, prestimulation of AgRP neurons for one hour caused animals to engage in vigorous pressing when the levers were subsequently made available (**Figure 5.3B, C**). This operant responding was specifically directed toward the food reward, because animals pressed the active lever much more frequently than the inactive lever (223 ± 29 for active lever vs. 28 ± 6 inactive, $p < 0.001$; **Figure 5.3B,C**). This response was also specific to AgRP neuron activation, because it was absent from sham stimulated mice that lacked ChR2 expression (**Figure 5.3D**). Thus prestimulation of AgRP neurons generates long-lasting motivation to work for food that persists even in the absence of continued AgRP neuron activity. This indicates that both appetitive and consummatory behaviors can be driven by a sustained signal from AgRP neurons.

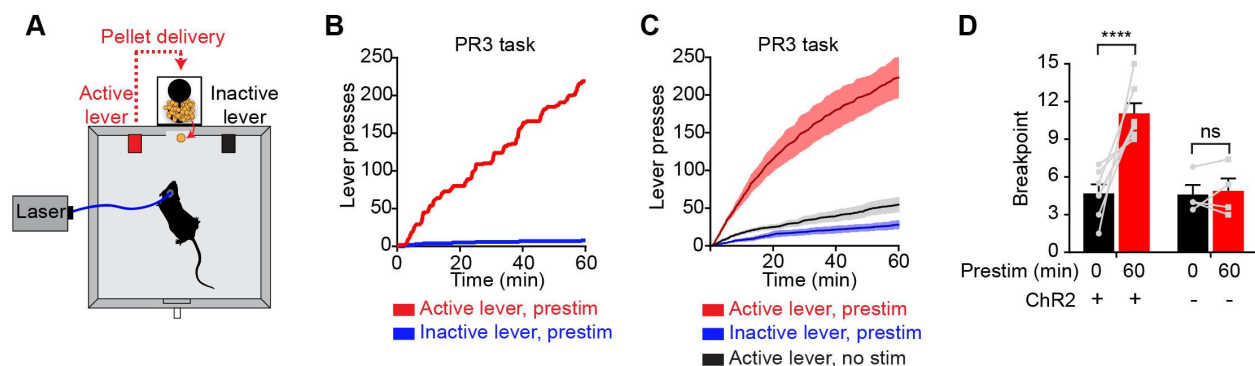


Figure 5.3. Prestimulation of AgRP neurons promotes sustained appetitive behavior. (A) Progressive ratio 3 lever press task. (B-D) Lever presses evoked by prestimulating AgRP neurons in progressive ratio 3 tasks ($n=7$). (B) Plots of cumulative lever presses by a representative mouse after 60 min prestimulation. (C) Plots of average cumulative lever presses from trials with or without prestimulation. Filled areas indicate S.E.M. (D) Analysis of total lever presses of ChR2⁺ and ChR2⁻ mice. Asterisks on top of brackets indicate significance levels for comparisons with the respective protocols, using one-way-ANOVA with Holm-Sidak's correction for multiple comparisons (**** $p \leq 0.0001$, *** $0.0001 < p \leq 0.001$, ** $0.001 < p \leq 0.01$, * $0.01 < p \leq 0.05$, ns $p > 0.05$).

AgRP neuron projections to the PVH, BNST and LHA are individually sufficient to generate persistent hunger

We next investigated the neural pathway that underlies these sustained behavioral effects. AgRP neurons project to several downstream targets in a primarily one-to-one configuration (Betley et al., 2013). Among these, the paraventricular hypothalamus (PVH), bed nucleus of the stria terminalis (BNST), and lateral hypothalamic area (LHA) are particularly strongly innervated by AgRP neuron axons (Broberger et al., 1998). Optogenetic stimulation of AgRP neuron terminals in each of these three areas during the act of feeding can drive voracious food consumption (Betley et al., 2013), but it remains unknown whether these same projections support feeding under more physiologic stimulation conditions, in which AgRP neurons are highly active only before food availability.

To test this, we implanted optical fibers above the PVH, BNST, or LHA of AgRP-ChR2 mice and then measured food intake following one hour of preparatory photostimulation (**Figure 5.4**). We found that prestimulation of AgRP neuron axons in all of these regions elicited robust food intake compared to non-stimulated controls (PVH: 0.55 ± 0.05 g vs. 0.11 ± 0.02 g, $p < 0.0001$; BNST: 0.38 ± 0.06 g vs. 0.14 ± 0.03 g, $p < 0.01$; LHA: 0.60 ± 0.01 g vs. 0.21 ± 0.05 g, $p < 0.001$ **Figure 5.4 and Figure 5.8**). Quantitative analysis of the relationship between prestimulation duration and food intake for ARC \rightarrow PVH projections revealed that this sustained response built up progressively over time (**Figure 5.8**), with kinetics similar to those observed for prestimulation of the soma (**Figure 5.1F**). These sustained effects were unaffected to introduction of a 10 minute delay between laser offset and the onset of food availability, indicating that they persist in the absence of ongoing feeding behavior (**Figure 5.4 and Figure 5.8**). To investigate the role of these pathways in appetitive behaviors, we prestimulated each projection for one hour and then measured lever pressing in a progressive ratio assay. All three projections supported vigorous and specific lever pressing (**Figure 5.4 and Figure 5.8**) to an extent that was comparable to the effect of stimulating all AgRP neurons in the ARC (**Figure**

5.4H). Thus at least three different projections of AgRP neurons are individually sufficiently to elicit the sustained feeding behavior that arises from AgRP neuron activity.

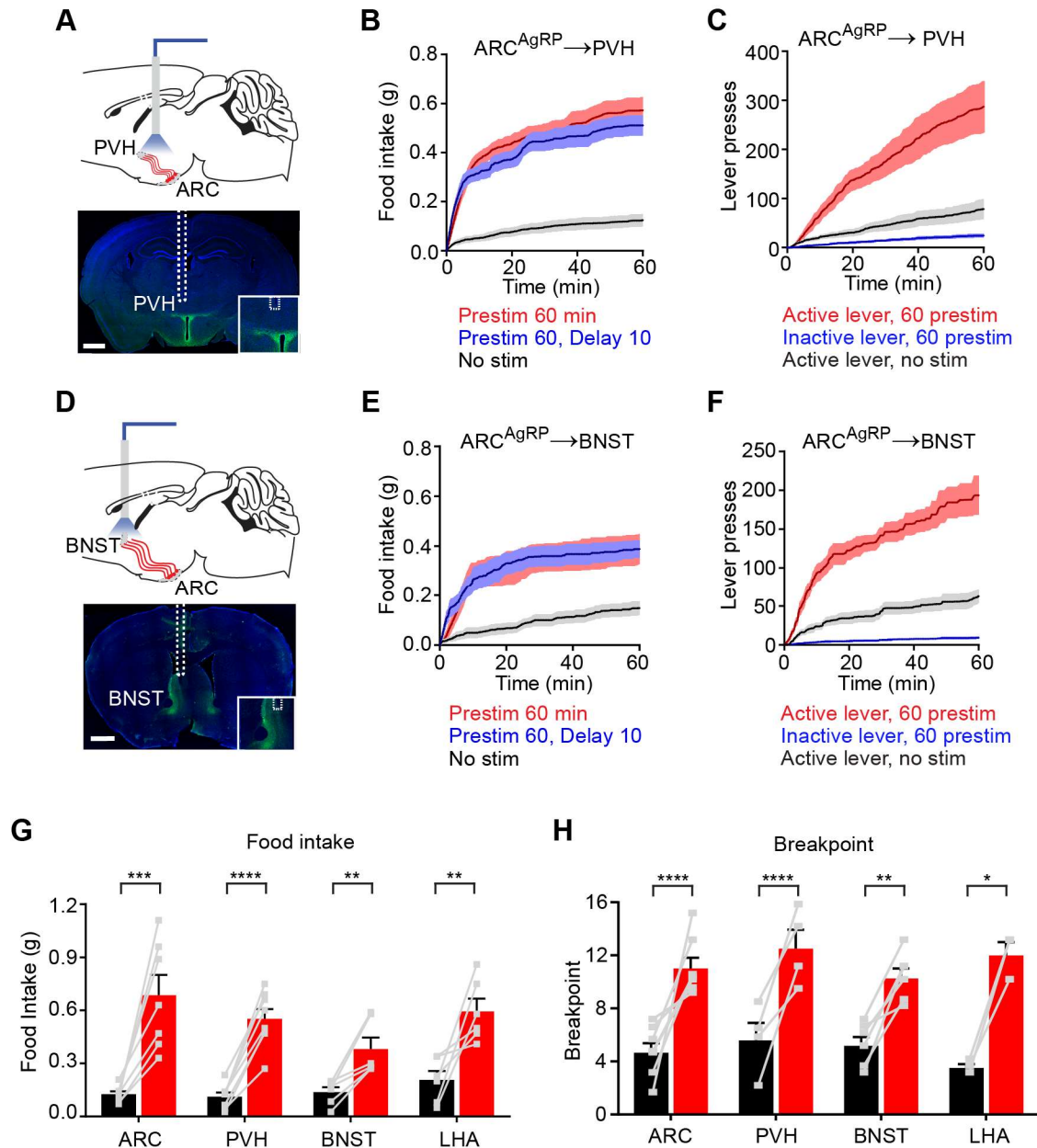


Figure 5.4. Projections of AgRP neurons to PVH, BNST or LHA are sufficient to prime feeding behavior. (A) Optical fiber placement above $AgRP^{ARC \rightarrow PVH}$. (B-C) Plots of cumulative food intake (B) and lever presses (C) evoked by prestimulating $AgRP^{ARC \rightarrow PVH}$ axonal terminals. Filled areas indicate S.E.M. (D) Optical fiber placement above $AgRP^{ARC \rightarrow BNST}$. (E-F) Plots of cumulative food intake (E) and lever presses (F) evoked by prestimulating $AgRP^{ARC \rightarrow BNST}$ axonal terminals. Filled areas indicate S.E.M. (G) 60min food intake evoked by 60min prestimulation of $AgRP^{ARC}$, $AgRP^{ARC \rightarrow PVH}$, $AgRP^{ARC \rightarrow BNST}$ and $AgRP^{ARC \rightarrow LHA}$ (red) and corresponding no stim controls (black). (H) Breakpoint in 60min progressive ratio 3 task reached by animals with 60min

prestimulation of AgRP^{ARC}, AgRP^{ARC→PVH}, AgRP^{ARC→BNST} and AgRP^{ARC→LHA} (red) and corresponding nostim controls (black). Asterisks on top of brackets indicate significance levels for comparisons with the respective protocols, using one-way-ANOVA with Holm-Sidak's correction for multiple comparisons (**** $p \leq 0.0001$, *** $0.0001 < p \leq 0.001$, ** $0.001 < p \leq 0.01$, * $0.01 < p \leq 0.05$, ns $p > 0.05$). ARC food intake n=8; ARC PR3 n=7; PVH food intake n=8; PVH PR3 n=4; BNST food intake n=6; BNST PR3 n=6; LHA food intake n=6; LHA PR3 n=3.

Prestimulation of AgRP neurons conditions appetite and flavor preference

The fact that AgRP neurons can drive feeding through a sustained mechanism implies that the underlying motivational processes must also be long-lasting. However the nature of the motivational signals that persist after AgRP neurons have been silenced is unknown. One important mechanism by which food deprivation motivates feeding is by enhancing the positively rewarding properties of food, such as its palatability (Berridge, 2004, 2009; Cabanac, 1971; Fulton, 2010; Lockie and Andrews, 2013; Rolls et al., 1980). We therefore considered the possibility that AgRP neuron activity might promote long-lasting potentiation of food's incentive value.

To test this, we investigated whether AgRP neuron prestimulation could condition appetite for specific foods. AgRP-ChR2 mice were acclimated to a feeding chamber that delivered pellets that had a similar energy density to their home cage chow, but had a distinct size, shape, and texture (**Figure 5.5A**; see Methods for additional information). We then tested mice in this chamber for pellet consumption during a one hour test period on eight consecutive days (**Figure 5.5B**). The trial was designed so that, on days 3, 5, and 7, the test period was immediately preceded by one hour of AgRP neuron prestimulation (**Figure 5.5B, blue**), whereas on the intervening days (days 1, 2, 4, 6, and 8), there was mock stimulation. Of note, mice had ad libitum access to chow in their home cage, and all animals were laser naïve at the beginning of the trial, meaning that day 3 was the first time they were exposed to photostimulation.

We found that mice consumed relatively few test pellets at baseline (trials 1 and 2; preconditioning), consistent with the fact that fed mice eat little during the light phase (**Figure**

5.5B, C, red). In trial 3, mice were prestimulated for one hour, and, as described above, this resulted in voracious pellet consumption (**Figure 5.5B red**). Strikingly, this pellet consumption remained strongly elevated in subsequent trials 4 and 6, even though these trials were not preceded by AgRP neuron stimulation (**Figure 5.5B, C red; post-conditioning**). This conditioned appetite was specific to the test conditions associated with AgRP neuron prestimulation, because it was not prevented by ad libitum access to chow in the home cage (**Figure 5.5A**) and was completely absent from sham stimulated control mice (**Figure 5.5B, gray**). This indicates that a single trial of AgRP neuron prestimulation can generate conditioned appetite for subsequently presented food.

We hypothesized that this conditioned appetite might reflect attribution of incentive value to the specific sensory properties of the test pellets (e.g. their taste or texture), caused by the fact that exposure to these pellets was experimentally paired with AgRP neuron prestimulation. This learned incentive value would then motivate the mice to eat those pellets in future trials even when not food deprived. A prediction of this model is that this specific appetite should undergo extinction if the test pellets are simply provided to the mice in their home cage, so that the pellets become dissociated from AgRP neuron prestimulation. This was indeed the case: providing the mice with overnight access to the test pellets abolished the conditioned appetite in the next trial (**Figure 5.5B,C red**). To test this a different way, we prepared a second cohort of laser naïve mice that were given ad libitum access to the test pellets in their home cage from the beginning of the trial (**Figure 5.5B,C black**). These animals showed no evidence of conditioned appetite when trained under otherwise identical conditions (**Figure 5.5B, black, days 4 and 6**). Thus AgRP neuron activity can condition appetite for specific foods that are consumed after AgRP neurons have shut off, such that these foods are later consumed in the absence of homeostatic need. This suggests that AgRP neuron prestimulation can attribute incentive value to the sensory properties of subsequently consumed food.

To probe this idea further, we examined whether animals could be trained to prefer a specific flavor by experimentally pairing that flavor with AgRP neuron prestimulation (**Figure 5.5D**). In a baseline trial, AgRP-ChR2 mice were given access two different flavors of non-caloric gels (strawberry and orange) and the amount of each consumed was recorded. Mice were then conditioned on four consecutive days by pairing access to the less preferred gel with 30 minutes of AgRP neuron prestimulation, whereas the preferred gel was paired with 30 minutes of mock stimulation (**Figure 5.5D**). The order of these conditioning sessions was randomized each day and they were separated by at least four hours. On day seven, mice were then tested by providing simultaneous access to both gels and measuring consumption of each. We found that this conditioning protocol robustly reversed the mice's flavor preference, such that the less preferred flavor became more preferred (**Figure 5.5E**). Thus animals learn to prefer flavors that are preceded by AgRP neuron activation, consistent with the idea that AgRP neuron activity induces a long-lasting potentiation of the rewarding sensory properties of food.

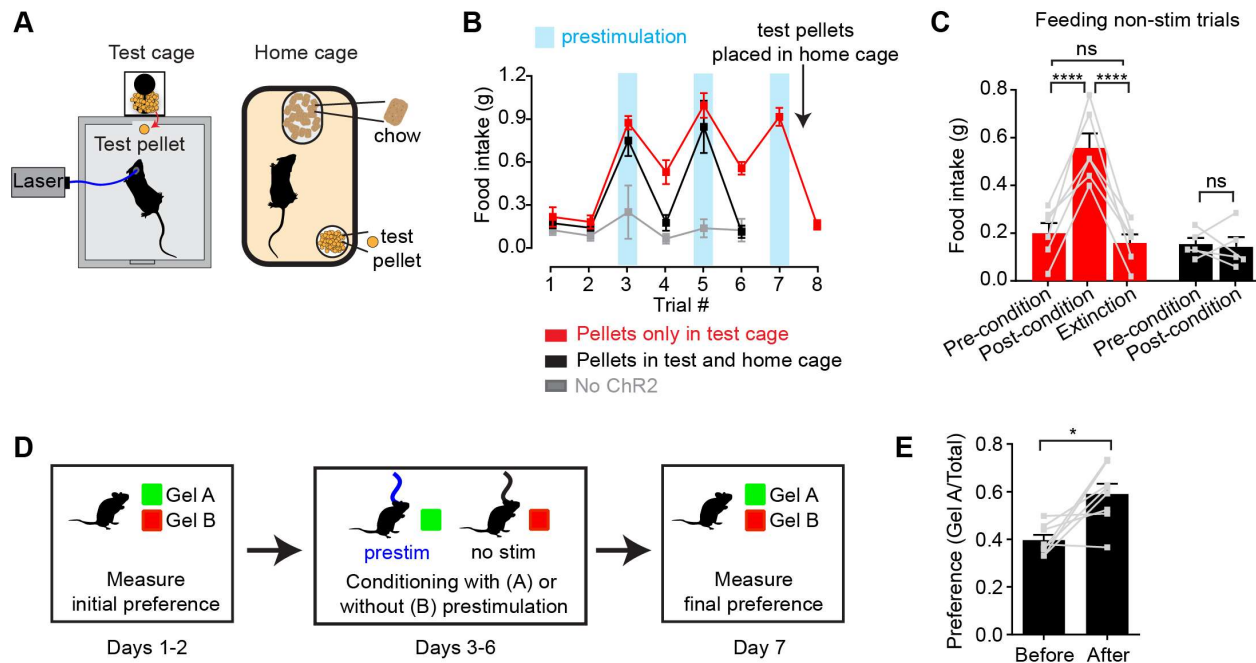


Figure 5.5. Prestimulation of AgRP neurons conditions appetite and flavor preference. (A) Schematic of conditioned appetite assay. Test pellets and home cage chow are similar in energy density but different in shape, size, and texture. Test pellets were either included in home cage or not, as indicated. (B-C) Average 60 min food intake of conditioned appetitive

experiments. (B) Food intake of AgRP-ChR2 mice without access to test pellets in homecage (red n=6) and with access to test pellets in homecage (black n=5), and WT mice without access to test pellets in homecage (grey n=3) through consecutive trials. Blue boxes indicate trials with 60 min prestimulation (trials 3,5,7), whereas in white trials animals were subjected to mock stimulation (trials 1,2,4,6,8). (C) Comparison among pre-conditioning, post-conditioning and extinction trials of AgRP-ChR2 mice with (black n=5) or without (red n=6) access to test pellets in homecage. Trial 1 and 2 are considered pre-conditioning, trial 4 and 6 are considered post-conditioning and trial 8 is considered extinction. (D) Conditioned flavor preference experiment. (E) Change of preference to conditioned flavor before and after 4 repeats of prestimulation conditioning assay (n=8). Asterisks on top of brackets indicate significance levels for comparisons with the respective protocols, using one-way-ANOVA with Holm-Sidak's correction for multiple comparisons (**** $p \leq 0.0001$, *** $0.0001 < p \leq 0.001$, ** $0.001 < p \leq 0.01$, * $0.01 < p \leq 0.05$, ns $p > 0.05$).

AgRP neuron stimulation is positively reinforcing

The preceding data suggest that AgRP neurons transmit a long-lasting, positive valence signal that potentiates the incentive value of food. The effect of this mechanism is to transform AgRP neuron firing before food availability into a sustained drive that can motivate feeding later. An important question is whether this positive valence mechanism is sufficiently strong to account for the dramatic instrumental responses (e.g. lever pressing, nose poking) that animals exhibit following AgRP neuron activation. Of note, a previous study reported that mice failed to perform operant responses in order to shut off AgRP neuron activity, indicating that these neurons do not motivate behavior by negative reinforcement (Betley et al., 2015), which we confirmed independently (**Figure 5.9**). However whether mice will perform these same actions in order to turn on AgRP neuron activity has never been tested.

We took laser naïve AgRP-ChR2 mice and acclimated them over three nights to behavioral chambers containing two levers, one of which triggered brief AgRP neuron photostimulation (5 s, 20 Hz) and the other of which was inactive (**Figure 5.6A**). Mice had ad libitum access to food during both training and testing. We then tested these mice in 150 minute trials during the light phase to see whether they would engage in operant responding for AgRP neuron stimulation. Strikingly, we found that mice engaged in lever pressing in order to optically stimulate their AgRP neurons (**Figure 5.6B**). This lever pressing was specifically directed

toward AgRP neuron self-stimulation, because it (1) was highly biased toward the active versus inactive lever (**Figure 5.6B, H**), (2) was greatly reduced in control mice that lacked ChR2 expression (**Figure 5.6H**), and (3) underwent rapid extinction when the active lever was uncoupled from the laser (**Figure 5.6D**). Importantly, the effectiveness of this lever pressing in stimulating AgRP neurons was confirmed by two separate measures. First, we observed reliable temporal coordination between lever pressing and food intake in mice allowed to self-stimulate: mice engaged in repeated cycles of lever pressing followed by food consumption (**Figure 5.6E, F**), whereas food consumption was greatly reduced when the lever was uncoupled from the laser (1.5 ± 0.2 g for active laser vs. 0.39 ± 0.07 g for inactive laser, $p < 0.001$). Second, we observed strong induction of the activity marker Fos in AgRP neurons from mice allowed to lever press for self-stimulation, whereas no Fos was observed in otherwise identical trials in which the laser was inactivated (**Figure 5.9**). Thus mice will actively lever press in order to stimulate their AgRP neurons, indicating that the activity of these cells is positively reinforcing under these conditions.

We considered two hypotheses for why AgRP neuron activity might be positively reinforcing. The first is that AgRP neuron firing is intrinsically rewarding, analogous to midbrain dopamine neurons (Corbett and Wise, 1980). The second is that AgRP neuron activity becomes rewarding specifically in the presence of food, because it magnifies food's intrinsic positive valence. In the latter case, mice may self-stimulate their AgRP neurons for one of two reasons: in order to enhance the incentive value of the food directly in front of them during the trial (hypothesis 2a), or because of a learned positive association that developed during training when mice lever pressed for self-stimulation in the presence of food (hypothesis 2b).

We performed a series of experiments to discriminate between these hypotheses. First, we tested whether mice trained to lever press in the presence of food would self-stimulate in a trial that lacked food. We found that they did, as self-stimulation remained robust even when

food was absent during the trial (**Figure 5.6C, H**). This indicates that the presence of food is not acutely required for the positively reinforcing effects of AgRP neuron activity.

To investigate this phenomenon further, we prepared a second cohort of laser naïve AgRP-ChR2 mice that were trained to lever press for AgRP neuron stimulation in an identical paradigm, except that food was absent during the overnight training sessions. We then tested whether these mice would lever press for self-stimulation. These mice were ad libitum fed, but food was absent during the testing. Under these conditions, we found that mice engaged in minimal lever pressing that was indistinguishable from control mice that lacked ChR2 expression (**Figure 5.6G, H**). This indicates that AgRP neuron stimulation is not intrinsically rewarding (hypothesis 1), but that prior experience self-stimulating AgRP neurons in the presence of food is sufficient for lever pressing to become positively reinforcing in food's absence (hypothesis 2b). Taken together, these data strongly support a model in which AgRP neuron activity results in a long-lasting potentiation of the rewarding properties of food. This sustained positive valence signal is sufficient to condition both Pavlovian and instrumental learning, and likely accounts for much of the behavioral response that is elicited by AgRP neuron activity.

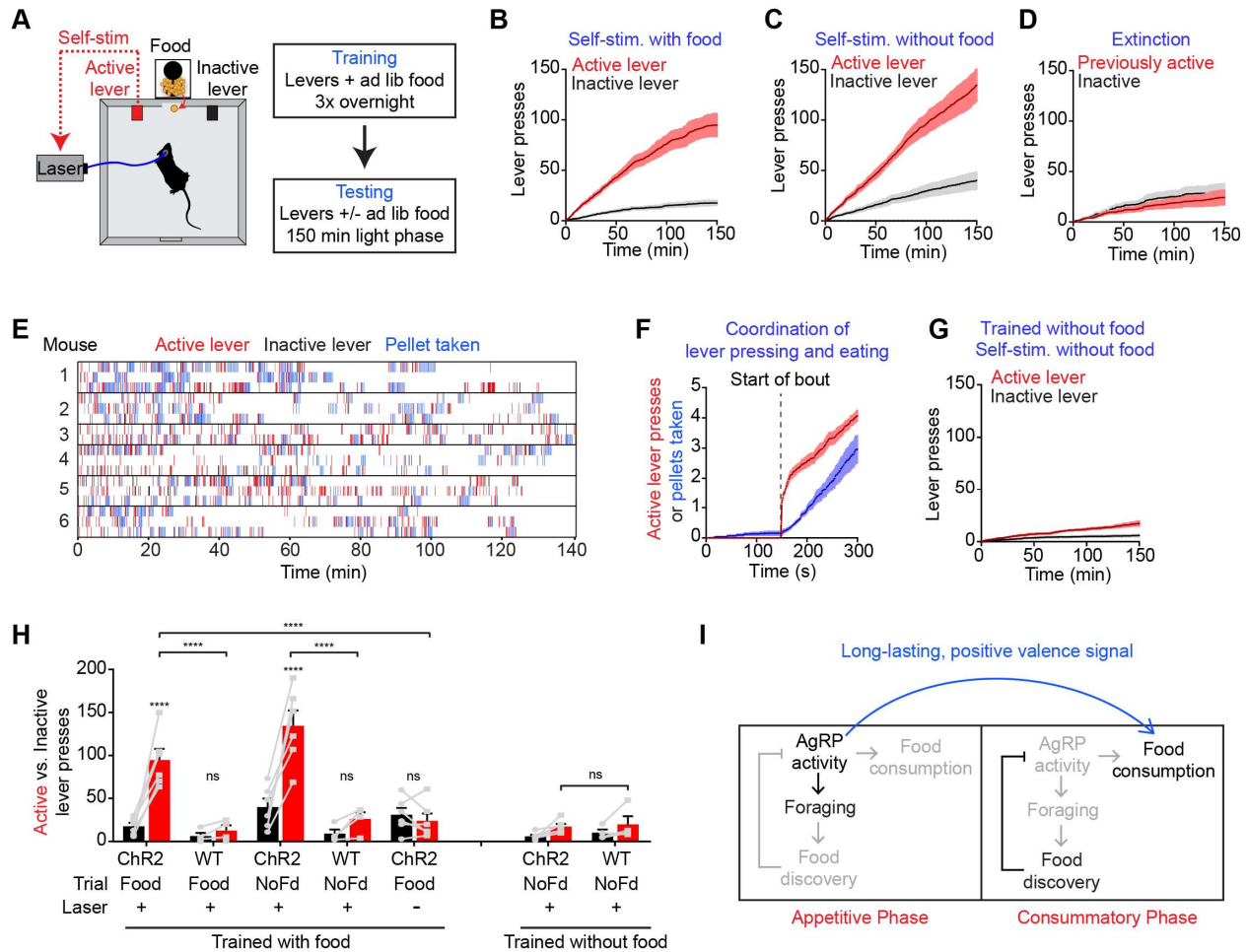


Figure 5.6. AgRP neuron activity is positively reinforcing in the presence of food.

(A) Schematic of the positive reinforcement protocol that tests whether animals will lever press to self-stimulate AgRP neurons. (B-D) Plots of cumulative active (red) and inactive lever presses (black) by mice conditioned with ad lib access to food (n=6). Filled areas indicate S.E.M. (B) Self-stimulation experiment with ad lib access to food pellets. (C) Self-stimulation experiment without access to food. (D) Self-stimulation experiment after extinction with ad lib access to food. (E-F) Temporal relationship between self-stimulation of AgRP neurons and food intake. Filled areas indicate SEM. (E) Raster plots of individual trials (2-3 repeats) of 6 different mice. (F) PSTH analysis of active lever presses and pellet consumption. Filled areas indicate SEM (n=6). Time zero is defined as the beginning of each active lever pressing bout. A bout is defined as a lever press train segregated from other lever presses by ≥ 5 min. (G) Plots of cumulative active (red) and inactive lever presses (black) by mice conditioned without food access (n=6). Self-stimulation experiments were conducted in the absence of food access. Filled areas indicate S.E.M. (H) Bar plots comparing total active (red) and inactive (black) lever presses of AgRP-ChR2 mice and WT control mice in self-stimulation experiment with ad lib (Food) or no (NoFd) access to food pellets. Asterisks on top of bar plots of active lever presses indicate significance levels compared to corresponding inactive lever presses and asterisks on top of brackets indicate significance levels for comparisons with the respective protocols, using one-way-ANOVA with Holm-Sidak's correction for multiple comparisons (**** $p \leq 0.0001$, *** $0.0001 < p \leq 0.001$, ** $0.001 < p \leq 0.01$, * $0.01 < p \leq 0.05$, ns $p > 0.05$). Trained with food: ChR2 food n=6, WT food n=4, ChR2 nofood n=6, WT nofood n=4; trained without food: ChR2 nofood n=6,

WT nofood n=4. **(I)** Model for control of feeding by AgRP neurons. During the appetitive phase, AgRP neuron activity drives food seeking. The sensory detection of food silences AgRP neuron activity. However animals still consume food during the subsequent consummatory phase because of a long-lasting, positive valence signal transmitted by AgRP neurons earlier, when food was unavailable.

DISCUSSION

AgRP neurons are a fundamental neural substrate of hunger. Nearly twenty years of investigation into the properties of these cells led to a widely accepted model for their function. The key tenets of this model were that (1) AgRP neuron activity drives feeding directly, and (2) the level of AgRP neuron activity is controlled by changes in hormones and nutrients. Both of these tenets were challenged by the recent discovery that AgRP neurons are rapidly inhibited by the sensory detection of food (Betley et al., 2015; Chen et al., 2015; Mandelblat-Cerf et al., 2015). Indeed, because AgRP neurons are inhibited before feeding begins, it has been unclear how these neurons are able to drive food consumption at all (Chen and Knight, 2016; Seeley and Berridge, 2015).

We hypothesized that AgRP neurons may drive feeding by transmitting a long-lasting signal that potentiates downstream circuits and persists after AgRP neuron firing has ceased (Chen and Knight, 2016). This would enable AgRP neuron activity before food discovery to drive feeding that occurs later, long after AgRP neurons have been silenced by sensory cues. Here we have shown that this is indeed a robust mechanism by which AgRP neurons can drive food consumption. We have shown that stimulation of AgRP neurons for as little as one minute is sufficient to increase subsequent food intake over baseline (**Figure 5.1F**); that this hunger signal builds up progressively over the course of 30-60 minutes, until prestimulated animals eat nearly as much food as mice fasted overnight (**Figure 5.1E**); and that this dramatic response is robust to insertion of a delay of tens of minutes between the offset of AgRP neuron stimulation

and the onset of feeding (**Figure 5.1H**). Thus these findings explain how the remarkable behavioral effects of AgRP neurons can be reconciled with their paradoxical natural dynamics.

Mechanisms underlying sustained hunger

It is usually assumed that a neuron driving a behavior will be most active during or immediately before the behavior's execution (Fields et al., 2007). For this reason, the possibility that AgRP neuron firing and feeding behavior could be separated in time by tens of minutes was unforeseen, and we are aware of few precedents in which such a vigorous and acute behavioral response can be elicited following such a long delay (Hoopfer et al., 2015; Kohatsu and Yamamoto, 2015). Consistent with this, we found no evidence for sustained behavioral effects following stimulation of an analogous population of neurons that control thirst (SFO^{Nos1} neurons): for these cells, drinking behavior was tightly timelocked to the laser stimulus (**Figure 5.2**). Intriguingly, AgRP neuron prestimulation also strongly potentiated appetitive behaviors, since prestimulated animals were willing to perform intense lever pressing in order to obtain a food reward (**Figures 5.3 and 5.4**). Thus the sustained effects of AgRP neuron activity are not restricted to consummatory actions such as licking, chewing, and swallowing, but also extend to flexible, goal oriented behaviors associated with food obtainment. This suggests that the entire "hunger drive" that motivates food seeking and consumption is transferred to a downstream circuit node during AgRP neuron firing, such that this drive becomes independent of continued AgRP neuron activity.

The mechanisms that underlie this sustained potentiation of feeding are unknown. The fact that these effects are robust to introduction of a 30 minute delay implies that they must result from a stable change in the internal state of the mouse, rather than some feedback process that requires interaction with food. This stable change would presumably be detected as the persistent activity (or inactivity) of a population of neurons downstream of AgRP neurons within the feeding circuit. Such cells would be predicted to integrate AgRP neuron activity over

time, so that they responded to rapid changes in AgRP neuron activity with a delay, thereby enabling feeding to continue after AgRP neurons have been silenced by sensory cues (Chen and Knight, 2016). We have shown that projections to the PVH, BNST, and LHA are each individually sufficient to drive long-lasting increases in food intake (**Figure 5.4**). In addition, a recent report showed that consumption of palatable foods can be potentiated by prestimulation of AgRP neuron projections to the parabrachial nucleus (Campos et al., 2016). Thus the persistent orexigenic effects of AgRP neuron activity do not depend on a single circuit node.

Mechanisms for generating persistent neural activity include both cell-intrinsic processes, such as changes in membrane conductances, as well as circuit level mechanisms, such as recurrent excitatory loops (Major and Tank, 2004; Wang, 2001). These mechanisms are often invoked to explain neural processes that have a duration of seconds, such as maintenance of working memory, rather than the behavioral potentiation that persists for tens of minutes described here. Whether similar or different mechanisms underlie the control of feeding by AgRP neurons remains unknown. Addressing this question will require detailed analysis of the dynamics and physiology of relevant downstream circuit elements, which may be the direct targets of AgRP neurons (Betley et al., 2013; Campos et al., 2016; Dietrich et al., 2012; Garfield et al., 2015; Padilla et al., 2016) or alternatively cells that are several synapses removed from the arcuate feeding circuit (Seeley and Berridge, 2015).

One point not addressed by our experiments is whether optical stimulation has a long-lasting effect on the activity of AgRP neurons themselves. While we have not measured how AgRP neurons respond to our stimulation protocol in vivo, available evidence suggests that optogenetic stimulation does not result in sustained activation of these cells. This evidence includes (1) the observation from in vivo optrode recordings (Mandelblat-Cerf et al., 2015) that ~5 minutes of intermittent 20 Hz optogenetic stimulation of AgRP neurons does not result in a sustained alteration of firing (31/33 neurons returned to baseline immediately upon laser offset, and the remaining two cells within two minutes); and (2) the finding from slice recordings that 30

minutes of intermittent 20 Hz optogenetic stimulation does not result in a sustained increase in AgRP neuron firing in vitro (AponTE et al., 2011). In addition, it is important to note that the sensory detection of food can inhibit AgRP neurons even in the presence of ongoing excitatory input, such as high dose ghrelin treatment (Chen et al., 2015). Therefore the presentation of food would likely inhibit any residual AgRP neuron activation that persisted after photostimulation, and consequently the interpretation of the experiments described here would be largely unchanged. Nevertheless, future experiments that record AgRP neuron activity in vivo in the context of different optogenetic stimulation paradigms will further clarify this issue.

The role of the neuropeptides NPY and AgRP in the sustained feeding response

One mechanism for the generation of persistent neural activity is the release of neuromodulators (Major and Tank, 2004), and AgRP neurons express two neuropeptides regulate feeding, NPY and AgRP (Clark et al., 1985; Fan et al., 1997; Hahn et al., 1998; Ollmann et al., 1997). In slice, NPY has been shown to induce long-lasting changes in membrane excitability and neurotransmitter release in certain contexts (Dubois et al., 2012; Fu et al., 2004; Roseberry et al., 2004). In addition, injections of NPY into the brain can drive voracious feeding with kinetics and duration that vary depending on the protocol (Clark et al., 1985; Morley et al., 1987a; Morley et al., 1987b). While some studies have concluded that NPY plays a largely redundant role in the regulation of feeding (Erickson et al., 1996; Krashes et al., 2013; Qian et al., 2002), others have suggested it is more essential (Bannon et al., 2000; Patel et al., 2006). Whether NPY signaling participates in the sustained potentiation of feeding described here remains to be determined.

Unlike NPY, the AgRP neuropeptide can potentiate food intake for as long as two weeks in certain contexts (Hagan et al., 2000; Krashes et al., 2013; Nakajima et al., 2016). However we believe that AgRP is unlikely to mediate the behavioral responses described here, for two reasons. First, the behavioral responses we observe following AgRP neuron prestimulation are

almost immediate, in that animals begin to eat within seconds of food presentation (**Figure 5.1**). By contrast the release of the AgRP neuropeptide requires at least two hours to affect feeding (Krashes et al., 2013). Thus the AgRP neuropeptide appears to act too slowly to explain our findings. Second, our projection stimulation experiments show that AgRP neuron projections to the PVH and BNST are both efficient in driving sustained feeding (**Figure 5.4**). However AgRP neuron projections to the BNST have been shown to function by targeting BNST neurons that do not express the melanocortin 4 receptor (MC4R), which is the target of AgRP (Garfield et al., 2015). This implies that the AgRP neuropeptide cannot be the molecule that drives feeding in our ARC → BNST stimulation experiments, and therefore that other neurotransmitters released by these cells (GABA or NPY) must underlie their sustained effects.

AgRP neurons drive feeding through a sustained positive valence mechanism

Food seeking and consumption are motivated behaviors. An important and unresolved question regards the nature of the motivational processes that AgRP neurons engage in order to promote feeding. Traditionally, motivational valence has been assigned by measuring the behavioral response to ongoing neural stimulation (Fields et al., 2007; Kravitz et al., 2012; Namburi et al., 2015). However, the discovery that AgRP neurons are rapidly inhibited by the sensory detection of food (Chen et al., 2015) and consequently drive food intake through a long-lasting, persistent mechanism (**Figures 5.1, 5.3, and 5.4**) implies that the motivational signals most relevant for food consumption are those that persist after AgRP neuron firing has ceased. These motivational signals have never been investigated.

To explore the properties of these long-lasting motivational cues, we stimulated AgRP neurons before food availability and then measured how this prestimulation affected the preference for subsequently presented foods. We found that prior AgRP neuron stimulation robustly conditioned flavor and food preference (**Figure 5.5**). This effect was sufficient to motivate mice following a single trial to overeat a test food that had been paired with AgRP

neuron prestimulation (**Figure 5.5B,C**). Importantly, this conditioned appetite was specific to the food paired with AgRP neuron prestimulation, because it could be blocked by ad libitum access to the paired food but not a different, unpaired food (**Figure 5.5B**). A similar phenomenon, known as “conditioned craving,” has been observed in rats that are fed a specific kind of pellet only when food deprived (Petrovich et al., 2007). The finding that this food-specific craving can be trained by AgRP neuron prestimulation argues that these neurons motivate feeding by potentiating the incentive salience or perceived rewarding properties of food encountered during a state of energy deficit (Seeley and Berridge, 2015). Of note, the idea that food deprivation can magnify food reward has long been recognized as a critical mechanism that drives feeding (Berridge, 2004; Cabanac, 1971), but the underlying neural mechanisms have been unclear. We propose that AgRP neurons are the origin of this effect.

A prediction of this positive valence model is that animals should engage in operant responding in order to stimulate AgRP neuron activity. We found that this is indeed the case, as animals will actively lever press in order to turn on (**Figure 5.6**) but not in order to turn off (**Figure 5.9**) AgRP neuron firing. Importantly, this instrumental responding required either that food was present during the trial (**Figure 5.6B**) or that animals had previously been allowed to self-stimulate in the presence of food, in order to learn this positive association (**Figure 5.6C**). This argues that AgRP neuron activity is not necessarily intrinsically rewarding, but that it attains positive valence specifically in the presence of food. This observation is again most readily explained by a model in which AgRP neurons enhance food’s intrinsically rewarding properties. By contrast, these findings do not support a model in which AgRP neurons motivate food consumption primarily through a negative valence signal (Betley et al., 2015), since animals do not self-administer aversive stimuli.

How can we reconcile our data with a prior report that AgRP neuron activity has negative valence? That study measured the valence of ongoing AgRP neuron firing in the absence of food and concluded that it was aversive, since animals avoided places and flavors associated

with elevated AgRP neuron activity (Betley et al., 2015). In contrast, we have measured here the valence that persists after AgRP neuron activity has ceased, because this corresponds to the natural activity pattern of these cells during food consumption (Chen et al., 2015). This has revealed that AgRP neurons transmit a previously unsuspected positive valence signal that can robustly condition appetite (**Figure 5.5**) and motivate instrumental responding (**Figure 5.6**). Therefore these data support an important role for a long-lasting, positive valence mechanism by which AgRP neurons motivate food consumption. Nevertheless, these arguments do not rule out an additional role for a negative valence signal that functions primarily prior to food discovery and contributes to food seeking or learning (Betley et al., 2015). Indeed, there is evidence that both positive and negative valence mechanisms contribute to the control of feeding behavior (Berridge, 2004; Bindra, 1976; Fulton, 2010; Hull, 1943; Lockie and Andrews, 2013). Investigation of the neural circuitry downstream of AgRP neurons may provide additional insight into how these parallel mechanisms are coordinated.

Optogenetic replay of the natural dynamics of AgRP neurons

Optogenetics enables selective manipulation of genetically defined cell types and thereby determination of their causal role in behavior (Adamantidis et al., 2015). An assumption implicit in most optogenetic experiments is that the pattern of artificial stimulation approximates the natural firing pattern of the cells, at least in its key features: otherwise, the relevance of any optically-elicited behavior is unclear. While this caveat is widely understood, the lack of information about the in vivo dynamics of many cell types has often precluded consideration of their natural firing patterns. For AgRP neurons, it was long assumed that these cells are highly active during feeding and only inhibited following food consumption, and this model guided the design of early optogenetic studies. However the discovery that AgRP neurons are inhibited by the sensory detection of food, and therefore have a firing pattern during feeding that is the opposite of what was believed, calls for reinvestigation of how these cells control behavior. Here

we have explored this question by using a prestimulation protocol that mimics the broad features of the natural dynamics of AgRP neurons. Using this new stimulation protocol, we are able to reconcile the paradoxical dynamics of AgRP neurons with their well-established function to promote feeding; identify novel mechanisms by which these neurons motivate behavior; and raise new questions about the downstream feeding circuit that await investigation.

METHODS

Mice

Mice were group housed on a 12:12 light:dark cycle with ad libitum access to water and mouse chow (PicoLab Rodent Diet 20, 5053 tablet, TestDiet). Adult mice (8-16 weeks old) were used for all experiments. For channelrhodopsin-2 expression in AGRP neurons, *Agrp-IRES-Cre* mice (Jackson Labs Stock 012899, *Agrp^{tm1(Cre)Lowl}/J*) were crossed with Ai32: *ROSA26-loxStoplox-ChR2-eYFP* (Jackson Labs stock 012569, B6;129S-*Gt(ROSA)26Sor^{tm32(CAG-COP4*H134R/EYFP)Hze/J}*) to generate double mutant animals. Wildtype C57BL/6J mice were used as controls. No statistical methods were used to determine sample sizes. Experimental protocols were approved by the University of California, San Francisco IACUC (Protocol AN133011) following the NIH guidelines for the Care and Use of Laboratory Animals.

Stereotaxic viral delivery and fiber implant

Recombinant AAV expressing ChETA_{TC} (AAV5-EF1 α -DIO-hChR2(E123T/T159C)-2A-mCherry-WPRE) was purchased from the UNC Vector Core. AAV was stereotaxically injected into the SFO of NOS1-IRES-Cre (Jackson Labs Stock 017526, *Nos1^{tm1(Cre)Mgmj}/J*) mice at 0.55 mm (A/P), -2.75 mm (D/V), 0 mm (M/L) relative to bregma.

Custom-made fiberoptic implants (0.39 NA \varnothing 200 μ m core Thorlabs FT200UMT and CFLC230-10) were installed above the SFO (bregma: AP: 0.55mm, DV: 2.45mm, ML: 0mm), the ARC (bregma: AP: -1.75mm, DV: dorsal surface -5.6mm, ML: -0.25mm), PVH (bregma: AP:

-0.75mm, DV: -4.3mm, ML: -0.2mm), BNST (bregma: AP: +0.5mm, DV: -4.2mm, ML: -0.55mm) or LHA (bregma: AP: -1.4mm; ML: -1.2mm; DV: -4.7mm).

Optogenetic stimulation

A 473 nm laser was modulated by Coulbourn Graphic State software through a TTL signal generator (Coulbourn H03-14) and synchronized with behavior experiments. The laser was split through a 4-way splitter (Fibersense and Signals) or passed through a single patch cable (Doric Lenses). The laser was then passed to custom-made fiber optic patch cables (Thorlabs FT200UMT, CFLC230-10; Fiber Instrument Sales F12774) through a rotary joint (Doric Lens FRJ 1x1). Patch cables were connected to the implants on mice through a zirconia mating sleeve (Thorlabs ADAL1). For opto-stimulation protocols, laser was modulated at 20 Hz on a 2 second ON and 3 second OFF cycle with 1 ms pulse width unless otherwise specified. Laser power was set within 15-20 mW at the terminal of patch cable unless otherwise specified. We estimated the light power at the ARC, PVH and BNST to be 4.02, 4.02 and 9.4 mW/mm² respectively. Effective power is likely lower due to loss at the cable-implant connection.

Functional evaluation of fiber placement

At the end of experiments, each AgRP-ChR2 mouse was further tested with a positive control protocol (60 min laser stimulation during food availability) to confirm correct fiber optic placement. Two AgRP-ChR2^{PVH} and two AgRP-ChR2^{LHA} mice that displayed a less than 20% increase of food intake during this positive control protocol were excluded.

Pre-stimulation evoked food intake

Mice were allowed to recover for seven days after implant surgery before experiments. In addition to regular chow, mice were supplied *ad libitum* with the food pellets used during testing (20 mg Bio-Serv F0163) in their home cage unless otherwise specified. Mice were habituated to

the behavioral chambers (Coulbourn H10-11M-TC with H10-11M-TC-NSF) and pellet dispensing systems (Coulbourn H14-01M-SP04 and H14-23M) for three days before the first experiment. Mice were provided ad libitum access to food and water unless otherwise specified and tested during the early phase of light cycle. All pre-stimulation food intake experiments follow this general structure: 70 min habituation/pre-stim period with no food access followed by 60 min food access. Pellet removal was detected using a built-in photo-sensor (Coulbourn H20-93). Food pellets left on the ground after each session were counted and deducted from the total food consumed.

To test whether stimulation of AgRP neuron soma or axonal terminals in the PVH, BNST, and LHA induces food intake, each mouse was tested in the following sequence of experiments on consecutive days: 1- 1- 2- 1- 2- 1- 1- 3- 1- 3- 1 (protocols are described in the table below). All mice were naïve (never stimulated by a laser previously) on the first day of these tests.

Protocol 1	70 min habituation		60 min food access
Protocol 2	10 min habituation	60 min opto-stim	60 min food access
Protocol 3	60 min opto-stim	10 min habituation	60 min food access
Positive control	70 min habituation		60 min food access with opto-stim

To examine the relationship between stimulation protocols and induced food intake, mice were tested with the following protocols once each in semi-randomized order:

69 min habituation	1 min opto-stim	60 min food access
65 min habituation	5 min opto-stim	60 min food access
55 min habituation	15 min opto-stim	60 min food access
40 min habituation	30 min opto-stim	60 min food access

10 min habituation	60 min opto-stim		60 min food access
10 min habituation	30 min opto-stim	30 min habituation	60 min food access
30 min habituation	30 min opto-stim	10 min habituation	60 min food access
30 min habituation	30 min opto-stim (10Hz; 4s ON, 1s OFF)		60 min food access
30 min habituation	30 min opto-stim (20Hz; 2s ON, 8s OFF)		60 min food access

Lickometer assay

Mice were habituated to the optical lickometer (Coulbourn H24-01M, H20-93) at least a week prior to experiments. Behavioral experiments were performed during the light cycle using the protocols described below.

pre-stimulation	70 min habituation no water access		30 min water access
no stimulation	10 min habituation no water access	60 min stimulation no water access	30 min water access
pre-stimulation + co-stimulation	45 min habituation + water access	30 min stimulation no water access	30 min stimulation + water access
co-stimulation	45 min habituation + water access		30 min stimulation + water access

During behavioral testing of SFO^{NOS1::}ChETA_{TC} mice, water access was prevented using a custom-made lickometer blocker. Co-stimulation data were based on experiments performed in (Zimmerman et al., 2016).

Progressive ratio testing

For training, mice were acutely food deprived 5 h before the start of dark cycle and trained with fr1 and fr7 protocols overnight until active lever presses exceeded 200. Mice were then acutely food deprived 5 h before the start of the dark cycle and trained with progressive ratio 3 (PR3) task for 1.5 h.

During the first 70 minutes of the testing protocol (habituation/pre-stim), access to the levers and pellet trough was blocked using a custom-cut acrylic board. At 70th minute of the protocol, the acrylic board was removed and a single pellet was delivered following pressing the active lever according to a PR3 schedule. Each experiment was repeats 2-7 times; no-stim and pre-stim are repeated the same number of times for each mouse.

Conditioned appetite assay

All mice were naïve (never stimulated by a laser previously) on the first day of these tests. Mice were provided with ad libitum regular chow and without any test pellets in their homecage from the beginning of the test unless otherwise specified. The regular chow was PicoLab Rodent Diet 20 (5053), which has an energy density of 3.43 kcal/g and macronutrient composition of approximately 21.0%:5.0%:53.4% Protein:Fat:Carbohydrate. The test pellets were BioServ Dustless Precision Pellets, which have an energy density of 3.35 kcal/gram and macronutrient composition of approximately 21.3%:3.8%:54%. The regular chow was formulated as an oval pellet of approximately 3/8 x 5/8 x 1 inch, whereas the test pellets were formulated as a much smaller, smooth round pellet (20 mg).

Each mouse was tested in the following sequence of experiments on consecutive days: 1- 1- 2- 1- 2- 1- 2-1 (protocols are described above in the pre-stimulation session). Protocol 2 with pre-stimulation was considered as a conditioning trial in this experiment. At the end of the 7th experiment or the third conditioning trial, *ad lib* amount of test pellets were put into the mice home cage in order to induce extinction of previously conditioned appetite.

Conditioned flavor preference assay

All mice were naïve (never stimulated by a laser previously) on the first day of these tests. Mice were first habituated to two differently flavored non-nutritive gels (Hunt's Snack Pack Sugar Free Strawberry & Orange) that were sweetened with sucralose. Mice were transferred to a

clean cage after initial habituation without test gel. Baseline flavor preference was determined in two separate food choice assays conducted in two consecutive days. Each food choice assay consists of 30 min habituation and 15 min food consumption. In the next 4 days, the following two protocols were used to condition the mice to their less preferred flavor with orders inverted each day.

30 min pre-stim	30 min consumption of less preferred gel (0.3 g provided)
30 min nostim	30 min consumption of preferred gel (0.3 g provided)

On the day following the last conditioning session, two food choice assays separated by 4 hours were conducted to determine the conditioned tasted preference.

Self-stimulation

Mice were initially habituated to the operant chamber and test pellets in the same way as mice in pre-stimulation evoked food intake assay. Each cohort was semi-randomly split into two groups (group A and group B). Of note, all mice were naïve to the lever (never exposed to a lever before) and to the laser stimulation on the first day of these tests. The lever on one side of the operant chamber was semi-randomly assigned to each mouse as the active lever. The lever location was counterbalanced within each group. The spatial localization of active lever and inactive lever was fixed for each mouse through the whole experiment.

Group A mice were initially tested with the following protocols to determine baseline lever pressing during the light phase:

<u>Food availability</u>	<u>Experiment Duration</u>	<u>Lever-laser pairing</u>	<u>Repeats</u>
<i>ad lib</i> food pellet access	2.5 h	off	1

Group A mice were then habituated overnight with the following protocol:

<u>Food availability</u>	<u>Experiment Duration</u>	<u>Lever-laser pairing</u>	<u>Repeats</u>
<i>ad lib</i> food pellet access	overnight	on	3

After conditioning, group A mice were then tested with the following protocol during the light phase:

<u>Food availability</u>	<u>Experiment Duration</u>	<u>Lever-laser pairing</u>	<u>Repeats</u>
<i>ad lib</i> food pellet access	2.5 h	on	2-3
no food access	2.5 h	on	2-3

To test memory extinction, group A mice were then conditioned with the following protocol:

<u>Food availability</u>	<u>Experiment Duration</u>	<u>Lever-laser pairing</u>	<u>Repeats</u>
<i>ad lib</i> food pellet access	2.5 h	off	3-4

The data from the last trial of the extinction experiments were compared to the pre-extinction trials in the analysis.

Group B mice were initially tested with the following protocols to determine baseline lever press during the light phase:

<u>Food availability</u>	<u>Experiment Duration</u>	<u>Lever-laser pairing</u>	<u>Repeats</u>
no food pellet access	2.5 h	off	1

Group B mice were then habituated overnight with the following protocol:

<u>Food availability</u>	<u>Experiment Duration</u>	<u>Lever-laser pairing</u>	<u>Repeats</u>
no food pellet access	Overnight	On	3

After conditioning, group B mice were then tested with the following protocol during the light phase:

<u>Food availability</u>	<u>Experiment Duration</u>	<u>Lever-laser pairing</u>	<u>Repeats</u>
no food pellet access	2.5 h	on	2-3

Negative Reinforcement Assay

AgRP-ChR2 mice with optical implants above the ARC were used in this experiment. Mice were naive to the lever (never exposed to a lever before) at the beginning of this experiment. The spatial localization of the active lever and inactive lever in the cage was counterbalanced within each cohort and fixed through the whole experiment.

Mice were then conditioned to active lever during the beginning of the dark phase for 2 hours for 3-4 times. During conditioning, each mouse received constant 20 Hz laser stimulation that could be turned off for 20 seconds by each press of the active lever. After three repeats of this conditioning protocol, mice were then tested with the same protocol during the light phase. Each trial lasted for 1 hour.

Fos staining following self-stimulation

Mice were tested with the self-stimulation protocol described above in the presence of food for 2.5. Immediately after the self-stimulation experiment, each mouse was perfused transcardially with PBS buffer followed by formalin. Brains were removed, postfixed in 4% PFA and transferred to PBS buffered 20% sucrose. Free floating sections (40 μ m) were prepared with a cryostat, blocked (3% BSA, 2% NGS, and 0.1% Triton-X in PBS for 2 h), and then incubated with primary antibody (chicken anti-GFP, Abcam, ab13970, 1:1,000; goat anti-Fos, Santa Cruz, SC52G, 1:500) overnight at 4°C. Samples were washed, incubated with secondary antibody (goat anti-chicken Alexa 488 secondary antibody; Invitrogen, 1:1000; donkey anti-goat Alexa 568 secondary antibody; Invitrogen, 1:1000) for 2 h at room temperature, washed, mounted,

and imaged with a confocal microscope. Images for direct comparison are imaged with the same settings.

To quantify the percentage of AgRP neurons that express Fos, we first identified 100 putative AgRP cells from each mouse based on GFP fluorescence using the ImageJ Cell Counter Plugin. We then manually quantified the presence or absence of Fos staining in those previously defined cells.

Immunofluorescence

Immunofluorescence was performed as previously described (Chen et al., 2015) using the following antibodies: Chicken anti-GFP (Aves Lab, GFP-1020, 1:1000); Goat anti-chicken Alexa-fluorophore 488 (Life Technologies A11039, 1:1,000).

Statistics

Raw behavioral data were analyzed with custom MATLAB scripts. Multiple measurements from the same mouse in the same experiment (e.g. on different days) were considered technical repeats and were averaged before statistical analysis. The average of these technical repeats for each mouse in each experiment was considered a single biological repeat and was used to determine sample size for statistical analysis. Data was analyzed by two-way ANOVA using Graphpad Prism 6 to test for an effect of genotype and stimulation protocol (experiments with WT control) or one-way ANOVA (experiments without WT control). Individual p-values were corrected using Holm-Sidak's multiple comparisons test. Regression analysis for experiments investigating feeding kinetics was performed using Graphpad.

SUPPLEMENTARY FIGURES

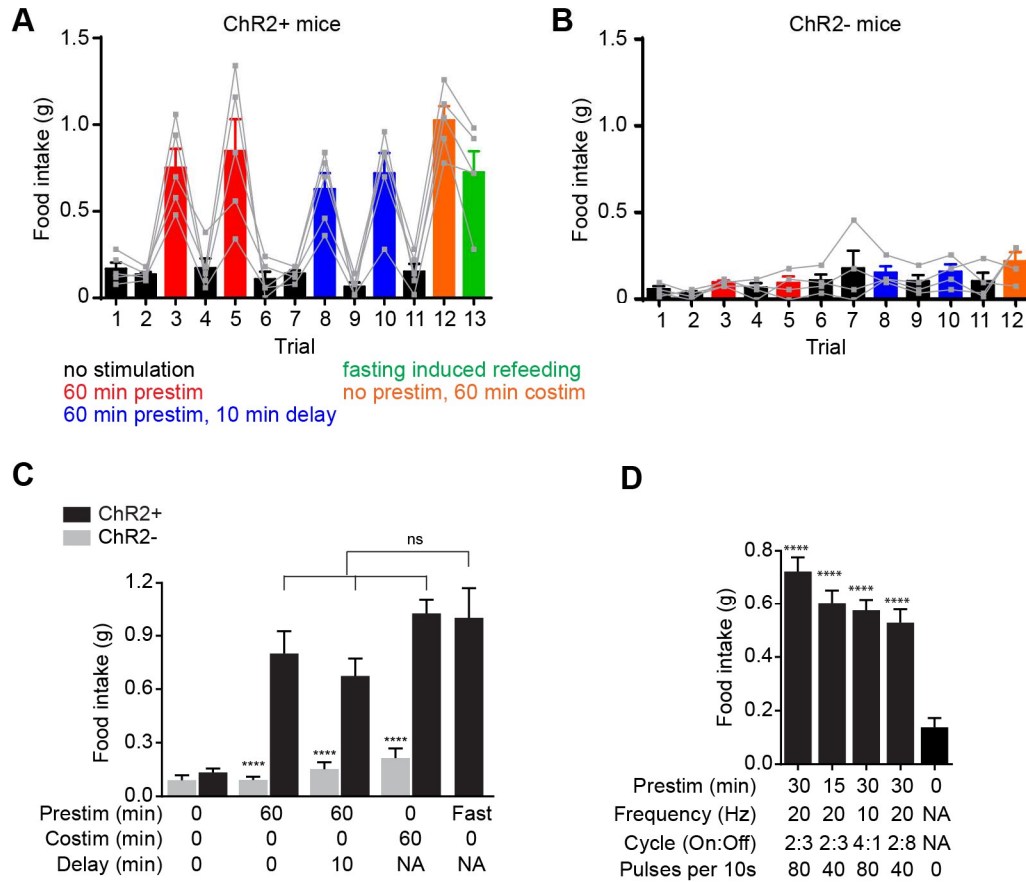


Figure 5.7. – Related to Figure 5.1. Prestimulation of AgRP neurons primes feeding. (A-B) 60 min food intake of (A) AgRP-ChR2 (n=5) and (B) WT control (n=4) mice in trials conducted in consecutive days. (C) Analysis of 60 min food intake of AgRP-ChR2 (n=5) and WT control (n=4) mice under different stimulation condition. Asterisks indicate significance level for comparison between WT and AgRP:ChR2 animals subjected to same stimulation protocol. ns, not significant. (D) Average 60 min food intake evoked by prestimulation with varied temporal structure of laser pulses (n=8). Asterisks on top of bar plots indicate significance levels compared to no stimulation control and asterisks on top of brackets indicate significance levels for comparisons with the respective protocols, using one-way-ANOVA with Holm-Sidak's correction for multiple comparisons (****p≤0.0001, ***0.0001<p≤0.001, **0.001<p≤0.01, *0.01<p≤0.05, ns p>0.05).

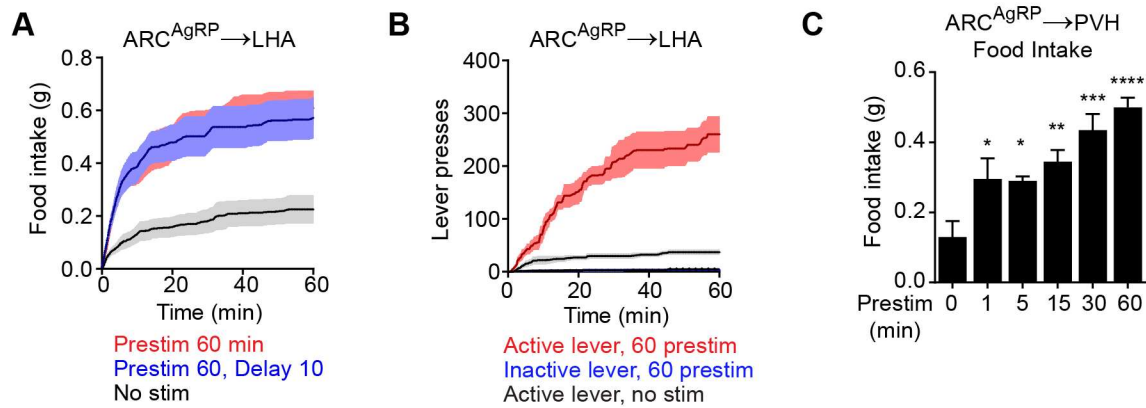


Figure 5.8. – Related to Figure 5.4. Prestimulation of specific AgRP neuron projections promotes feeding.

(A) Plots of cumulative food intake for prestimulation $AgRP^{ARC \rightarrow LHA}$ projections. Filled area indicates SEM (n=6). **(B)** Plots of cumulative lever presses for prestimulation of $AgRP^{ARC \rightarrow LHA}$ projections. Filled area indicates SEM (n=3). **(C)** Food intake evoked by prestimulation of $AgRP^{ARC \rightarrow PVH}$ projections of varied duration (n=4). Asterisks indicate significance levels for comparison to no prestimulation adjusted with Holm-Sidak's correction for multiple comparisons (**** $p \leq 0.0001$, *** $0.0001 < p \leq 0.001$, ** $0.001 < p \leq 0.01$, * $0.01 < p \leq 0.05$).

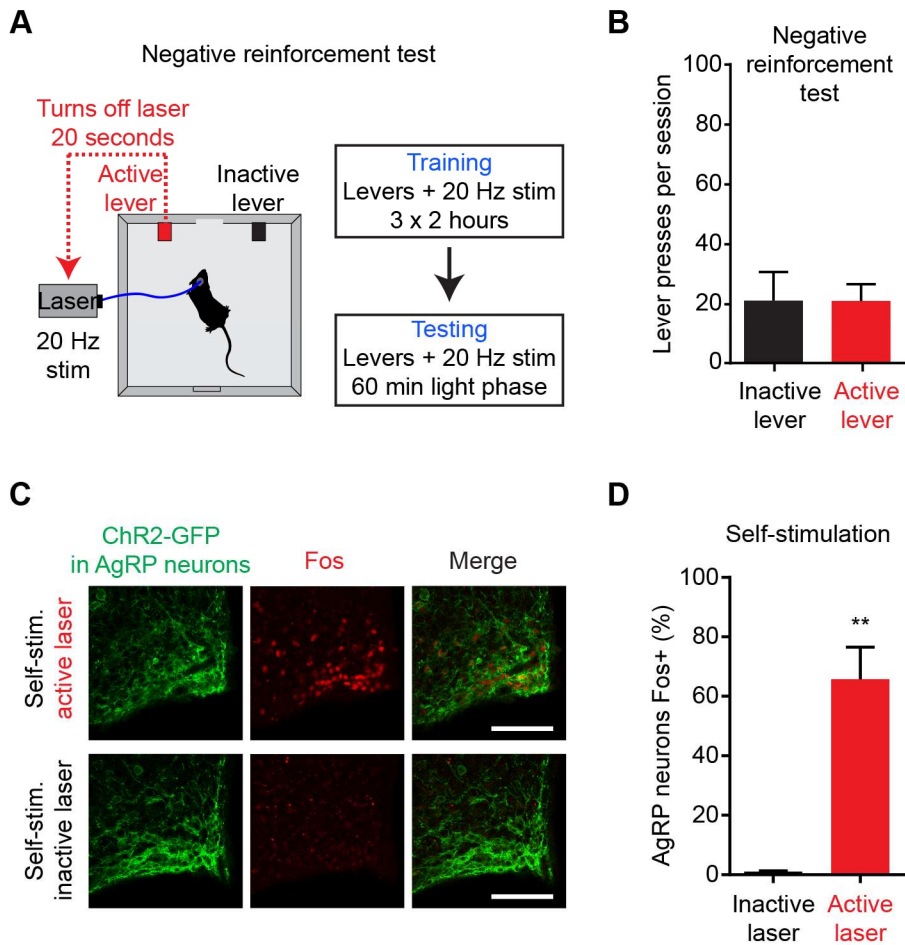


Figure 5.9. – Related to Figure 5.6. AgRP neurons support positive, but not negative, reinforcement.

(A) Schematic of the negative reinforcement protocol that tests whether animals will lever press to shut off AgRP neuron activity. **(B)** Number of presses for the active and inactive lever in a 60 minute negative reinforcement test ($n=6$). **(C)** Induction of Fos expression in AgRP neurons of mice that are allowed to self-stimulate by lever pressing (top), but not in mice in which the lever has been disconnected from the laser (bottom). **(D)** Quantification of the percentage of AgRP neurons that express Fos in each group ($n=3$). Asterisks indicate a significant difference in Fos expression between the two groups by an unpaired, two-tailed t-test. (** $0.001 < p \leq 0.01$).

References

- Acuna-Goycolea, C., and van den Pol, A.N. (2005). Peptide YY3-36 inhibits both anorexigenic proopiomelanocortin and orexigenic neuropeptide Y neurons: Implications for hypothalamic regulation of energy homeostasis. *Journal of Neuroscience* 25, 10510-10519.
- Adamantidis, A., Arber, S., Bains, J.S., Bamberg, E., Bonci, A., Buzsaki, G., Cardin, J.A., Costa, R.M., Dan, Y., Goda, Y., *et al.* (2015). Optogenetics: 10 years after ChR2 in neurons--views from the community. *Nature neuroscience* 18, 1202-1212.
- Ammar, A.A., Nergardh, R., Fredholm, B.B., Brodin, U., and Sodersten, P. (2005). Intake inhibition by NPY and CCK-8: A challenge of the notion of NPY as an "Orexigen". *Behavioural brain research* 161, 82-87.
- Andermann, M.L., and Lowell, B.B. (2017). Toward a Wiring Diagram Understanding of Appetite Control. *Neuron* 95, 757-778.
- Andrews, Z.B., Liu, Z.W., Wallingford, N., Erion, D.M., Borok, E., Friedman, J.M., Tschop, M.H., Shanabrough, M., Cline, G., Shulman, G.I., *et al.* (2008). UCP2 mediates ghrelin's action on NPY/AgRP neurons by lowering free radicals. *Nature* 454, 846-851.
- Aponte, Y., Atasoy, D., and Sternson, S.M. (2011). AGRP neurons are sufficient to orchestrate feeding behavior rapidly and without training. *Nature neuroscience* 14, 351-355.
- Atasoy, D., Betley, J.N., Su, H.H., and Sternson, S.M. (2012). Deconstruction of a neural circuit for hunger. *Nature* 488, 172-177.
- Balthasar, N., Dalgaard, L.T., Lee, C.E., Yu, J., Funahashi, H., Williams, T., Ferreira, M., Tang, V., McGovern, R.A., Kenny, C.D., *et al.* (2005). Divergence of melanocortin pathways in the control of food intake and energy expenditure. *Cell* 123, 493-505.
- Bannon, A.W., Seda, J., Carmouche, M., Francis, J.M., Norman, M.H., Karbon, B., and McCaleb, M.L. (2000). Behavioral characterization of neuropeptide Y knockout mice. *Brain Res* 868, 79-87.
- Barrachina, M.D., Martinez, V., Wang, L.X., Wei, J.Y., and Tache, Y. (1997). Synergistic interaction between leptin and cholecystokinin to reduce short-term food intake in lean mice. *Proceedings of the National Academy of Sciences of the United States of America* 94, 10455-10460.
- Batterham, R.L., Cowley, M.A., Small, C.J., Herzog, H., Cohen, M.A., Dakin, C.L., Wren, A.M., Brynes, A.E., Low, M.J., Ghatei, M.A., *et al.* (2002). Gut hormone PYY(3-36) physiologically inhibits food intake. *Nature* 418, 650-654.
- Becskei, C., Lutz, T.A., and Riediger, T. (2008). Glucose reverses fasting-induced activation in the arcuate nucleus of mice. *Neuroreport* 19, 105-109.
- Berridge, K.C. (2004). Motivation concepts in behavioral neuroscience. *Physiology & behavior* 81, 179-209.

- Berridge, K.C. (2007). The debate over dopamine's role in reward: the case for incentive salience. *Psychopharmacology* 191, 391-431.
- Berridge, K.C. (2009). 'Liking' and 'wanting' food rewards: brain substrates and roles in eating disorders. *Physiology & behavior* 97, 537-550.
- Berthoud, H.R. (2008). The vagus nerve, food intake and obesity. *Regulatory peptides* 149, 15-25.
- Betley, J.N., Cao, Z.F., Ritola, K.D., and Sternson, S.M. (2013). Parallel, redundant circuit organization for homeostatic control of feeding behavior. *Cell* 155, 1337-1350.
- Betley, J.N., Xu, S., Cao, Z.F., Gong, R., Magnus, C.J., Yu, Y., and Sternson, S.M. (2015). Neurons for hunger and thirst transmit a negative-valence teaching signal. *Nature* 521, 180-185.
- Beutler, L.R., Chen, Y., Ahn, J.S., Lin, Y.C., Essner, R.A., and Knight, Z.A. (2017). Dynamics of Gut-Brain Communication Underlying Hunger. *Neuron* 96, 461-475 e465.
- Bindra, D. (1976). *A theory of intelligent behavior* (New York: Wiley).
- Blouet, C., and Schwartz, G.J. (2010). Hypothalamic nutrient sensing in the control of energy homeostasis. *Behavioural brain research* 209, 1-12.
- Brand, J.G., Cagan, R.H., and Naim, M. (1982). Chemical senses in the release of gastric and pancreatic secretions. *Annual review of nutrition* 2, 249-276.
- Broberger, C., Johansen, J., Johansson, C., Schalling, M., and Hokfelt, T. (1998). The neuropeptide Y/agouti gene-related protein (AGRP) brain circuitry in normal, anorectic, and monosodium glutamate-treated mice. *Proceedings of the National Academy of Sciences of the United States of America* 95, 15043-15048.
- Broberger, C., Landry, M., Wong, H., Walsh, J.N., and Hokfelt, T. (1997). Subtypes Y1 and Y2 of the neuropeptide Y receptor are respectively expressed in pro-opiomelanocortin- and neuropeptide-Y-containing neurons of the rat hypothalamic arcuate nucleus. *Neuroendocrinology* 66, 393-408.
- Burnett, C.J., Li, C., Webber, E., Tsaousidou, E., Xue, S.Y., Bruning, J.C., and Krashes, M.J. (2016). Hunger-Driven Motivational State Competition. *Neuron* 92, 187-201.
- Cabanac, M. (1971). Physiological role of pleasure. *Science* 173, 1103-1107.
- Campos, C.A., Bowen, A.J., Schwartz, M.W., and Palmiter, R.D. (2016). Parabrachial CGRP Neurons Control Meal Termination. *Cell Metab* 23, 811-820.
- Cannon, W.B. (1929). Organization for Physiological Homeostasis. *Physiological Reviews* 9, 399-431.

- Cecil, J.E., Castiglione, K., French, S., Francis, J., and Read, N.W. (1998). Effects of intragastric infusions of fat and carbohydrate on appetite ratings and food intake from a test meal. *Appetite* 30, 65-77.
- Chen, T.W., Wardill, T.J., Sun, Y., Pulver, S.R., Renninger, S.L., Baohan, A., Schreiter, E.R., Kerr, R.A., Orger, M.B., Jayaraman, V., *et al.* (2013). Ultrasensitive fluorescent proteins for imaging neuronal activity. *Nature* 499, 295-300.
- Chen, Y., and Knight, Z.A. (2016). Making sense of the sensory regulation of hunger neurons. *Bioessays* 38, 316-324.
- Chen, Y., Lin, Y.C., Kuo, T.W., and Knight, Z.A. (2015). Sensory detection of food rapidly modulates arcuate feeding circuits. *Cell* 160, 829-841.
- Chen, Y., Lin, Y.C., Zimmerman, C.A., Essner, R.A., and Knight, Z.A. (2016). Hunger neurons drive feeding through a sustained, positive reinforcement signal. *Elife* 5.
- Claret, M., Smith, M.A., Batterham, R.L., Selman, C., Choudhury, A.I., Fryer, L.G., Clements, M., Al-Qassab, H., Heffron, H., Xu, A.W., *et al.* (2007). AMPK is essential for energy homeostasis regulation and glucose sensing by POMC and AgRP neurons. *J Clin Invest* 117, 2325-2336.
- Clark, J.T., Kalra, P.S., and Kalra, S.P. (1985). Neuropeptide Y stimulates feeding but inhibits sexual behavior in rats. *Endocrinology* 117, 2435-2442.
- Clemmensen, C., Muller, T.D., Woods, S.C., Berthoud, H.R., Seeley, R.J., and Tschop, M.H. (2017). Gut-Brain Cross-Talk in Metabolic Control. *Cell* 168, 758-774.
- Cone, R.D. (2005). Anatomy and regulation of the central melanocortin system. *Nature neuroscience* 8, 571-578.
- Corbett, D., and Wise, R.A. (1980). Intracranial self-stimulation in relation to the ascending dopaminergic systems of the midbrain: a moveable electrode mapping study. *Brain Res* 185, 1-15.
- Cowley, M.A., Smart, J.L., Rubinstein, M., Cerdan, M.G., Diano, S., Horvath, T.L., Cone, R.D., and Low, M.J. (2001). Leptin activates anorexigenic POMC neurons through a neural network in the arcuate nucleus. *Nature* 411, 480-484.
- Cowley, M.A., Smith, R.G., Diano, S., Tschop, M., Pronchuk, N., Grove, K.L., Strasburger, C.J., Bidlingmaier, M., Esterman, M., Heiman, M.L., *et al.* (2003). The distribution and mechanism of action of ghrelin in the CNS demonstrates a novel hypothalamic circuit regulating energy homeostasis. *Neuron* 37, 649-661.
- Cui, G., Jun, S.B., Jin, X., Pham, M.D., Vogel, S.S., Lovinger, D.M., and Costa, R.M. (2013). Concurrent activation of striatal direct and indirect pathways during action initiation. *Nature* 494, 238-242.

Cummings, D.E., and Overduin, J. (2007). Gastrointestinal regulation of food intake. *Journal of Clinical Investigation* 117, 13-23.

Davis, J.D., and Campbell, C.S. (1973). Peripheral control of meal size in the rat. Effect of sham feeding on meal size and drinking rate. *Journal of comparative and physiological psychology* 83, 379-387.

Davis, J.D., and Smith, G.P. (1990). Learning to sham feed: behavioral adjustments to loss of physiological postingestional stimuli. *The American journal of physiology* 259, R1228-1235.

Day, D.E., Keen-Rhinehart, E., and Bartness, T.J. (2005). Role of NPY and its receptor subtypes in foraging, food hoarding, and food intake by Siberian hamsters. *American journal of physiology Regulatory, integrative and comparative physiology* 289, R29-36.

Dietrich, M.O., Bober, J., Ferreira, J.G., Tellez, L.A., Mineur, Y.S., Souza, D.O., Gao, X.B., Picciotto, M.R., Araujo, I., Liu, Z.W., *et al.* (2012). AgRP neurons regulate development of dopamine neuronal plasticity and nonfood-associated behaviors. *Nature neuroscience* 15, 1108-1110.

Dietrich, M.O., Liu, Z.W., and Horvath, T.L. (2013). Mitochondrial dynamics controlled by mitofusins regulate AgRP neuronal activity and diet-induced obesity. *Cell* 155, 188-199.

Dubois, C.J., Ramamoorthy, P., Whim, M.D., and Liu, S.J. (2012). Activation of NPY type 5 receptors induces a long-lasting increase in spontaneous GABA release from cerebellar inhibitory interneurons. *J Neurophysiol* 107, 1655-1665.

Erickson, J.C., Clegg, K.E., and Palmiter, R.D. (1996). Sensitivity to leptin and susceptibility to seizures of mice lacking neuropeptide Y. *Nature* 381, 415-421.

Fan, W., Boston, B.A., Kesterson, R.A., Hruby, V.J., and Cone, R.D. (1997). Role of melanocortinergic neurons in feeding and the agouti obesity syndrome. *Nature* 385, 165-168.

Farooqi, I.S., Keogh, J.M., Yeo, G.S., Lank, E.J., Cheetham, T., and O'Rahilly, S. (2003). Clinical spectrum of obesity and mutations in the melanocortin 4 receptor gene. *The New England journal of medicine* 348, 1085-1095.

Farooqi, I.S., Yeo, G.S., Keogh, J.M., Aminian, S., Jebb, S.A., Butler, G., Cheetham, T., and O'Rahilly, S. (2000). Dominant and recessive inheritance of morbid obesity associated with melanocortin 4 receptor deficiency. *J Clin Invest* 106, 271-279.

Feldman, M., and Richardson, C.T. (1986). Role of thought, sight, smell, and taste of food in the cephalic phase of gastric acid secretion in humans. *Gastroenterology* 90, 428-433.

Fenselau, H., Campbell, J.N., Verstegen, A.M., Madara, J.C., Xu, J., Shah, B.P., Resch, J.M., Yang, Z., Mandelblat-Cerf, Y., Livneh, Y., *et al.* (2017). A rapidly acting glutamatergic ARC->PVH satiety circuit postsynaptically regulated by alpha-MSH. *Nature neuroscience* 20, 42-51.

Fields, H.L., Hjelmstad, G.O., Margolis, E.B., and Nicola, S.M. (2007). Ventral tegmental area neurons in learned appetitive behavior and positive reinforcement. *Annual review of neuroscience* 30, 289-316.

Friedman, J. (2014). 20 YEARS OF LEPTIN: Leptin at 20: an overview. *The Journal of endocrinology* 223, T1-T8.

Friedman, J.M., and Halaas, J.L. (1998). Leptin and the regulation of body weight in mammals. *Nature* 395, 763-770.

Fu, L.Y., Acuna-Goycolea, C., and van den Pol, A.N. (2004). Neuropeptide Y inhibits hypocretin/orexin neurons by multiple presynaptic and postsynaptic mechanisms: tonic depression of the hypothalamic arousal system. *The Journal of neuroscience : the official journal of the Society for Neuroscience* 24, 8741-8751.

Fulton, S. (2010). Appetite and reward. *Front Neuroendocrinol* 31, 85-103.

Gao, Q., and Horvath, T.L. (2007). Neurobiology of feeding and energy expenditure. *Annual review of neuroscience* 30, 367-398.

Garfield, A.S., Li, C., Madara, J.C., Shah, B.P., Webber, E., Steger, J.S., Campbell, J.N., Gavrilova, O., Lee, C.E., Olson, D.P., *et al.* (2015). A neural basis for melanocortin-4 receptor-regulated appetite. *Nature neuroscience* 18, 863-871.

Garfield, A.S., Shah, B.P., Burgess, C.R., Li, M.M., Li, C., Steger, J.S., Madara, J.C., Campbell, J.N., Kroeger, D., Scammell, T.E., *et al.* (2016). Dynamic GABAergic afferent modulation of AgRP neurons. *Nature neuroscience* 19, 1628-1635.

Grill, H.J., and Norgren, R. (1978). Chronically decerebrate rats demonstrate satiation but not bait shyness. *Science* 201, 267-269.

Gropp, E., Shanabrough, M., Borok, E., Xu, A.W., Janoschek, R., Buch, T., Plum, L., Balthasar, N., Hampel, B., Waisman, A., *et al.* (2005). Agouti-related peptide-expressing neurons are mandatory for feeding. *Nature neuroscience* 8, 1289-1291.

Gunaydin, L.A., Grosenick, L., Finkelstein, J.C., Kauvar, I.V., Fenno, L.E., Adhikari, A., Lammel, S., Mirzabekov, J.J., Airan, R.D., Zalocusky, K.A., *et al.* (2014). Natural neural projection dynamics underlying social behavior. *Cell* 157, 1535-1551.

Hagan, M.M., Rushing, P.A., Pritchard, L.M., Schwartz, M.W., Strack, A.M., Van Der Ploeg, L.H., Woods, S.C., and Seeley, R.J. (2000). Long-term orexigenic effects of AgRP-(83---132) involve mechanisms other than melanocortin receptor blockade. *American journal of physiology Regulatory, integrative and comparative physiology* 279, R47-52.

Hahn, T.M., Breininger, J.F., Baskin, D.G., and Schwartz, M.W. (1998). Coexpression of Agrp and NPY in fasting-activated hypothalamic neurons. *Nature neuroscience* 1, 271-272.

Halatchev, I.G., Ellacott, K.L., Fan, W., and Cone, R.D. (2004). Peptide YY3-36 inhibits food intake in mice through a melanocortin-4 receptor-independent mechanism. *Endocrinology* 145, 2585-2590.

Hentges, S.T., Nishiyama, M., Overstreet, L.S., Stenzel-Poore, M., Williams, J.T., and Low, M.J. (2004). GABA release from proopiomelanocortin neurons. *The Journal of neuroscience : the official journal of the Society for Neuroscience* 24, 1578-1583.

Hetherington, A.W., and Ranson, S.W. (1939). Experimental hypothalamico-hypophyseal obesity in the rat. *Proceedings of the Society for Experimental Biology and Medicine* 41, 465-466.

Hinney, A., Schmidt, A., Nottebom, K., Heibult, O., Becker, I., Ziegler, A., Gerber, G., Sina, M., Gorg, T., Mayer, H., *et al.* (1999). Several mutations in the melanocortin-4 receptor gene including a nonsense and a frameshift mutation associated with dominantly inherited obesity in humans. *The Journal of clinical endocrinology and metabolism* 84, 1483-1486.

Hodos, W. (1961). Progressive ratio as a measure of reward strength. *Science* 134, 943-944.

Hoopfer, E.D., Jung, Y., Inagaki, H.K., Rubin, G.M., and Anderson, D.J. (2015). P1 interneurons promote a persistent internal state that enhances inter-male aggression in *Drosophila*. *Elife* 4.

Horvath, T.L. (2005). The hardship of obesity: a soft-wired hypothalamus. *Nature neuroscience* 8, 561-565.

Horvath, T.L., and Diano, S. (2004). The floating blueprint of hypothalamic feeding circuits. *Nature reviews Neuroscience* 5, 662-667.

Hull, C.L. (1943). *Principles of behavior, an introduction to behavior theory* (New York,: D. Appleton-Century Company).

Huszar, D., Lynch, C.A., Fairchild-Huntress, V., Dunmore, J.H., Fang, Q., Berkemeier, L.R., Gu, W., Kesterson, R.A., Boston, B.A., Cone, R.D., *et al.* (1997). Targeted disruption of the melanocortin-4 receptor results in obesity in mice. *Cell* 88, 131-141.

Janowitz, H.D., Hollander, F., Orringer, D., Levy, M.H., Winkelstein, A., Kaufman, R., and Margolin, S.G. (1950). A quantitative study of the gastric secretory response to sham feeding in a human subject. *Gastroenterology* 16, 104-116.

Jennings, J.H., Rizzi, G., Stamatakis, A.M., Ung, R.L., and Stuber, G.D. (2013). The inhibitory circuit architecture of the lateral hypothalamus orchestrates feeding. *Science* 341, 1517-1521.

Jerlhag, E., Egecioglu, E., Dickson, S.L., Andersson, M., Svensson, L., and Engel, J.A. (2006). Ghrelin stimulates locomotor activity and accumbal dopamine-overflow via central cholinergic systems in mice: implications for its involvement in brain reward. *Addiction biology* 11, 45-54.

Kanatani, A., Mashiko, S., Murai, N., Sugimoto, N., Ito, J., Fukuroda, T., Fukami, T., Morin, N., MacNeil, D.J., Van der Ploeg, L.H., *et al.* (2000). Role of the Y1 receptor in the regulation of

neuropeptide Y-mediated feeding: comparison of wild-type, Y1 receptor-deficient, and Y5 receptor-deficient mice. *Endocrinology* *141*, 1011-1016.

Kermani, M., and Eliassi, A. (2012). Gastric acid secretion induced by paraventricular nucleus microinjection of orexin A is mediated through activation of neuropeptide Yergic system. *Neuroscience* *226*, 81-88.

Klajner, F., Herman, C.P., Polivy, J., and Chhabra, R. (1981). Human obesity, dieting, and anticipatory salivation to food. *Physiology & behavior* *27*, 195-198.

Koda, S., Date, Y., Murakami, N., Shimbara, T., Hanada, T., Toshinai, K., Nijjima, A., Furuya, M., Inomata, N., Osuye, K., *et al.* (2005). The role of the vagal nerve in peripheral PYY3-36-induced feeding reduction in rats. *Endocrinology* *146*, 2369-2375.

Kohatsu, S., and Yamamoto, D. (2015). Visually induced initiation of *Drosophila* innate courtship-like following pursuit is mediated by central excitatory state. *Nat Commun* *6*, 6457.

Krashes, M.J., Koda, S., Ye, C., Rogan, S.C., Adams, A.C., Cusher, D.S., Maratos-Flier, E., Roth, B.L., and Lowell, B.B. (2011). Rapid, reversible activation of AgRP neurons drives feeding behavior in mice. *J Clin Invest* *121*, 1424-1428.

Krashes, M.J., Lowell, B.B., and Garfield, A.S. (2016). Melanocortin-4 receptor-regulated energy homeostasis. *Nature neuroscience* *19*, 206-219.

Krashes, M.J., Shah, B.P., Koda, S., and Lowell, B.B. (2013). Rapid versus delayed stimulation of feeding by the endogenously released AgRP neuron mediators GABA, NPY, and AgRP. *Cell Metab* *18*, 588-595.

Krashes, M.J., Shah, B.P., Madara, J.C., Olson, D.P., Strohlic, D.E., Garfield, A.S., Vong, L., Pei, H., Watabe-Uchida, M., Uchida, N., *et al.* (2014). An excitatory paraventricular nucleus to AgRP neuron circuit that drives hunger. *Nature* *507*, 238-242.

Kravitz, A.V., Tye, L.D., and Kreitzer, A.C. (2012). Distinct roles for direct and indirect pathway striatal neurons in reinforcement. *Nature neuroscience* *15*, 816-818.

LeGall-Salmon, E., Stevens, W.D., and Levy, J.R. (1999). Total parenteral nutrition increases serum leptin concentration in hospitalized, undernourished patients. *JPEN J Parenter Enteral Nutr* *23*, 38-42.

Lima, S.Q., Hromadka, T., Znamenskiy, P., and Zador, A.M. (2009). PINP: a new method of tagging neuronal populations for identification during in vivo electrophysiological recording. *PLoS one* *4*, e6099.

Liu, T., Kong, D., Shah, B.P., Ye, C., Koda, S., Saunders, A., Ding, J.B., Yang, Z., Sabatini, B.L., and Lowell, B.B. (2012). Fasting activation of AgRP neurons requires NMDA receptors and involves spinogenesis and increased excitatory tone. *Neuron* *73*, 511-522.

Lockie, S.H., and Andrews, Z.B. (2013). The hormonal signature of energy deficit: Increasing the value of food reward. *Molecular metabolism* *2*, 329-336.

- Lu, D.S., Willard, D., Patel, I.R., Kadwell, S., Overton, L., Kost, T., Luther, M., Chen, W.B., Woychik, R.P., Wilkison, W.O., *et al.* (1994). Agouti Protein Is an Antagonist of the Melanocyte-Stimulating-Hormone Receptor. *Nature* 371, 799-802.
- Luo, L. (2015). *Principles of neurobiology* (New York, NY: Garland Science).
- Luquet, S., Perez, F.A., Hnasko, T.S., and Palmiter, R.D. (2005). NPY/AgRP neurons are essential for feeding in adult mice but can be ablated in neonates. *Science* 310, 683-685.
- Major, G., and Tank, D. (2004). Persistent neural activity: prevalence and mechanisms. *Curr Opin Neurobiol* 14, 675-684.
- Mandelblat-Cerf, Y., Ramesh, R.N., Burgess, C.R., Patella, P., Yang, Z., Lowell, B.B., and Andermann, M.L. (2015). Arcuate hypothalamic AgRP and putative POMC neurons show opposite changes in spiking across multiple timescales. *Elife* 4.
- Marsh, D.J., Hollopeter, G., Kafer, K.E., and Palmiter, R.D. (1998). Role of the Y5 neuropeptide Y receptor in feeding and obesity. *Nat Med* 4, 718-721.
- Morley, J.E., Hernandez, E.N., and Flood, J.F. (1987a). Neuropeptide Y increases food intake in mice. *The American journal of physiology* 253, R516-522.
- Morley, J.E., Levine, A.S., Gosnell, B.A., Kneip, J., and Grace, M. (1987b). Effect of neuropeptide Y on ingestive behaviors in the rat. *The American journal of physiology* 252, R599-609.
- Myers, M.G., Munzberg, H., Leininger, G.M., and Leshan, R.L. (2009). The Geometry of Leptin Action in the Brain: More Complicated Than a Simple ARC. *Cell Metabolism* 9, 117-123.
- Nakajima, K., Cui, Z., Li, C., Meister, J., Cui, Y., Fu, O., Smith, A.S., Jain, S., Lowell, B.B., Krashes, M.J., *et al.* (2016). Gs-coupled GPCR signalling in AgRP neurons triggers sustained increase in food intake. *Nat Commun* 7, 10268.
- Nakazato, M., Murakami, N., Date, Y., Kojima, M., Matsuo, H., Kangawa, K., and Matsukura, S. (2001). A role for ghrelin in the central regulation of feeding. *Nature* 409, 194-198.
- Namburi, P., Beyeler, A., Yorozu, S., Calhoon, G.G., Halbert, S.A., Wichmann, R., Holden, S.S., Mertens, K.L., Anahtar, M., Felix-Ortiz, A.C., *et al.* (2015). A circuit mechanism for differentiating positive and negative associations. *Nature* 520, 675-678.
- Oka, Y., Ye, M., and Zuker, C.S. (2015). Thirst driving and suppressing signals encoded by distinct neural populations in the brain. *Nature* 520, 349-352.
- Ollmann, M.M., Wilson, B.D., Yang, Y.K., Kerns, J.A., Chen, Y., Gantz, I., and Barsh, G.S. (1997). Antagonism of central melanocortin receptors in vitro and in vivo by agouti-related protein. *Science* 278, 135-138.

Padilla, S.L., Qiu, J., Soden, M.E., Sanz, E., Nestor, C.C., Barker, F.D., Quintana, A., Zweifel, L.S., Ronnekleiv, O.K., Kelly, M.J., *et al.* (2016). Agouti-related peptide neural circuits mediate adaptive behaviors in the starved state. *Nature neuroscience* 19, 734-741.

Parkinson, J.R., Dhillon, W.S., Small, C.J., Chaudhri, O.B., Bewick, G.A., Pritchard, I., Moore, S., Ghatei, M.A., and Bloom, S.R. (2008). PYY3-36 injection in mice produces an acute anorexigenic effect followed by a delayed orexigenic effect not observed with other anorexigenic gut hormones. *Am J Physiol Endocrinol Metab* 294, E698-708.

Patel, H.R., Qi, Y., Hawkins, E.J., Hileman, S.M., Elmquist, J.K., Imai, Y., and Ahima, R.S. (2006). Neuropeptide Y deficiency attenuates responses to fasting and high-fat diet in obesity-prone mice. *Diabetes* 55, 3091-3098.

Pavlov, I.P. (1902). *The work of the digestive glands* (London: Charles Griffin Co. Ltd.).

Petrovich, G.D., Ross, C.A., Gallagher, M., and Holland, P.C. (2007). Learned contextual cue potentiates eating in rats. *Physiology & behavior* 90, 362-367.

Pinto, S., Roseberry, A.G., Liu, H., Diano, S., Shanabrough, M., Cai, X., Friedman, J.M., and Horvath, T.L. (2004). Rapid rewiring of arcuate nucleus feeding circuits by leptin. *Science* 304, 110-115.

Poggioli, R., Vergoni, A.V., and Bertolini, A. (1986). ACTH-(1-24) and alpha-MSH antagonize feeding behavior stimulated by kappa opiate agonists. *Peptides* 7, 843-848.

Power, M.L., and Schulkin, J. (2008). Anticipatory physiological regulation in feeding biology: cephalic phase responses. *Appetite* 50, 194-206.

Powley, T.L. (1977). The ventromedial hypothalamic syndrome, satiety, and a cephalic phase hypothesis. *Psychol Rev* 84, 89-126.

Qian, S., Chen, H., Weingarh, D., Trumbauer, M.E., Novi, D.E., Guan, X., Yu, H., Shen, Z., Feng, Y., Frazier, E., *et al.* (2002). Neither agouti-related protein nor neuropeptide Y is critically required for the regulation of energy homeostasis in mice. *Mol Cell Biol* 22, 5027-5035.

Reidelberger, R.D. (1994). Cholecystokinin and control of food intake. *J Nutr* 124, 1327S-1333S.

Richter, C.P. (1942). *Total self-regulatory functions in animals and human beings*. Harvey Lecture Series 38, 63-103.

Riediger, T., Bothe, C., Becskei, C., and Lutz, T.A. (2004). Peptide YY directly inhibits ghrelin-activated neurons of the arcuate nucleus and reverses fasting-induced c-Fos expression. *Neuroendocrinology* 79, 317-326.

Rolls, E.T., Burton, M.J., and Mora, F. (1980). Neurophysiological analysis of brain-stimulation reward in the monkey. *Brain Res* 194, 339-357.

- Roseberry, A.G., Liu, H., Jackson, A.C., Cai, X., and Friedman, J.M. (2004). Neuropeptide Y-mediated inhibition of proopiomelanocortin neurons in the arcuate nucleus shows enhanced desensitization in ob/ob mice. *Neuron* 41, 711-722.
- Schneeberger, M., Dietrich, M.O., Sebastian, D., Imbernon, M., Castano, C., Garcia, A., Esteban, Y., Gonzalez-Franquesa, A., Rodriguez, I.C., Bortolozzi, A., *et al.* (2013). Mitofusin 2 in POMC neurons connects ER stress with leptin resistance and energy imbalance. *Cell* 155, 172-187.
- Schwartz, M.W., Baskin, D.G., Bukowski, T.R., Kuijper, J.L., Foster, D., Lasser, G., Prunkard, D.E., Porte, D., Woods, S.C., Seeley, R.J., *et al.* (1996). Specificity of leptin action on elevated blood glucose levels and hypothalamic neuropeptide Y gene expression in ob/ob mice. *Diabetes* 45, 531-535.
- Schwartz, M.W., Woods, S.C., Porte, D., Jr., Seeley, R.J., and Baskin, D.G. (2000). Central nervous system control of food intake. *Nature* 404, 661-671.
- Sederholm, F., Ammar, A.A., and Sodersten, P. (2002). Intake inhibition by NPY: role of appetitive ingestive behavior and aversion. *Physiology & behavior* 75, 567-575.
- Seeley, R.J., and Berridge, K.C. (2015). The hunger games. *Cell* 160, 805-806.
- Seeley, R.J., Yagaloff, K.A., Fisher, S.L., Burn, P., Thiele, T.E., van Dijk, G., Baskin, D.G., and Schwartz, M.W. (1997). Melanocortin receptors in leptin effects. *Nature* 390, 349.
- Skinner, B.F. (1938). *The behavior of organisms* (New York,: Appleton-Century-Crofts).
- Smith, G.P. (2000). The controls of eating: a shift from nutritional homeostasis to behavioral neuroscience. *Nutrition* 16, 814-820.
- Sohn, J.W., Elmquist, J.K., and Williams, K.W. (2013). Neuronal circuits that regulate feeding behavior and metabolism. *Trends Neurosci* 36, 504-512.
- Spiegelman, B.M., and Flier, J.S. (2001). Obesity and the regulation of energy balance. *Cell* 104, 531-543.
- Steculorum, S.M., Ruud, J., Karakasilioti, I., Backes, H., Engstrom Ruud, L., Timper, K., Hess, M.E., Tsaousidou, E., Mauer, J., Vogt, M.C., *et al.* (2016). AgRP Neurons Control Systemic Insulin Sensitivity via Myostatin Expression in Brown Adipose Tissue. *Cell* 165, 125-138.
- Steffens, A.B. (1976). Influence of the oral cavity on insulin release in the rat. *The American journal of physiology* 230, 1411-1415.
- Stephens, T.W., Basinski, M., Bristow, P.K., Buevalleskey, J.M., Burgett, S.G., Craft, L., Hale, J., Hoffmann, J., Hsiung, H.M., Kriauciunas, A., *et al.* (1995). The Role of Neuropeptide-Y in the Antiobesity Action of the Obese Gene-Product. *Nature* 377, 530-532.
- Sternson, S.M., and Eiselt, A.K. (2017). Three Pillars for the Neural Control of Appetite. *Annu Rev Physiol* 79, 401-423.

- Sternson, S.M., Shepherd, G.M., and Friedman, J.M. (2005). Topographic mapping of VMH --> arcuate nucleus microcircuits and their reorganization by fasting. *Nature neuroscience* 8, 1356-1363.
- Stratton, R.J., and Elia, M. (1999). The effects of enteral tube feeding and parenteral nutrition on appetite sensations and food intake in health and disease. *Clin Nutr* 18, 63-70.
- Stratton, R.J., Stubbs, R.J., and Elia, M. (2003). Short-term continuous enteral tube feeding schedules did not suppress appetite and food intake in healthy men in a placebo-controlled trial. *J Nutr* 133, 2570-2576.
- Stratton, R.J., Stubbs, R.J., and Elia, M. (2008). Bolus tube feeding suppresses food intake and circulating ghrelin concentrations in healthy subjects in a short-term placebo-controlled trial. *Am J Clin Nutr* 88, 77-83.
- Stricker, E.M., and Hoffmann, M.L. (2007). Presystemic signals in the control of thirst, salt appetite, and vasopressin secretion. *Physiology & behavior* 91, 404-412.
- Strubbe, J.H., and Steffens, A.B. (1975). Rapid insulin release after ingestion of a meal in the unanesthetized rat. *The American journal of physiology* 229, 1019-1022.
- Su, Z., Alhadeff, A.L., and Betley, J.N. (2017). Nutritive, Post-ingestive Signals Are the Primary Regulators of AgRP Neuron Activity. *Cell Rep* 21, 2724-2736.
- Takahashi, K.A., and Cone, R.D. (2005). Fasting induces a large, leptin-dependent increase in the intrinsic action potential frequency of orexigenic arcuate nucleus neuropeptide Y/Agouti-related protein neurons. *Endocrinology* 146, 1043-1047.
- Takahashi, N., Okumura, T., Yamada, H., and Kohgo, Y. (1999). Stimulation of gastric acid secretion by centrally administered orexin-A in conscious rats. *Biochemical and biophysical research communications* 254, 623-627.
- Tan, K., Knight, Z.A., and Friedman, J.M. (2014). Ablation of AgRP neurons impairs adaption to restricted feeding. *Molecular metabolism* 3, 694-704.
- Tellez, L.A., Medina, S., Han, W.F., Ferreira, J.G., Licona-Limon, P., Ren, X.Y., Lam, T.T., Schwartz, G.J., and de Araujo, I.E. (2013). A Gut Lipid Messenger Links Excess Dietary Fat to Dopamine Deficiency. *Science* 341, 800-802.
- Tolhurst, G., Reimann, F., and Gribble, F.M. (2012). Intestinal sensing of nutrients. *Handb Exp Pharmacol*, 309-335.
- Tong, Q., Ye, C.P., Jones, J.E., Elmquist, J.K., and Lowell, B.B. (2008). Synaptic release of GABA by AgRP neurons is required for normal regulation of energy balance. *Nature neuroscience* 11, 998-1000.
- Vaisse, C., Clement, K., Durand, E., Hercberg, S., Guy-Grand, B., and Froguel, P. (2000). Melanocortin-4 receptor mutations are a frequent and heterogeneous cause of morbid obesity. *J Clin Invest* 106, 253-262.

- van den Top, M., Lee, K., Whyment, A.D., Blanks, A.M., and Spanswick, D. (2004). Orexigen-sensitive NPY/AgRP pacemaker neurons in the hypothalamic arcuate nucleus. *Nature neuroscience* 7, 493-494.
- Vong, L., Ye, C., Yang, Z., Choi, B., Chua, S., Jr., and Lowell, B.B. (2011). Leptin action on GABAergic neurons prevents obesity and reduces inhibitory tone to POMC neurons. *Neuron* 71, 142-154.
- Wang, D., He, X., Zhao, Z., Feng, Q., Lin, R., Sun, Y., Ding, T., Xu, F., Luo, M., and Zhan, C. (2015). Whole-brain mapping of the direct inputs and axonal projections of POMC and AgRP neurons. *Front Neuroanat* 9, 40.
- Wang, X.J. (2001). Synaptic reverberation underlying mnemonic persistent activity. *Trends Neurosci* 24, 455-463.
- Weigle, D.S. (1994). Appetite and the regulation of body composition. *FASEB journal : official publication of the Federation of American Societies for Experimental Biology* 8, 302-310.
- Weingarten, H.P., and Kulikovsky, O.T. (1989). Taste-to-postingestive consequence conditioning: is the rise in sham feeding with repeated experience a learning phenomenon? *Physiology & behavior* 45, 471-476.
- Williams, K.W., and Elmquist, J.K. (2012). From neuroanatomy to behavior: central integration of peripheral signals regulating feeding behavior. *Nature neuroscience* 15, 1350-1355.
- Wolf, S.G., and Wolff, H.G. (1943). *Human gastric function, an experimental of a man and his stomach* (London, New York etc.: Oxford university press).
- Woods, S.C. (1991). The eating paradox: how we tolerate food. *Psychol Rev* 98, 488-505.
- Woods, S.C., Figlewicz, D.P., Madden, L., Porte, D., Jr., Sipols, A.J., and Seeley, R.J. (1998). NPY and food intake: discrepancies in the model. *Regulatory peptides* 75-76, 403-408.
- Woods, S.C., and Kuskosky, P.J. (1976). Classically conditioned changes of blood glucose level. *Psychosomatic medicine* 38, 201-219.
- Woods, S.C., and Ramsay, D.S. (2007). Homeostasis: beyond Curt Richter. *Appetite* 49, 388-398.
- Woods, S.C., Vasselli, J.R., Kaestner, E., Szakmary, G.A., Milburn, P., and Vitiello, M.V. (1977). Conditioned insulin secretion and meal feeding in rats. *Journal of comparative and physiological psychology* 91, 128-133.
- Wu, Q., Boyle, M.P., and Palmiter, R.D. (2009). Loss of GABAergic signaling by AgRP neurons to the parabrachial nucleus leads to starvation. *Cell* 137, 1225-1234.
- Wu, Q., Clark, M.S., and Palmiter, R.D. (2012). Deciphering a neuronal circuit that mediates appetite. *Nature* 483, 594-597.

Wu, Q., Howell, M.P., Cowley, M.A., and Palmiter, R.D. (2008). Starvation after AgRP neuron ablation is independent of melanocortin signaling. *Proceedings of the National Academy of Sciences of the United States of America* *105*, 2687-2692.

Yang, Y., Atasoy, D., Su, H.H., and Sternson, S.M. (2011). Hunger states switch a flip-flop memory circuit via a synaptic AMPK-dependent positive feedback loop. *Cell* *146*, 992-1003.

Yeo, G.S., Farooqi, I.S., Aminian, S., Halsall, D.J., Stanhope, R.G., and O'Rahilly, S. (1998). A frameshift mutation in MC4R associated with dominantly inherited human obesity. *Nat Genet* *20*, 111-112.

Young, R.C., Gibbs, J., Antin, J., Holt, J., and Smith, G.P. (1974). Absence of satiety during sham feeding in the rat. *Journal of comparative and physiological psychology* *87*, 795-800.

Zafra, M.A., Molina, F., and Puerto, A. (2006). The neural/cephalic phase reflexes in the physiology of nutrition. *Neuroscience and biobehavioral reviews* *30*, 1032-1044.

Zhan, C., Zhou, J., Feng, Q., Zhang, J.E., Lin, S., Bao, J., Wu, P., and Luo, M. (2013). Acute and long-term suppression of feeding behavior by POMC neurons in the brainstem and hypothalamus, respectively. *The Journal of neuroscience : the official journal of the Society for Neuroscience* *33*, 3624-3632.

Zimmerman, C.A., Lin, Y.C., Leib, D.E., Guo, L., Huey, E.L., Daly, G.E., Chen, Y., and Knight, Z.A. (2016). Thirst neurons anticipate the homeostatic consequences of eating and drinking. *Nature*.

Ziv, Y., Burns, L.D., Cocker, E.D., Hamel, E.O., Ghosh, K.K., Kitch, L.J., El Gamal, A., and Schnitzer, M.J. (2013). Long-term dynamics of CA1 hippocampal place codes. *Nature neuroscience* *16*, 264-266.

Publishing Agreement

It is the policy of the University to encourage the distribution of all theses, dissertations, and manuscripts. Copies of all UCSF theses, dissertations, and manuscripts will be routed to the library via the Graduate Division. The library will make all theses, dissertations, and manuscripts accessible to the public and will preserve these to the best of their abilities, in perpetuity.

I hereby grant permission to the Graduate Division of the University of California, San Francisco to release copies of my thesis, dissertation, or manuscript to the Campus Library to provide access and preservation, in whole or in part, in perpetuity.

Author Signature _____ Date _____